E.U. GRADUATE SCHOOL OF NATURAL AND APPLIED SCIENCES

# EGE UNIVERSITY

# PREPARATION AND CHARACTERIZATION OF POLYMER BASED NANOCOMPOSITE ELECTRODES AND THEIR APPLICATION TO DETERMINATION OF ARSENIC IN REAL SAMPLES

**Meryem GÖKDUMAN**

**Supervised by: Prof. Dr. Zekerya DURSUN**

**Deparment of Chemistry**
**Presentation Date: 09.09.2016**

**Bornova-İZMİR**

**2016**

**EGE UNIVERSITY GRADUATE SCHOOL OF APPLIED AND NATURAL SCIENCES**

**(MASTER OF SCIENCE THESIS)**

# PREPARATION AND CHARACTERIZATION OF POLYMER BASED NANOCOMPOSITE ELECTRODES AND THEIR APPLICATION TO DETERMINATION OF ARSENIC IN REAL SAMPLES

**Meryem GÖKDUMAN**

**Supervisor: Prof. Dr. Zekerya DURSUN**

**Department of Chemistry**

**Date of Presentation: 09.09.2016**

**Bornova-İZMİR**

**2016**

**Meryem Gökduman** tarafından **Yüksek Lisans** tezi olarak sunulan **"Preparation and characterization of polymer based nanocomposite electrodes and their application to determination of arsenic in real samples"** başlıklı bu çalışma E.Ü. Lisansüstü Eğitim ve Öğretim Yönetmeliği ile E.Ü. Fen Bilimleri Enstitüsü Eğitim ve Öğretim Yönergesi'nin ilgili hükümleri uyarınca tarafımızdan değerlendirilerek savunmaya değer bulunmuş ve **09.09.2016** tarihinde yapılan tez savunma sınavında aday oybirliği ile başarılı bulunmuştur.

**Jüri Üyeleri:** **İmza**

**Jüri Başkanı : Prof. Dr. Zekerya DURSUN.....**

**Raporter Üye : Doç. Dr. Nur Erdem AKSUNER .....**

**Üye : Doç. Dr. Süleyman Koçak .....**

# ÖZET

## POLİMER MODİFİYE EDİLMİŞ NANOKOMPOZİT ELEKTROTLARIN HAZIRLANMASI, KARAKTERİZASYONU VE ARSENİK TAYİNİNE UYGULANMASI

GÖKDUMAN, Meryem

Yüksek Lisans Tezi, Kimya Anabilim Dalı

Tez Danışmanı: Prof. Dr. Zekerya DURSUN

Eylül, 2016

Nanoteknoloji ve nanobilimdeki gelişmelerin son yıllarda hızla artmasıyla fizik, kimya ve biyoloji konusunda bilgi sağlayan sensör çalışmaşarı da artmıştır. Geleneksel elektrotlar her uygulamada yeterli olmadığı için farklı analitlere karşı katalitik etkinliği ve seçimliliği yüksek farklı yüzeylere ihtiyaç duyulmuştur. Bu amaca yönelik yüksek iletkenliği olan, etkin ve geniş yüzeye alanına sahip grafen oksit ve iletken polimer filmlerin metal nanoparçacıklar ile birleştirilmesiyle yeni nesil elektrot malzemeleri oluşturulmuştur.

İki bölümden oluşan bu tez çalışmasının ilk kısmında Brodie metodu ile grafen sentezi yapılmış ve metal nanoparçacıklar, poli(p-aminofenol) polimer film ve grafen oksit modifiye elektrotlar hazırlanarak, elektrokatalitik yükseltgenmeyle arsenik tayini yapılmıştır. 0.1 M HCI çözeltisi içinde arseniğin en yüksek yükseltgenme pikini altın nano parçacıkların polimer film yüzeyinde biriktirildiği koşullarda gözlenmiştir (Au/PPAP/GO/GCE). Yalın camımsı karbon elektrot arseniğe yanıt vermezken Au/PPAP/GO/GCE ile akım Au/GO/PPAP/GCE ve Au/GO/GCE'den daha yüksek çıkmıştır. Au/Ni/PPAP/GO/GCE, Au/Cu/PPAP/GO/GCE ve Au/Pt/PPAP/GO/GCE elektrotlar da denenmiş fakat en iyi yanıtı Au/PPAP/GO/GCE vermiştir.

İkinci kısımda ise metal nanoparçacıklar ile modifiye, PCR (polycresolred) polimer film elektrotlar hazırlanarak, arsenik tayini yapılmıştır. 0.1 M HCI ortamında Au/PCR/GCE ile arsenik en iyi yükseltgenme pikini vermiştir.

Bimetalik nano parçacık modifiye polycresolred film glassy karbon elektrot ile polycresolred film glassy karbon elektrot karşılaştırıldığında, altın modifiye polycresolred film glassy karbon elektrotta yanıt alınmıştır.

Tüm polimer ve grafen oksit ile modifiye edilmiş elektrot yüzeyleri ve onların metal nano parçacık kaplı formları taramalı elektron mikroskopu ve X-ışını kırınım spektroskopisi ile karakterize edilmiştir.

**Anahtar sözcükler:** Atomik Kuvvet Mikroskobu (AFM), arsenik, grafen oksit, metal nano parçacık, cresol red, poli-aminofenol, Taramalı elektron mikroskobu (SEM), voltammetri.

## ABSTRACT

# PREPARATION AND CHARACTERIZATION OF POLYMER BASED NANOCOMPOSITE ELECTRODES AND THEIR APPLICATION TO DETERMINATION OF ARSENIC IN REAL SAMPLES

GÖKDUMAN, Meryem

MSc in Chemistry Deparment

Supervisor: Prof. Dr. Zekerya DURSUN

Eylül, 2016

In recent years, sensor studies which provide information on physic, chemistry and biology were increased with the progress on nanoscience and nanotechnology. Because of the insufficient behaviour of conventional electrodes in some applications, the necessity of different active surfaces which were more selective and catalytically active towards analytes. The combination of metal nano particles with conductive polymers and graphene oxide which have high conductivity and wide active surface area were used as important new electrode materials.

In the first part of this thesis which consisted of two different sections, graphene oxide was synthesized with Brodie method and it was used as working electrode. Metal nano particles, poly(p-aminophenol) and graphene oxide modified glassy carbon electrode was prepared and their effect on arsenic oxidation peak was investigated. The best catalytic activity towards arsenic oxidation reaction in 0.1M HCI solution was obtained for existence of Au nanoparticles on the polymer surface (Au/PPAP/GO/GCE). However bare glassy carbon electrode wasn't response for arsenic; Au/GO/GCE, Au/GO/PPAP/GCE and Au//PPAP/GO/GCE had good response for arsenic. Among these modified electrodes, the best current was obtained from Au/PPAP/GO/GCE. Also, using different metal nanoparticles before Au nanoparticles; Au/Cu/PPAP/GO/GCE,

Au/Ni/PPAP/GO/GCE and Au/Pt/PPAP/GO/GCE were obtained. As a result, their current were not high as Au/PPAP/GO/GCE.

Second part of this thesis, polycresol red (PCR) film modified electrodes were used for arsenic oxidation. The best catalytic activity towards arsenic oxidation in 0.1 M HCI solution. Au nanoparticles and polycresol red modified glassy carbon electrore used for working electrode and $10^{-6}$ M arsenic was detected.

All polymer and carbon nanotube modified electrode surfaces were characterized by X-ray diffraction spectroscopy and scanning electron microscopy.

**Keywords:** Atomic Force Microscopy (AFM), carbon nanotube, glucose, metal nano particles, nitrite, oxygen, poly-aminophenol, Scanning electron microscopy (SEM), voltammetry, X-ray Diffraction (XRD).

# ACKNOWLEDGEMENT

I would like to express my indepted gratitude to my supervisor Prof. Dr. Zekerya DURSUN for his encouragement, patience and valuable guidance during the whole period of my research.

I am very grateful to, Res. Asst.Dr. Şükriye KARABİBEROĞLU, Res. Asst. Dr. Aydan ELÇİ, Dr. Çağri KOÇAK and PhD Student Ceren KARAKAŞ for their friendly assistance, collaboration and fellowships during my laboratory studies.

Also I would like to thank to Dr. Ayşegül Şeker ERDOĞAN, Associate Doç. Dr. Özgür ARAR, Ph.D. Student Müge ŞATIR and Kemal Volkan ÖZDOKUR for their help and friendship.

Finally, I would like to thank my mother Cansel GÖKDUMAN and my father Mehmet GÖKDUMAN for immortal confidence, their support and encouragement for my education.

Meryem GÖKDUMAN

2016 İZMİR

# CONTENTS

Page

## CONTENTS (continued)

Page

## CONTENTS (continued)

Page

## CONTENTS (continued)

Page

## CONTENTS (continued)

Page

# LIST OF FIGURES

## LIST OF FIGURES (continued)

Figure Page

## LIST OF FIGURES (continued)

Figure Page

## LIST OF FIGURES (continued)

Figure Page

## LIST OF FIGURES (continued)

Figure Page

# LIST OF TABLES

## ABBREVIATIONS

| Symbol | Explanation |
|---|---|
| A | Electrode area |
| AFM | Atomic force microscopy |
| C | Analyte concentration |
| CE | Capillary Electrophoresis |
| CFC | Carbon reinforced material |
| CFME | Carbon fibre micro electrophoresis |
| CL | Chemiluminescence |
| CNT | Carbon Nanotubes |
| $C_{ox}$ | Concentration of oxidized form |
| $C_{red}$ | Concentration of reduced form |
| CV | Cyclic Voltammetry |
| D | Diffussion coefficient |
| DME | dropping mercury electrode |
| DPV | Differential Pulse Voltammetry |
| $E^0$ | The standart potential |
| Ep | Peak potential |
| Epa | Anodic peak potential |
| Epc | Cathodic peak potential |
| Eq | Equation |
| FIA | Flow injection analysis |
| GCE | Glassy carbon electrode |
| $i_l$ | Limiting current |
| $i_{pa}$ | Anodic peak current |
| $i_{pc}$ | Cathodic peak current |
| LOD | Limit of Detection |
| LR | Lineer range |
| MNP | Metal nano particle |
| MWCNT | Multiwalled Carbon Nanotubes |
| NPV | Normal pulse voltammetry |
| GO | Graphene oxide |
| PCR | Polycresolred |
| PPAP | Poly(p-aminophenol) |

| | |
|---|---|
| Red | Reduced form |
| SAM | Self-assemblied monolayer |
| SEM | Scanning Electron Microscopy |
| SDS | Sodium dodecil sulphate |
| SPE | screen printed electrode |
| SWCNT | Single Walled Carbon Nanotubes |
| V | Scan rate |

## 1. INTRODUCTION

In the last 20 years, scientists have been increasingly interested in a multidisciplinary field which is considered as ***nanoscience and nanotechnology***. The terminology started with 'colloids' about 150 years ago let the scientists began to understand that objects in the nanometer size range have special properties and behavior.

There has been an increasing growth of nanoscience and technology in the last few years, primarily because of the availability of new strategies for the synthesis of nanomaterials and new tools for characterization and manipulation. Several methods of synthesizing nanoparticles, nanowires and nanotubes, and their assemblies, have been discovered (Cao, 2004).

Recently, scientists are focused on carbon based materials which are very critical for nano-sciences. Fullerenes, nanotubes, graphene oxides and graphenes are typical council of nano-structured carbons. Carbon nanotubes (CNTs), have received increasing interest because of their unique properties such as high surface area, significant electrical conductivity, extremely high mechanical strength and good chemical stability. Carbon nanotubes have wide application field as sensitive sensors for some analysts such as coenzymes, neurotransmitters, nucleic acids and also oxygen reduction reaction (Rivas, et al., 2007).

The common nanomaterials generally include nanoparticles, nanowires, nanotubes, nanocapsules, nanostructured alloys and polymers, nanoporous solids. It is also worth to say that chemists have synthesized molecular entities nanometric dimension, nanometer-sized metal particles or metal nanoparticles (MNP) are object of great interest in modern chemical research due to their unique electrical, magnetic, optical and other properties which are individual from both those of the bulk metal and those of isolated atoms and molecules (Haudy, et al., 2006).

Electrochemical studies with nanosized particles involve them to be accessible to the electrode surface where the potential can be controlled. This can be provided either by using the metallic colloid along with an inert and planar

electrode or by attaching the nanoparticle onto a conducting matrix (Cheetam, et al., 2004).

Polymer film electrodes have received great attention due to their wide applications such as chemical sensors and biosensors fields. Porous structure improves their use as supporting material for the development of new catalytic and electrocatalytic materials. These electrodes have many adventages such as; supporting the electrocatalytic properties of substrates, decreasing the overpotential, increasing the reaction rate and enhancing reproducibility and stability of the electrode response in the term of electrocatalysis. Polymer film modified electrodes can be produced with several methods. Among these methods, electropolymerization is promising for immobilizing polymers on various conductive substrates due to the deposition can be contolled by adjusting the electrochemical parameters. (Hathoot, et al., 2012). Conducting polymers also offer a chemical stable film to electrode surface which offer a selective and sensitive opportunity for the determination of many biological and pharmaceutically important molecules. Polymer film surface was also used as prior material for the preparation of metal nanoparticles modification for electrocatalytic electrode reactions ( Biallozor and Kupniewska, 2005).

The most common CPs used as supporting materials are conjugated polymers with heteroatoms in main chain as polyaniline (PANI), polythiophene (PTh) and their derivatives. Due to their high electrical conductivity, it is possible to shuttle the electrons through polymer chains between the electrodes and dispersed metal particles, where the electrocatalytic reaction forms. For this reason, these composite materials can achieve an effiecent electrocatalysis and offer the use of conducting polymers as supporting matrices for the immobilization of catalytically active noble metal particles (Antolini, et al., 2009).

Electrocatalytic oxidation of arsenic has been studied over the past few years due to the great importance of toxic effect and prior pollutant in drinking water. Because of arsenic pollution detecting of arsenic is getting more and more important. A vast number of metals, in particular, platinum, gold, copper, nickel, and palladium have been used as electrode materials in many applications (Taniguchi, et al., 2004).

### 1. 1 The Aim of The Thesis

This thesis mainly comprises in two parts. The first part include that synthesis of graphene oxide and then preparation of graphene oxide, poly (p-aminophenol) (PPAP) and different metal nano particles (Ni, Cu, Fe, Pt, Au) modified glassy carbon electrodes for detection of arsenic.

The second part include that the poly(cresolred) (PCR) was covered on electrode. The PCR/GCE modified with Au nano particles by electrochemical depositionand then the modified electrodes were used electrochemical determination of arsenic in acidic solutions. The morphology and chemical properties of modified electrode surfaces were characterized with scanning electron microscopy and X-ray photoelectron spectroscopy.

### 1. 2 Graphene

Carbon which is the most important element in the universe, have symbol C that is a member of group 14 on the periodic table. There are three naturally occurring isotopes, with $^{12}$ C and $^{13}$ C being stable, while $^{14}$ C is radioactive, decaying with a half-life of about 5,730 years. Carbon is one of the few elements known since antiquity. There are several allotropes of carbon such as graphite, diamond, and amorphous carbon occurs which are best known,in a great variety of species and has been developed to a large number of highly specialised applications as structural and functional materials (Li et. all, 2015).

Fullerenes, carbon nanotubes, carbon anions and graphene are carbon based structures which are called nano-structured materials. These new carbon materials play a major role in nano-science.

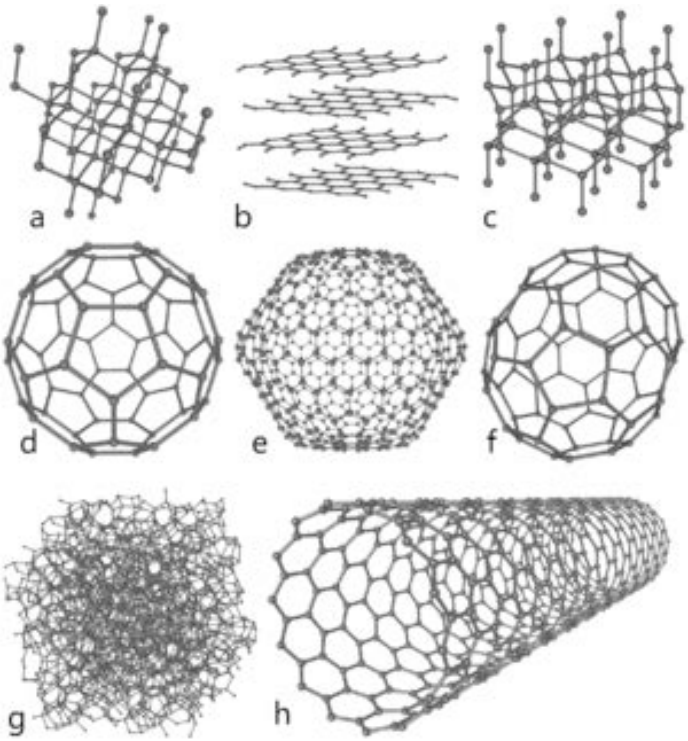


**Figure 1.1** Eight allotropes of carbon: a) Diamond, b) Graphite, c) Lonsdaleite, d) $C_{60}$ (Buckminsterfullerene or buckyball), e) $C_{540}$, f) $C_{70}$, g) Amorphous carbon, and h) single-walledcarbon nanotube or buckytube.

A fullerene is any molecule composed of carbon in the form of a hollow sphere, ellipsoid, tube and many other shapes. Fullerenes, were discovered in 1985 by Kroto et al. while investigating the nature of carbon present in interstellar space. The discovery of fullerenes greatly expanded the number of known carbon allotropes, which until recently were limited to graphite, diamond, and amorphous carbon. The coordination at every carbon atom in fullerenes is not planar, but slightly pyramidalized, with some $sp^3$ character present in the essentially $sp^2$ carbons.

Carbon nanotubes (CNTs) are allotropes of carbon with a cylindrical nanostructure which were discovered by Iijima in 1991. Using a transmission electron microscope (TEM), they have been characterized as a new carbon material. Their properties and potential applications have been paid much attention since their discovery (Dresselhaus et al., 2001). Nanotubes have been constructed with length-to-diameter ratio of up to 132,000,000:1, significantly larger than for any other material (Wang et al., 2009). Nanotubes are categorized as single-walled nanotubes (SWNTs) and multi-walled nanotubes (MWNTs). Individual nanotubes naturally align themselves into "ropes" held together by van

der Waals forces, more specifically, pi-stacking. As a result, a carbon nanotube can bend easily but still is very strong.

As described in Figure 1.2 graphene sheets are rolled up in different directions to form different structured carbon nanotubes. Figure describes that O and A are crystallographically equivalent on the graphene sheet, where X-axis is placed paralle to one side of the honeycomb lattice.

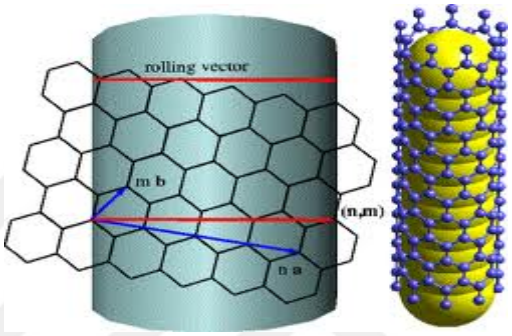


**Figure 1.2** A single walled carbon nanotube structure

The points O and A can be connected by a vector $\boldsymbol{C_h} = n\boldsymbol{a}_1 + \boldsymbol{ma_2}$, where $\mathbf{a_1}$ and $\mathbf{a_2}$ are unit vectors for the honeycomb lattice of the graphene sheet. Next, can drawn normal to C *h* at points **0** and **A** to obtain lines OB and AB′. If it is known superimpose OB onto AB′, obtain cylinder of carbon atoms that constitutes a carbon nanotube when properly capped at both ends with half of a fullerene. Such a single-wall carbon nanotube is uniquely determined by the integers ***(n,m).*** However, from an experimental standpoint, it is more suitable to refer to each carbon nanotube by its diameter $\boldsymbol{dt} = Ch/\pi$ and the chiral angle θ depending on the chiral angle, a single-wall carbon nanotube can have three basic geometries; armchair with θ = 30″, and chiral with 0 < θ < 30″, as depicted in Figure 1.3.

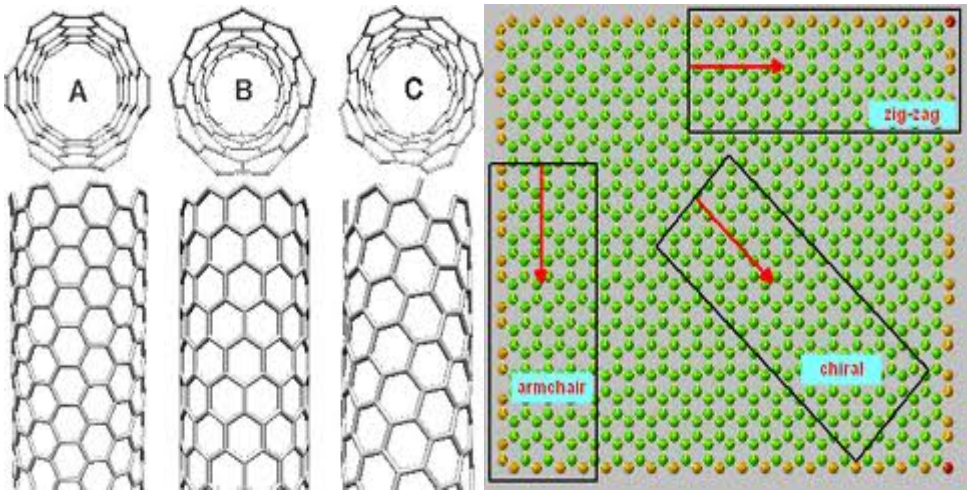


**Figure 1.3** Three basic geometric structure of carbon nanotubes (a) armchair, (b) zigzag, (c) chiral

The structure of carbon nanotube influences its properties such as density, conductance and lattice structure. It is known that some nanotubes are conductors, that is, they are metallic, wheras some are semiconductors. The wider diameter of carbon nanotube behaves like graphite and the narrower diameter of carbon nanotube's intrinsic properties depend on type (Cao, G., 2004).

According to the mathematical laws of Euler; to close the tube, at least 12 pentagons are necessary. Figure 1.4 shows the end sides of nanotubes.

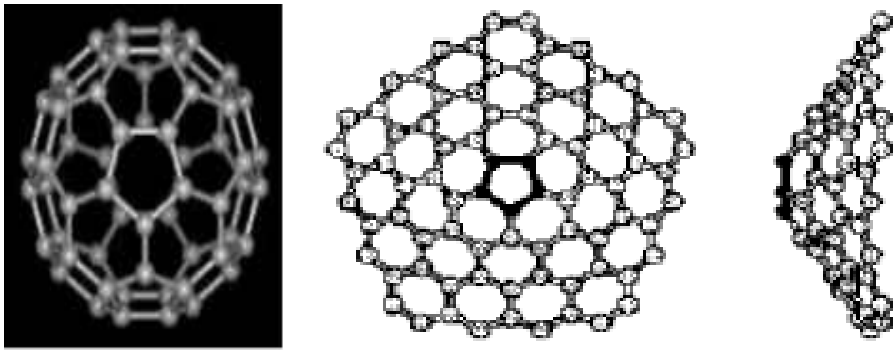

**Figure 1.4** End sides of carbon nanotubes

### 1. 3 Synthesis of Graphene Oxide and Graphene

Graphene is pure carbon in the form of a very thin, transparent, two dimensional, one atom thick of graphite. Although it has very low weight (100 times stronger than steel) it conduct the heat and electricity with a great efficiency (Li et al., 2015). Graphene has a theoretical specific surface area (SSA)

of 2630 $m^2/g$. This is much larger than that reported to date for carbon black (typically smaller than 900 $m^2/g$) or for carbon nanotubes (CNTs), from ≈100 to 1000 $m^2/g$ and is similar to activated carbon In Figure 1.5, graphene sheets are rolled up in different directions to form different structured carbon nanotubes.

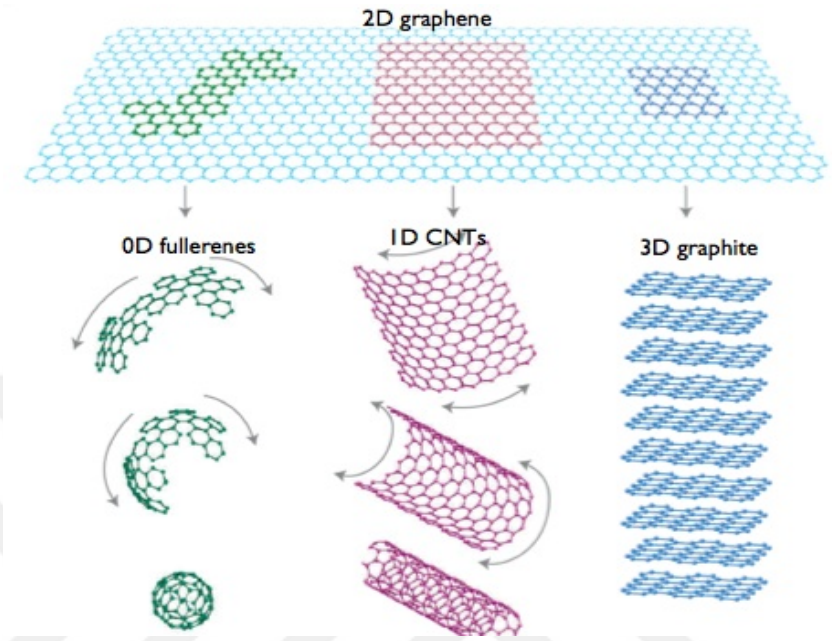


**Figure 1.5** Different structured carbon nantubes

There are many ways to synthesize graphene, such as;

- ✓ Exfoliation
- ✓ Adhesive tape
- ✓ Wedge-based mechanical exfoliation
- ✓ Reduction of graphene oxide
- ✓ Sugar method
- ✓ Shearing
- ✓ Sonication
- ✓ Solvent-aided

- ✓ Solvent/surfactant-aided
- ✓ Immiscible liquids
- ✓ Molten salts
- ✓ Epitaxy
- ✓ Nanotube slicing
- ✓ Carbon dioxide reduction
- ✓ Spin coating
- ✓ Supersonic spray
- ✓ Intercalation
- ✓ Laser
- ✓ Microwave assisted oxidation

Among these preparation methods, solution-based reduction of graphite oxide is attractive for its easy operation in recent years.

Graphene oxide was first prepared by Oxford chemist Benjamin C. Brodie in 1859, by treating graphite with a mixture of potassium chlorate and fuming nitric acid (Brodie, 1859). He reported synthesis of "paper-like foils" with 0.05 mm thickness. In 1957 Hummers and Offeman developed a safer, quicker, and more efficient process called The Hummers' Method, using a mixture of sulfuric acid ($H_2SO_4$), sodium nitrate ($NaNO_3$), and potassium permanganate ($KMnO_4$) which is still widely used, often with some modifications (Hummers, et al., 1958).

Among these methods, Hummers' method is popular for the following reasons. First, $KClO_3$ was replaced by $KMnO_4$ as the oxidation agent. In this

condition, the by products of toxic gas were eliminated and the securities of experiments were improved. Moreover, the oxidation time was shortened, and last it was easy to exfoliate the resulted product in water.

Graphene oxide shows remarkable differences depending on degree and oxidation and synthesis method. For example temperature point of explosive exfoliation is generally higher for graphene oxide prepared by Brodie method compared to Hummers graphene oxide, the difference is up to 100 degrees with the same heating rates. Hydration and solvation properties of Brodie and Hummers graphene oxides are also significantly different (Luzan, et al., 2013).

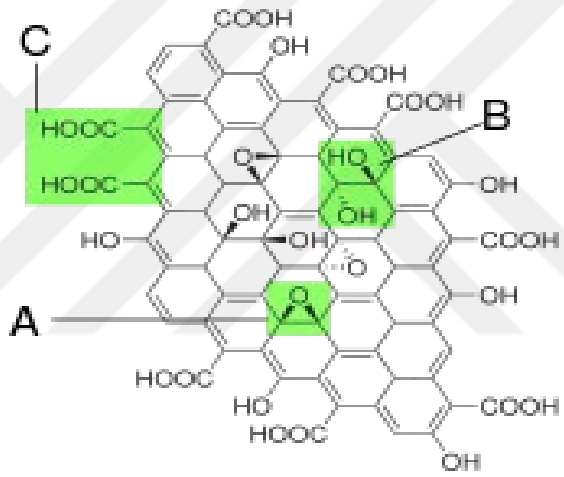


**Figure 1.6** Graphene oxide structure proposed in 1998 with functional groups. **A:** Epoxy bridges, **B:**Hydroxyl groups, **C:** Pairwise carboxyl groups.

Recently a mixture of $H_2SO_4$ and $KMnO_4$ has been used to cut open carbon nanotubes lengthwise, resulting in microscopic flat ribbons of graphene, a few atoms wide, with the edges "capped" by oxygen atoms (=O) or hydroxyl groups (-OH) (Kosynkin, et al., 2009).

Graphite (Graphene) oxide (GO) has also been prepared by using a "bottom-up" synthesis method (Tang-Lau method) in which the sole source is glucose, the process is safer, simpler, and more environmentally friendly compared to traditionally “top-down” method, in which strong oxidizers are involved. Another

important advantage of Tang-Lau method is control of thickness, ranging from monolayer to multilayers by adjusting growth parameters (Tang, et al., 2012).

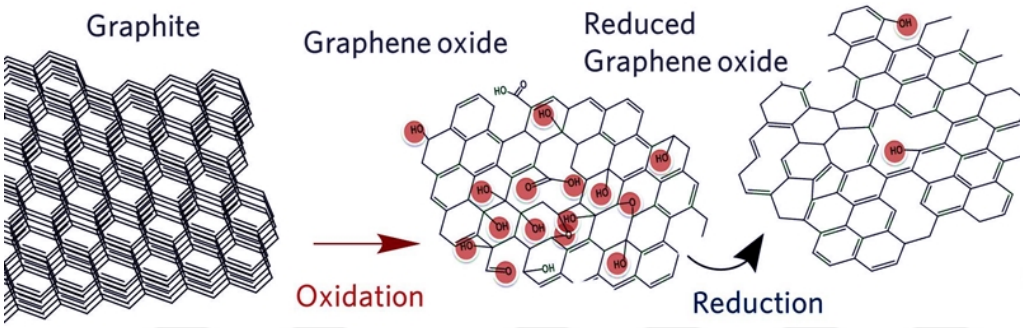


**Figure 1.7** Oxidation of graphite oxide

Figure 1.7 shows synthesis of graphene oxide and graphene. Firstly, by oxidation of graphite, graphene oxide occurs and then; by reduction of graphene oxide, graphene sheets occur.

Graphene oxide and graphene have wide using areas and applications:

- ✓ Optical applications
- ✓ Coating
- ✓ Water purification
- ✓ DNA analysis application
- ✓ Flexible rechargeable battery electrode
- ✓ Drug-delivery material
- ✓ Composite materials
- ✓ Photovoltaics and energy storage

Last two decades number of studies have done using or modifying graphe as a sensitive electrode. Rosy et. al., have been developed using graphene meodified palladium (Pd) sensor. Graphene was synthesized in the laboratory and the

electrochemical response towards norepinephrine (NE) determination was studied. The modified sensor exhibitied excellent electrocatalytic activity for the oxidation of NE. In the 0.5 µM– 500 µM NE concentration range in phosphate buffer of pH 7.2, using palladium modified graphene electrode, the detection limit and quantification 67.44 nM and 224.80 nM, respectively. Because of the detection sensitivities of bare and modified Pd sensors were 0.851 µA $mM^{-1}$ and 17.428 µA $mM^{-1}$, this modified electrode was successfully applied for the determination of NE in pharmaceutical dosage forms and human urine samples.

In another study, a nanocomposite electrode prepared by graphene and $SnO_2$ nanosheets was used to modify a N-hexylpyridinium hexafluorophosphate based carbon ionic liquid electrode. Electrochemical behaviors of dopamine on the electrode were evaluated by cyclic and differential pulse voltammetry. The results showed that graphene-$SnO_2$ nanocomposite electrode displayed high electrocatalytic activity to the oxidation of dopamine. Under the optimum conditions, the oxidation peak current was proportional to the DA concentration in the range from 0.5 to 500.0 µM with a detection limit of 0.13 µM (S/N = 3) (Sun, et. al., 2013).

In other study; for detection of uric acid, reduced graphene oxide material based modified electrode was prepared. To make more sensitive electrode material, reduced graphene oxide film with various oxygen functionalities were prepared through electro-reduction at different reduction potentials and their electrocatalytic activities for UA oxidation were examined. The partially electro-reduced graphene oxide (pERGO) electrode with the content of oxygen functionalities was showed the highest current sensivity towards UA (Zhang, et. al., 2014).

According to another study, indium thin electrode (ITO) modified with electrochemically reduced graphene oxide (ERGO) without any glue reagents were used for determination of uric acid in the presence of ascorbic acid. This modified electrode showed an exellent electrocatalytic effect towards uric acid. Differential pulse voltammetry (DPV) was used to determine the linear uric acid detection range (0.3–100 µM) and the detection limit (0.3 µM) (Khan, et. al., 2013).

In another study, graphene oxide (GO), nickel oxide nanoparticles (NiONPs)/GO/glassy carbon (GC) modified electrode was prepared by

electrodeposition of NiONPs on the GC surface as a supercapasitor and nonenzymatic glucose sensor. The results indicated that GO was partially reduced and three-dimensional NiONPs were electrochemically synthesized on the surface of GO. Compared with NiONPs/GC electrode, NiONPs/GO/GC modified electrode showed more excellent conductivity, more superior electrochemical capacitive behavior and better electrocatalytic oxidation of glucose, applying for the electrochemical detection of glucose. The linear range for glucose is from 3.13 µM to 3.05 mM with the detection limit of 1.0 µM (Yuan, et. al., 2013).

Graphene and reduced graphene oxide have been also widely used for determination of heavy metals in different matrixes. An in situ modified Hummers method (without the use of any surfactants) has been used for the deposition of bismuth (Bi) particles on to the surface of reduced graphene oxide (RGO) sheets. It was characterized by X-ray diffraction (XRD) and Fourier transform infarred (FTIR) spectroscopy, Raman spectroscopy, transmission electron microscopy (TEM), thermo- gravimetry (TG) and differential scanning calorimetry (DSC). The morphology of the RGO/Bi nanocomposites provides a better choice as an electrode material for detection of heavy metal ions because of its better functional properties over the Bi film electrode. Trace analysis of heavy metal ions such as $Cd^{+2}$, $Pb^{+2}$, $Cu^{+2}$ and $Zn^{+2}$ in water is carried out by stripping voltammetric analysis using RGO/Bi nanocomposite as an electrode material. The three sigma detection limits at different deposition potential for $Cd^{2+}$, $Pb^{2+}$, $Zn^{2+}$ and $Cu^{2+}$ were obtained as 2.8, 0.55, 17 and 26 µg/L, respectively. Copper detection using Bi-film electrode was a big challenge, which has been resolved using the RGO/Bi nanocomposite electrode (Sahoo, et. al., 2013).

### 1. 4 Conductive Electroactive Polymers

Recently, conducting polymers have attracted much interest in the development of sensors due to their electrical properties. Conducting electroactive polymers (CEPs) were investigated in the mid-1970s. this culminated in 2000 when the Nobel Prize was awarded to Alan MacDiarmid, Alan Heeger and Hideki Shirakawa for their discovery and development of conducting polymers. Applying industrial development of conducting polymer products has provided the fundamental understanding of the chemistry, physics, and material science (Wallace, et al., 2009).

Inherently conducting polymers, also known as ‘synthetic metals’ are polymers with a highly π-conjucated polymeric chain (Lu et, al., 2011). Electrically conducting polymers have in common a significant overlap of delocalised π-electrons along the polymer chain, and several suitable structures. Typical conducting polymers include polyacetylene (PA), polyaniline (PANI), polypyrrole (PPy), polythiophene (PTh), poly(para-phenylene) (PPP), poly(phenylenevinylene) (PPV), polyfuran (PF), etc. which are shown in Figure 1.8

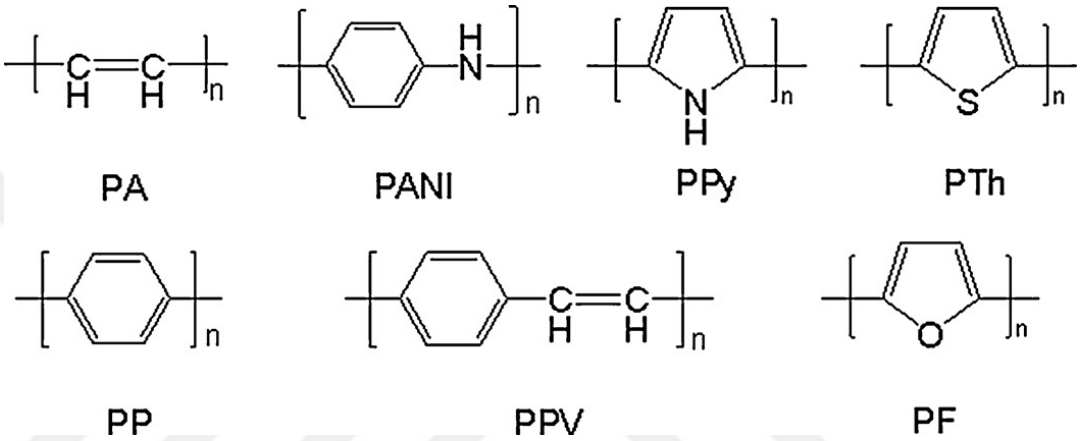


**Figure 1.8** Some conjugated conducting polymers (2011 X. Lu et al.)

The high conductivity makes these polymers using for electro-optic, sensors, absorbing and corrosion protective material and large surface area of nanomaterials.

CPs can be synthesized in two ways: chemically and electrochemically methods. These two methods have some advantages and disadvantages which are shown in Table 1.1.

**Table 1. 1** Comparison of chemical and electrochemical CP polymerization

| Polymerization | Chemical polymerization | Electrochemical polymerization |
|---|---|---|
| **Advantages** | Larger-scale production is possible<br>Post-covalent modification of bulk CP is possible<br>More options to modify CP | Thin film<br>Synthesis is not complex<br>Entrapment of molecules in CP<br>Doping is simultaneous |
| **Disadvantages** | Not esasy to make thin films<br>Synthesis is complex | Removing the film from electrode surface is hard |

.

### 1. 4. 1 Applications of CEPs

Conducting polymers are keys to technology because of their large-scale applications which are listed below:

- Chemical sensors
- Biosensors
- Transistors
- Data storage
- Supercapacitor
- Tuators
- Batteries
- Optically transparent conducting material

- Photovoltaic cells
- Surface protection
- Electrocatalysis
- Substituent for carbon nanomaterial
- Molecular devices and modified electrodes

### 1. 4. 2 Studies at polymer modified electrodes

Polymer films are obtained by different methods as dip coating, vapor deposition and spin-coating which require toxic solvents and some special equipments. Besides this methods electrochemical techniques are simple methods that provide a uniform and strongly adherent conducting polymer films with better conductivity at electrode surface by cheaper way ( MacDiarmid, 1997).

Modifications of the GCE surface with poly(3,4-ethylenedioxythiophene) (PEDOT), nafion and multi-walled carbon nanotubes were tested to evaluate possible sensor performance enhancements. Nafion gave the best results so the sensors were successfully applied for determination of caffeine content in drugs (Torres et al., 2014).

The electrochemical polymerization of the EDOT was carried out by the cyclic voltammetry (CV) and as a result PEDOT modified electrodes were obtained. This PEDOT (poly(3,4-ethylenedioxy) thiophene) modified electrode was developed as a chemical sensor electrode and used for simultaneous measurement of various combination of dopamine ascorbate anion (Vasantha et al., 2006).

The PANOA poly(aniline-co-o-aminophenol) copolymer was strongly catalyzed the reaction of arsenate in NaCI solution and it was used as a probe to determine arsenate directly. Electrocatalytic reduction of arsenate depended on pH and applied potential (Mu et al., 2009).

Bobacka and coworkers studied usage of several conducting polymers including poly(3-octylthiophene), poly(3,4-ethylenedioxythiophene) (PEDOT) and polypyrrole (PPy) with various dopants and they showed that conducting polymers have more significant effect on the sensivity and selectivity of the modified electrodes towards the metal ions (Bobacka et al., 2005).

Conducting polymer modified electrodes (CPME) in their dopes and undoped forms were used for determination of heavy metals by anodic stripping voltammetry. EDTA-functionalized CPME were used for the detection of various metal ions at different pHs (Rahman et al., 2003).

Electropolimerization of pyrogallol at the glassy carbon electrode in PBS (pH 7.0) gave a water-insoluble and stable film on the electrode surface. This poly(pyrogallol) film electrode was used for determination of Sb(III) by differential anodic stripping voltammetry. Under optimized conditions, the calibration curve was linear in the range $5.0x10^{-9}$ to $1.0x10^{-7}$ M Sb(III) (10 min accumulation). A detection limit of $4x10^{-10}$ M Sb(III) (0.05 ppb) (S/N=3) was found (Beng Khoo et al., 1998).

In another study, a novel polytaurine nano gold film has been fabricated on a glassy carbon electrode (GCE) and ITO by using CV. The modified GCE electrode was successfully applied for detection of arsenic in real drinking water and lab analysis (Rajkumar et al., 2011).

### 1.5 Poly(p-aminophenol)

Aminophenol is an organic compound with the formula $C_6H_4(OH)NH_2$. Aminophenol isomers (o-aminophenol (o-AP), p-aminophenol (p-AP), and m-aminophenol (m-AP)) are important industrial raw materials that are widely used as chemical inhibitors, petroleum additives, and synthetic intermediates. Figure 1.9 shows the three isomers of aminophenol.

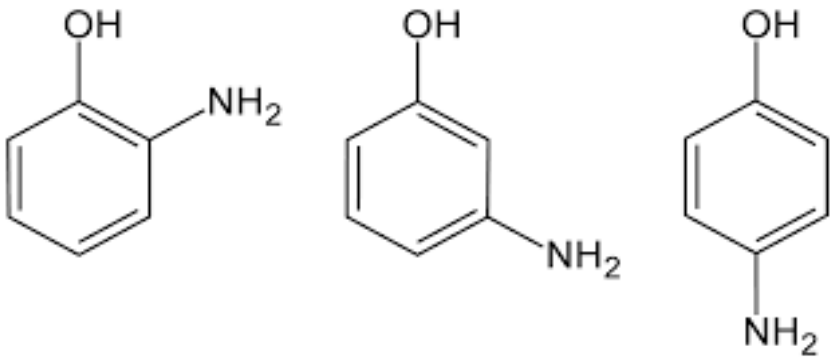


**Figure 1.9** Three isomers of aminophenol. From left to the right : o-aminophenol, m-aminophenol, p-aminophenol.

Also, the current interest in polimerization of polymers (especially polp(p-aminophenol)) is well documented in by the growing literature data. In Figure 1.10, the polimerization of p-aminophenol is shown. The use of PPAP for practical purpose, whatever the applicative field, is closely related to its chemical structure. The ability of cation capturing, for example, has been attributed to the simultaneous presence of hydroxyl and amino groups of the polymer backbone with availablel one pair electrons, which is consistent with the 1,4- substituted molecular structure proposed by Zhang. Recently, a nanocomposite of graphene and PPAP was electrosynthesized which exhibited high specific capacitance, rate capability and cycling stability as a supercapacitor electrode. This behavior was due to the synergetic effect of PPAP and graphene nanosheets related to hydrogen bonding and stacking. Also as for molecularly imprinted polymer, the applications of PPAP take advantage of the formation of hydrogenbonds between the template and–$NH_2$ and–OH groups present along the polymer skeleton.

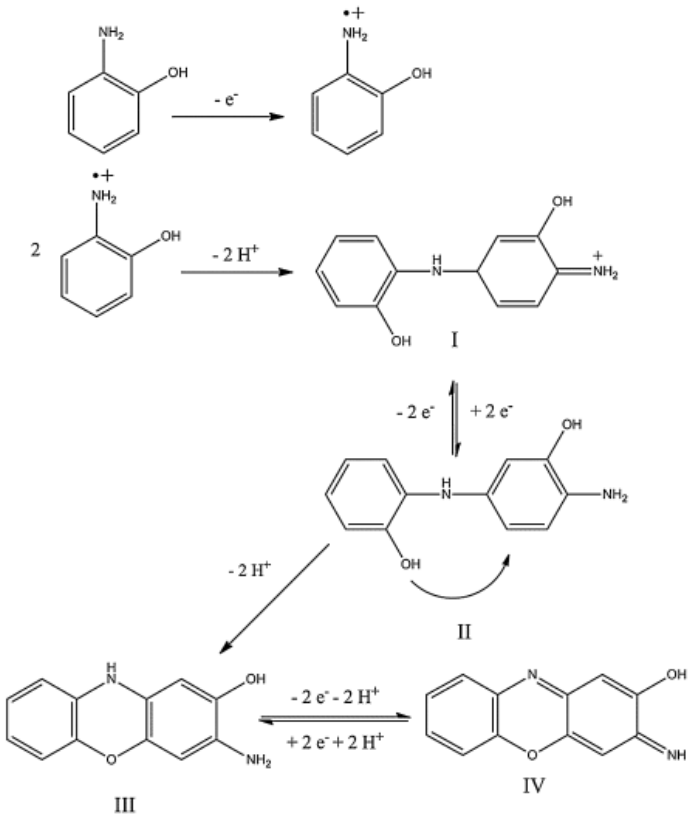


**Figure 1.10** Polimerization of p-aminophenol

### 1.6 Cresol Red

Cresol red (*o*-Cresolsulfonephthalein) is a triarylmethane dye frequently used for monitoring the pH in aquaria. It is also widely used molecular biology reactions and color maker. Figure 1.11 shows the structure of cresol red.

Recently, polymerization of cresol red has some applications in electrochemistry. Chen, at. Al., were studied glassy carbon electrode (GCE) modified with electropolymerized films of cresol red in pH 5.6 phosphate buffer solution (PBS) by cyclic voltammetry (CV). The modified electrode showed an excellent electrocatalytic effect on the oxidation of norepinephrine (NE). According the results, the peak current increases linearly with the concentration of NE in the range of $3\times10^{-6}$–$3\times10^{-5}$ M by the differential pulse voltammetry. The detection limit was $2\times10^{-7}$ M. The modified electrode can also separate the electrochemical responses of norepinephrine and ascorbic acid (AA). The separation between the anodic peak potentials of NE and AA was 190 mV by the cyclic voltammetry. And the responses to NE and AA at the modified electrode were relatively independent (Chen, et. al., 2005).

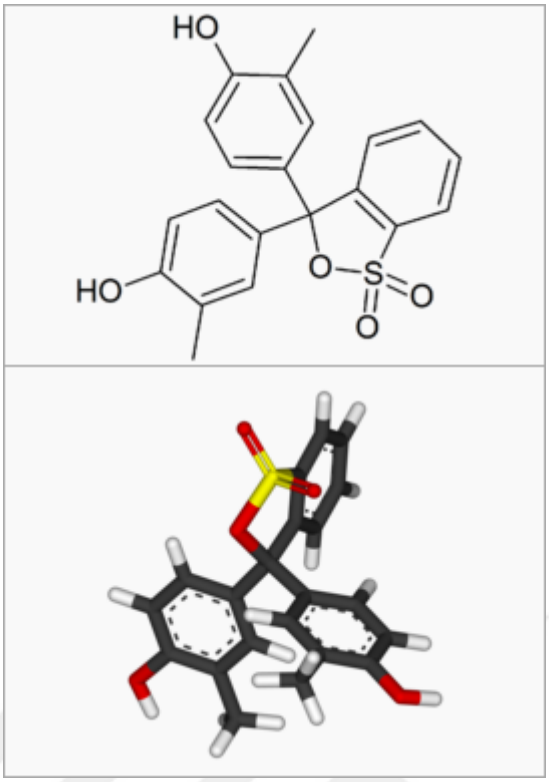


**Figure 1.11** The structure of cresol red

In other study, polycresol p (o-cresol) has been synthesized by cyclic voltammetry technique in acidic medium using sulfuric acid as an electrolyte at 30$^{o}$C. The electrosynthesized polymer was characterized by X-ray diffraction (XRD) and scanning electron microscope (SEM). The adsorption properties of the fabricated polymer were investigated for adsorptive removal of Pb (II) ions from aqueous solutions. Various physico-chemical parameters such as pH, initial metal ion concentration, and equilibrium contact time were studied. Optimum conditions were found to be 6 for pH and 4 h for contact time. In addition, the adsorption isotherms were obtained using Pb(II) solutions of concentrations ranging from 50 to 250 mg/l. The adsorption process was found to follow pseudo-second-order reaction kinetics and Freundlich adsorption isotherms (Sayyah, et. al., 2014).

## 1.7 Metal Nano Particles

In recent years, nonaomaterials such as nanometer-sized metal particles has become increasingly important in modern chemical research.

However metal nanoparticles have a great role in many applications, they have some disadvantages like fragile and unstable surface area.

Because of being unstable; ligands, capping agents, surfactans, phthalocyanines, carbon nanotubes and polymers can be used stabilizing support material for metal nanoparticles. Among these materials, conducting polymers and carbon nanotubes provide good electron-ion conductivity and proton conductivity. The porous structure of polymers and carbon nanotubes can allow easily dispersion of metal nanoparticles.

There are exist diferent synthesis methods for metal nanoparticles, it can be categorized in two main group: physical methods and chemical methods.

**Physical Methods**

- Metal-vapour synthesis
- Laser ablation
- Solvated metal-atom dispersion
- Sonoelectrochemistry
- Microwave irridation

**Chemical Methods**

- Salt reduction
- Electrochemical reduction
- Thermal reaction
- Ligand removal from organometallic
- Photolysis of metal compounds

- Radiolytic methods

The production of many semiconductors can be made of nanoparticles of heavy metal (Cd, Zn, etc), lantanides and their compounds (Doria et al., 2012). On the other hand, inorganic lanthanide based nanoparticles are applied in a range of biotechnologies (Abid et al., 2013).

Metal particles can be divided into three groups according their dispersion type; 1 to 30–50 nm called as nanometric or ultradispersed, 30–50 to 100-500 nm called as submicrometric or highly dispersed, and also 100–500 to 1000 nm called as Micrometric (Muraviev, 2005).

The significant role of chemistry was seen in the synthesis and characterization of nanosized metarials of nanoparticles, carbon nanotubes, metals/oxides and semiconductors, composites involving ceramics (Cheetam et al., 2004).

Metal nano particles can be synthesized with different techniques. Such as synthesis of semiconductor nanoparticles in solutions of the corresponding salts by controlled addition of anions (cations) or by hydrolysis another one is preparation of nanoparticles as a result of phase transformations, third one is the synthesis of nanoparticles in aerosol and finally by electrochemical methods.

Among all methods mentioned above, the electrochemically synthesis of metal nanoparticles is one of the most appropriate method to obtain uniformly dispersed nano particle on the stabilized conducting material modified electrode surface. The electrodeposition method is an advantageous method that which has low cost, taken short time, a high purity of the particles, more easily controls the nano particules dimensions, lower particle size distribution compare to chemical and physical methods. Morover, the electrodeposition method includes the ability to uniformly coat non-planar substrates, to plate over wide areas, and to deposit a nanocomposite to an overall thickness much larger than can be usually achieved by vacuum deposition methods (Heflin, et al., 2004).

Due to their unique electrical, magnetic, optical and other properties which improve catalytic activity, the analytical sensitivity and selectivity, metal nano

particules modified electrodes widely used in chemical researchs. Noble metal nano-structures like Au, Pt and Pd have attracted tremendous attention in recent decades, because of their excellent optical, electrochemical and electronic properties, which are different from those of bulk metal materials.

In another work silver nanoparticles were mixed with a solution of Nafion and modified to glassy carbon electrode. This modified electrodes were used for the detection of arsenic (Prakash et al., 2012), polyphenols (Rawal et al., 2011), antimony (Renedo et al., 2007), pesticides (Kumaravel et al., 2010) and glucose (Ren et al., 2005).

In the study of Lan et al., gold-palladium bimetallic nanoparticles modified glassy carbon electrode was used for determination of arsenin (III) by anodic stripping voltammetry. The (Au-Pd) nanoparticles modified electrode was performed in solutions of pH 4.5 which contains different concentrations of arsenite. A good response was exhibited towards As(III) with a limit of detection of 0.025 ppb (Lan et al., 2012).

In another study, Cui et al., electrochemical sensor was developed for arsenic detection. By using a magnetic $Fe_3O_4$ nanoparticles and gold nanoparticles, glassy carbon electrode was modified. The AuNPs/$Fe_3O_4$/GCE gave the best result in comparison with AuNPs/GCE and the developed method was successfully used to determine arsenic(III) in real water samples (Cui et al., 2012).

## 1. 8 Arsenic

### 1.8.1 Chemical properties of arsenic

Arsenic is a chemical element with symbol As and atomic number 33. Arsenic occurs in many minerals, usually in conjunction with sulfur and metals, and also as a pure elemental crystal. Arsenic is a metalloid. It can exist in various allotropes, although only the gray form has important use in industry.

Arsenic has more than fifty identified different arsenic containing chemical species.The most widespread arsenic species in the worl are presented in Table 1.2. (Rajakovic et al., 2013). Arsenic occurs four oxidation states ($As^{3+}$, $As^{5+}$, $As^{0}$ and $As^{3-}$). The major forms of inorganic arsenic in water are arsenate ions (As(V), $H_2AsO_4$ or $HAsO_4^-$) and arsenite ions (As(III) and $H_3AsO_3$), organic arsenic forms are monomethylarsonic acid (MMA) and dimethyl arsenic acid (DMA) (Li et al., 2012).

**Table 1.2.** Names, abbreviation and structure of the most common arsenic species

| Name of arsenic species | Abbreviation | Structure |
|---|---|---|
| Arsenous acid, arsenite | As(III) | $H_3AsO_3$, $H_2AsO_3^-$, $HAsO_3^{2-}$, $AsO_3^{3-}$ |
| Arsenic acid, arsenate | As(V) | $H_3AsO_4$, $H_2AsO_4^-$, $HAsO_4^{2-}$, $AsO_4^{3-}$ |
| Monomethylarsenic acid | MMA | $CH_3AsO(OH)_2$ |
| Dimethylarsinic acid | DMA | $(CH_3)_2AsO(OH)$ |
| Trimethylarsine oxide | TMAO | $(CH_3)_3AsO$ |
| Trimethylarsoniopropionate | TMAP | $(CH_3)_3As^+CH_2CH_2COO^-$ |
| Tetramethylarsonium ion | TETRA, TMA | $(CH_3)_4As^+$ |
| Arsenobetaine | AB | $(CH_3)_3As^+CH_2COOH$ |
| Arsenocholine | AC | $(CH_3)_3As^+CH_2CH_2OH$ |
| Dimethylarsinyolacetic acid | DMAA | $(CH_3)_2AsOCH_2COOH$ |
| Phenylarsine oxide | PAO | $C_6H_5AsO$ |
| Phenylarsonic acid | PAA | $C_6H_5AsO(OH)_2$ |
| Arsenosugars $C_7H_{14}AsO_3CH_2CH(OH)CH_2R$ | | |
| Arsenosugar 1 (glycerol sugar) | – | R=OH |
| Arsenosugar 2 (phosphate sugar) | – | $R=OP(O)(O^-)OCH_2CH(OH)CH_2OH$ |
| Arsenosugar 3 (sulphonate sugar) | – | $R=SO_3^-$ |
| Arsenosugar 4 (sulphate sugar) | – | $R=OSO_3^-$ |

### 1.8.2 Arsenic in the environment

A Arsenic can be found naturally on earth in small concentrations. It occurs in soil and minerals and it may enter air, water and land through wind-blown dust and water run-off. Arsenic in the atmosphere comes from various sources: vulcanoes release about 3000 tonnes per year and microorganisms release volatile methylarsines to the extent of 20.000 tonnes per year, but human activity is responsible for much more: 80.000 tonnes of arsenic per year are released by the burning of fossil fuels.

- ✓ Smelting of metals

- ✓ Pharmaceutical industry
- ✓ Pesticide manufacture
- ✓ Wood preservative
- ✓ Cattle and sheep dips
- ✓ Feed additives
- ✓ Dye stuffs
- ✓ Semiconductor manufacture

It is widely found in the Earth's crust and increasingly being found in drinking water in many places in the world (Giacomino et al., 2011). Some countries, such as China, Bangaldesh, Vietnam,India, Chile, USA and Canada, suffer from As contamination (Liu et al., 2014).

Arsenic contaminated water typically contains arsenous acid and arsenic acid or their derivatives. Their names as "acids" is a formality, these species are not aggressive acids but are merely the soluble forms of arsenic near neutral pH. These compounds are extracted from the underlying rocks that surround the aquifer. Arsenic acid tends to exist as the ions $[HAsO_4]^{2-}$ and $[H_2AsO_4]^-$ in neutral water, whereas arsenous acid is not ionized. Figure 1.12 shows the major forms of arsenic which are mostly found in water.

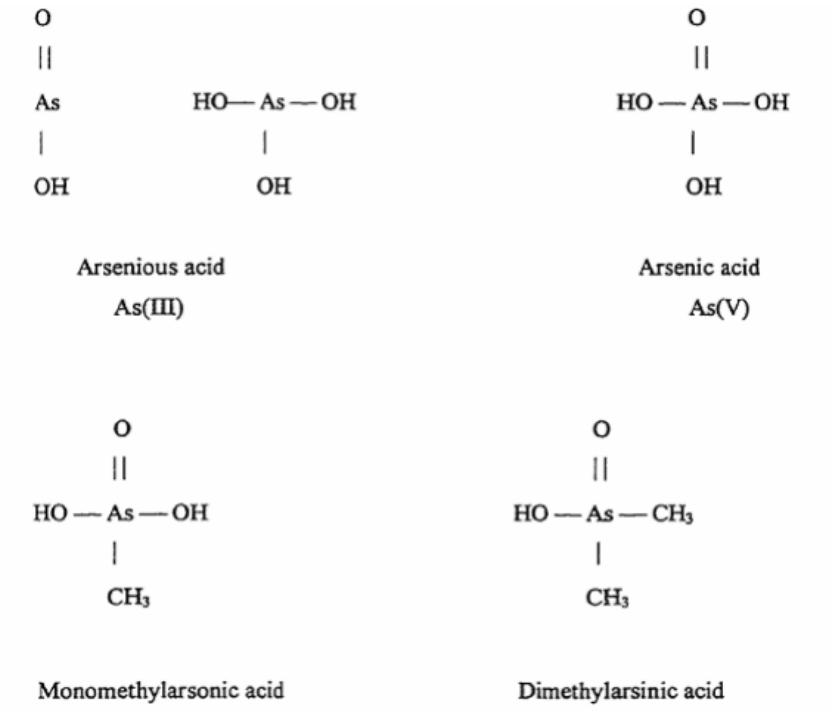


**Figure 1.12** Major forms of arsenic found in water.

### 1.8.3 Arsenic toxicity

As(III) and As(V) are the most common toxic forms of inorganic arsenic present in drinking water. Biologically, As(III) is generally recognized to be more toxic than As(V). To humans, arsenite is about 60 times more toxic than arsenate. When taken by humans and animals, inorganic As(V) is transformed to As(III), followed by methylation to monomethyl arsenic (MMA) and dimethyl arsenic (DMA) which are much less toxic forms (Jain & Ali, 2000). The toxicity order of arsenic species is arsenite > arsenate > MMA > DMA.

Long term exposure to arsenic in drinking water can cause a lot of adverse effects including skin lesions, respiratory, cardiovascular, genotoxic, mutagenic and cardiovascular effects (Gibbon et al., 2011).

A very high exposure to inorganic arsenic can cause infertility and miscarriages with women, and it can cause skin disturbances, declined resistance to infections, heart disruptions and brain damage with both men and women. Finally, inorganic arsenic can damage DNA.

On the contrary to the inorganic arsenic, organic arsenic can cause neither cancer, nor DNA damage. But exposure to high doses may cause certain effects to human health, such as nerve injury and stomachaches.

Arsenic poisoning effected many people and high level of arsenic increasingly found in drinking water in many countries such as Bangaldesh, India, Great Britain, Thailand, Mexico and within the U.S in California, Oregon, Masshusetts, Marine and new Hampshire (Camacho, et. al., 2011).

Because of these health effects as it mentioned above, arsenic detection has become a great interests in all over the worl. All the studies have been carrying out to decrease the level of arsenic in drinking water. This level is 10 ppb according the World Health Organizations (WHO) report.

### 1.8.4 Studies for arsenic detection

Recently, as we know, several voltammetric techniques were developed and researched for determination of inorganic arsenic, such as cyclic voltammetry (CV), square wave voltammetry (SWV), linear sweep voltammetry (LSV) and differential pulse voltammetry (DPV). SWV and DPV are effective among these techniques because they can offer better sensitivity and higher signal. To achive detection of trace amount of arsenic, stripping based analysis techniques are more effective. Because of pre-concentration step, As is deposited onto the electrode from the solution (Liu et al., 2014).

To compare with various analytical techniques, modified electrodes such as polymer, metal nanoparticles modified lecetrodes show a special attention to detect arsenic due to its easy preparation (Rajkumar et al., 2011).

In their study, poly taurine nano gold film has been fabricated on glassy carbon electrode and ITO using cyclic voltammetry. Poly taurine nano gold film modified GCE has been used successfully for detection of arsenic in tap water, spring water and mineral water. It detected the arsenic in a linear range of 6 to 28 µM with the detection limit of 0.46 µM in lab samples.

As it mentioned above, conductive polymers are good alternative because of its electrochemical activity. Therefore, a conductive polymer could be used to remove arsenate and arsenite ions from the aqueous solution. In their research, they used poly(aniline-co-o-aminophenol) (PANO) and deposited on the glassy carbon electrode to investigate electrocatalytic reduction of arsenate in NaCI solution (Zhang et al., 2009).

Recently, the use of nanoparticulate gold, supported on carbon subsrates has been allowed the trace determination of arsenic and reduced the interference (Xiao et al., 2008).

In another research, GCE electrode was modified by casting gold-palladium (Au-Pd) nanoparticles onto its surface and by stripping voltammetry and then it is used for detection of As(III). Modified electrode was performed in pH 4.5 supporting solution which is containing different concentrations of arsenite. Au-Pd modified GCE performed good response towards As(III) with detection limit of 0.25 µg/kg which is lower than 10 µg/kg limit (Lan, et. al., 2012).

Krause and his friends prepared bismuth modified exfoliated graphite electrode in the detection of arsenic in water. At a -600 mV potential, bismuth film was electrodeposited onto an exfoliated graphite (EG) electrode. In As(III) solutions, EG-Bi modified electrode was performed in optimum conditions of pH 6 by square wave anodic stripping voltammetry at a deposition potential of -600 mV and 180 s pre-concentration time. As a result, detection limit was found 5 µg/kg and observed that this modified electrode didn't interefe cations except Cu(II) (Krause, et. al., 2014).

Silver nanoparticles (AgNPs) built-in chitosan modified glassy carbon electrode (GCE) has been prepared for sensitive detection of As(III) by differential pulse anodic stripping voltammetry (DPASV). This modified electrode (AgNPs/CT/GCE) was characterized by SEM, TEM, XRD, FTIR, Uv-Vis. Nanostructured modified electrode showed wide linear range (10-100 ppb), with 0.309 ppb high sensitivity and 1.20 ppb detection limit. In the presence of Cu and other organics, it showed a stable performance (Prakash, et. al., 2012).

In other study, electro reduced graphene oxide (EGO) was prepared by the oxidation of exfoliated graphite by using Hummers method. It was dropped (10 µl) onto the GCE surface and after drying, in 1 M HCI media, 1 mM Pb (II) modified by cyclic voltammetry. The detection limit of arsenic is found to be 10 nM (Ramesha, et. al., 2011).

Liu and his team was worked with graphene oxide for As detection. An electroreduced graphene oxide-Au nanoparticles composite film was electrodeposited onto GCE surface by cyclic voltammetry. The modified ERGO-AuNPs/GCE was used to determine As(III) in 0.2 M HCI by anodic stripping voltammetry. Under optimum conditions, the detection limit was found 2.7 nM (0.20 ppb, S/N = 3) with a 12.2 µA/µM. this modified electrode successfully applied for analysis of As(III) in real water samples (Liu, et. al., 2013).

In recent study, Toor and his friends prepared Au/$Fe_3O_4$ nanocomposite modified GCE electrode for detection of arsenic. Gold (Au) nanoparticles (NPs) were synthesized by one step chemical reduction of chloroauric acid in presence of trisodium citrate and sodium borohydrate, while $Fe_3O_4$ NPs were synthesized by co-precipitation. These NPs (Au & $Fe_3O_4$) were mixed in different ratios. It was characterized SEM, Uv-Vis and FTIR. The (Au & $Fe_3O_4$) mixture was deposited on glassy carbon electrodes using simple drop casting method and characterized for their electrochemical response using $K_3FeCN_6$ as redox probe. The electrochemical response of optimized modified electrode toward As (III) was examined with cyclic voltammetry and Linear Sweep Voltammetry (LSV). The results shows that synthesized nanocomposites have very good potential towards As (III) and can be optimized further for low level detection of it (Toor, et. al., 2015)

### 1. 9 Fundamentals of Voltammetric Techniques

Historically, the branch of electrochemistry we now call voltammetry developed from the discovery of polarography in 1922 by the Czech chemist Jaroslav Heyrovsky, received the 1959 Nobel Prize in chemistry. The early voltammetric methods experienced a number of difficulties, making them less than ideal for routine analytical use. Voltammetry is one of the most important electroanalytical methods used in analytical chemistry and various industrial

processes. Voltammetry is the name of a group of electrochemical techniques. In voltammetry, information about an analyte is obtained by measuring the current as the potential is varied.

The common characteristic of all voltammetric techniques is that they involve the application of a potential (E) to an electrode and the monitoring of the resulting current (i) flowing through the electrochemical cell. In many cases the applied potential is varied or the current is monitored over a period of time (t). Thus, voltammograms are obtained as some function of E, i, and t. Voltammetric techniques are considered active techniques (as opposed to passive techniques such as potentiometry) because the applied potential does a change in the concentration of an electroactive species at the electrode surface by electrochemically reducing or oxidizing it.

The various voltammetric techniques have many analytical advantages including excellent sensitivity with a very large useful linear concentration range for both inorganic and organic species ($10^{-12}$ to $10^{-1}$ mol $L^{-1}$), a large number of useful solvents and electrolytes, a wide range of temperatures, rapid analysis times (seconds) and simultaneous determination of several analytes.

The existence of polarized electrodes was recognized and utilized in a practical way. All voltammograms are recorded with a three-electrode system consisting of a reference, counter and the working electrode.

In voltammetry, the applied potential, as calculated by the Nernst equations, controls the concentrations of the redox species at the electrode surface ($c_O{}^0$ and $c_R{}^0$). The current resulting from the redox process, (known as the faradaic current) is related to the material flux at the electrode-solution interface and is described by Fick's diffusion law. For a reversible electrochemical reaction, which can be described by Oxidation (Ox)+ne ⇆ Reduction (Red), the application of a potential E forces the respective concentrations of Ox and Red at the surface of the electrode (that is, $c^0{}_{Ox}$and $c^0{}_{Red}$) to a ratio in compliance with the Nernst equation:

$$E = E^0 + 2.3\ RT/nF \log c^0{}_{Red} / c^0{}_{Ox}$$

where, $C_O$ and $C_R$ are the concentrations of the oxidized and reduced forms of the electroactive species at the electrode surface. $E^0$ is the standart electrode potential for redox reaction.

Many different voltammetric techniques have been developed based on this current-voltage relationship, and have proven to be be extremely valuable tools for analyzing trace metals in solutions, determining complexation in organic and inorganic systems, studying kinetics and diffusion, etc. The most widely used voltammetric methods can be classified as:

A) Direct current methods: D.C. Polarography, Linear sweep voltammetry, Sampled D.C. Polarography, Hydrodynamic voltammetry

B) Pulse methods: Normal pulse voltammetry, Differential pulse voltammetry, Square wave voltammetry, Cyclic voltammetry

C) Stripping voltammetry: Anodic stripping voltammetry, Cathodic stripping voltammetry, Adsorptive stripping voltammetry

D) Alternating current methods

### 1.9.1 Polarography

Polarography is a subclass of voltammetry in which the working electrode is dropping mercure. Due to special properties of this electrode, is wide cathodic range. Polarography has been widely used for the determination of many important reducible species.

This technique was invented by J. Heyrovsky in Czechoslovakia in 1922. The excitation signal used in conventional (DC) polarography is a linearly increasing potential ramp. We can obtain the IIkovic equation for the limiting diffusion current ($I_d$)

$$I_d = k.n.F.D^{1/2}.m_r^{2/3}.t^{1/6}.c$$

Where k is a constant which includes π and the density of mercury, and with the Faraday constant (F) has been evaluated at 708 for max current and 607 for average current, D is the diffusion coefficient of the depolarizer in the medium ($cm^2/s$), n is the number of electrons exchanged in the electrode reaction, m is the

mass flow rate of Hg through the capillary (mg/sec), and t is the drop lifetime in seconds, and c is depolarizer concentration in mol/$cm^3$.

### 1.9.2 Pulse voltammetry

The potential step is the basis of pulse voltammetry. Pulse techniques were initially developed for the dropping mercury electrode, the objective being to synchronize the oulses with drop growth and reduce the capaticive current contribution by current sampling at the end of the drop life. After applying a pulse of potential, the capaticive current dies away faster than the faradaic current; thus the current is measured at the end of the pulse (Bard and Faulkner, 2001).

Normal pulse voltammetry uses a series of potential pulses of increasing amplitude. Between the pulses the electrode is kept a constant potential at which no reaction of the analytes occurs. The amplitude of pulse increases linearly with each drop. The current is measured abour 40 ms after the pulse is applied, at which time the contribution of the charging current is nearly zero. In addition, because of the short pulse duration, the diffusion layer is thinner than that of DC polarography and hence the faradaic current is increased and normal pulse polarpgraphy will be 5-10 times more sensitive than DC polarography. The limit of detection is about $10^{-7}$ to $10^{-8}$ (mol/L) for NPV technique. NPV is also a very good technique for determining diffusion coefficient.

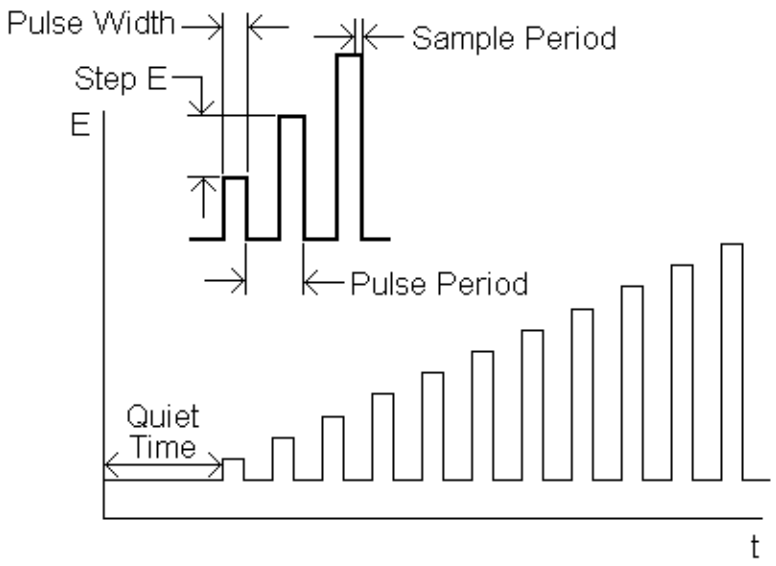


**Figure 1.13** The Schematic representation of waveform of normal pulse voltammetry.

Differential pulse voltammetry (DPV) is an extremely useful technique for measuring trace levels of organics and inorganic species. DPV is similar to NPV but with two important differences: the base potential is incremented between pulses, these increments being equal and the current is measured immediately before pulse application and at the end of the pulse: the difference between the two currents is registered.

Two current samples are taken during each drop's life time. One is taken immediately before applying the potential pulse, and the second drop is dislodged. For each cycle the first current difference value is instrumentally subtracted from the second. A plot of this current difference versus applied (dc ramp) potential produces a stepped peak-shaped incremental derivative voltammogram. (Figure 1.14 ).

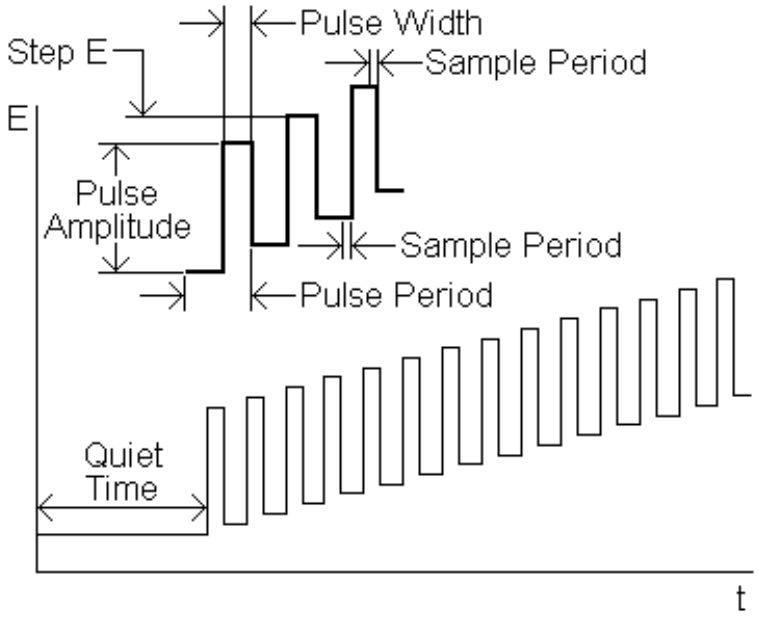


**Figure 1.14** Differential pulse voltammetry scheme of application of potentials.

### 1.9.3 Cyclic voltammetry

The theory of cyclic voltammetry has been extended to include electron transfer reactions which are described by the electrochemical rate equation. As a result of theoretical calculations made it possible to measure standard rate constants for electron transfer. The power of cyclic voltammetry results from its ability to rapidly provide considerable information on the thermodynamics of redox processes and the kinetics of heterogeneous electron transfer reactions and on coupled chemical reactions or adsorption processes.

When the scan rate is constant and the initial and switching potentials are known, one can easily convert time to potential, and the usual protocol is to record current vs. applied potential. A typical voltammogram is given in Figure 1.13b (Wang, 2000).

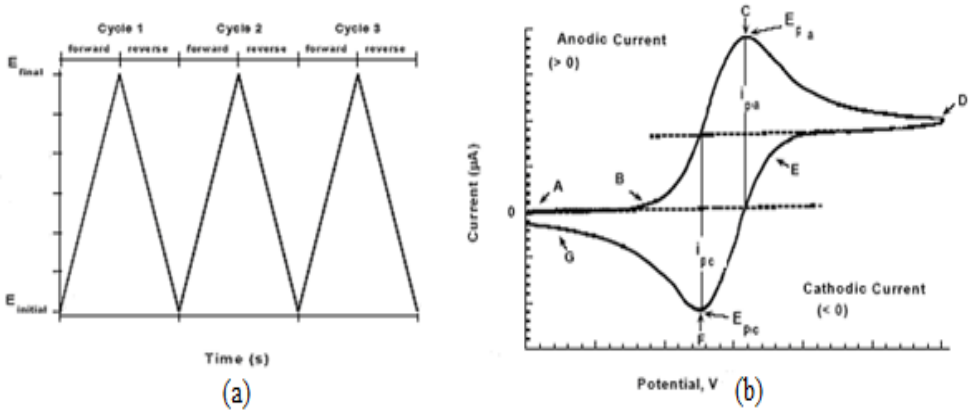


**Figure 1.15 a**) A cyclic voltammetry potential waveform with switching potentials **b)** The expected response of a reversible redox couple during a single potential cycle

In cyclic voltammetry, the system is described as “reversible” when the electrode kinetics is much faster than the rate of diffusion. The Nernst equation is the final boundary condition for a reversible system. The system is described as “irreversible” when the electrode kinetics is slower than the rate of diffusion.

For an irreversible reaction of the type one-electron, one-step reaction $Ox+e^- \leftrightarrows$ Red, linear scan and cyclic voltammetry give the same voltammetric profile, since no inverse peak emerges on changing the scan direction.

### 1.9.4 Stripping voltammetry

Stripping voltammetry involves the pre-concentration of an analyte on the surface of the working electrode before running a voltammetric scan. Pre-concentrating an analyte on the surface of the working electrode can be accomplished by applying a potential to the working electrode for a certain amount of time. The three most commonly used variations are anodic stripping voltammetry (ASV), cathodic stripping voltammetry (CSV), and adsorptive stripping voltammetry (AdSV). The amount of time the potential is held during the pre-concentration step, while consistently stirring the solution, directly affects the sensitivity of the electrochemical method, lowering the detection limits of certain analytes.

Although ASV, CSV, and AdSV have their own unique properties, these methods have two steps in common. First step, the analyte species in the sample solution is concentrated onto or into a working electrode. It is a preconcentration step that results in the high sensitivity that can be achieved. During the second

step, the preconcentrated analyte is measured or stripped from the electrode by the application of a potential scan. Any number of potential waveforms can be used for the stripping step (that is, differential pulse, square wave, linear sweep, or stairca.se). The most common are differential pulse and square wave.

### 1.9.5 Square-Wave voltammetry

Square-wave voltammetry (SWV) is one of the newest pulse techniques. (Osteryoung and Osteryoung, 1985). It was little used in the beginning owing to difficulties with the controlling electronics. With advances in instrumentation square-wave voltammetry became more popular as an important voltammetric technique (Shah, 2010). This technique consists of the application of a square-wave of constant amplitude superimposed on a staircase wave form (Figure 1.14). The current is sampled twice in each pulse period; at the reverse half cycle and the forward haft cycle. During each square-wave cycle, once at the end of the forward pulse that gives rise to the oxidative current component, and once at the end of the backward pulse that gives rise to the reduction current component. The difference between the two currents is then displayed as a function of the resultant potential. This minimizes the effect of charging current and so high sensitivity is achieved. The resulting peak-shaped voltammogram is symmetrical about the half-wave potential and the peak current is proportional to the concentration (Figure 1.15). The detection limit for SWV is $10^{-7}$ to $10^{-8}$ M. It seems that this technique will gain considerable use for the analysis of inorganic and organic species. The SWV is rapid, sensitive and consumed less analyte than the other pulsed techniques.

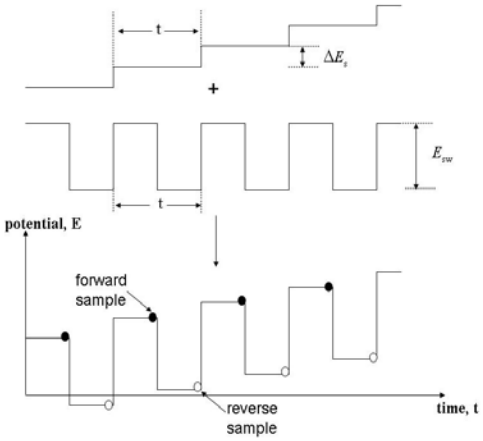


**Figure 1.16** Schematic waveform of pulses superimposed on a staircase for SWV.

## 1. 10 Surface Characterization Techniques and Aplications

The developments in material sciences have increased demand for surface characterization techniques to improve the function and quality of target surface. Characterization of surface properties is important in many research fields of material science, including heterogeneous catalysis, activity of metal surfaces, semiconductor thin-film technology, corrosion resistance and studies of the behavior and functions of biological membranes. Desired surface properties such as optical, electrical, chemical or mechanical are affected from the surface structure and composition. In this connection, also, surface characterization techniques such as scanning electron microscopy (SEM), transmission electron microscopy (TEM), scanning tunnelling microscopy (STM) and atomic force microscopy (AFM) and X-Ray Photoelectron Spectroscopy (XPS) are very usefull instruments for the understanding of catalytic activities of modified electrode surface having a important place in electrochemical studies.

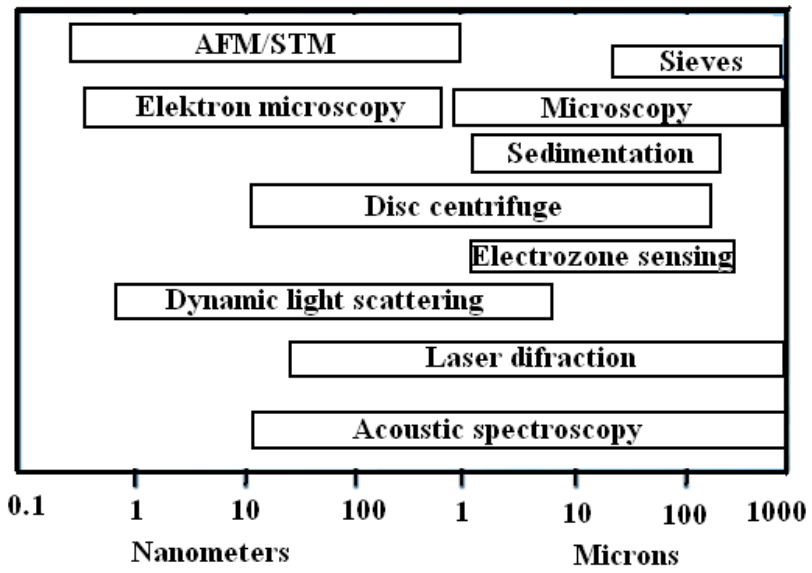


**Figure 1.17** Comparison of the imaging of many types 2D and 3D profiling and imaging instruments (Rosenauer, 2003).

### 1. 10. 1 Scanning electron microscope (SEM)

The SEM is the most importamt electron-optical instrument for the investigation of bulk specimens. An electron probe is produced by two- or three-stage demagnification of the smallest cross section of the electron beam after acceleration.

This electron probe, 2-10 nm in diameter, is scanned in a raster over a region of the specimen. The smallest diameter of the electron probe is limited by the minimum acceptable probe current, which lies in the range $10^{-12}$-$10^{-11}$ A. This value is determined by the need to generate an adequated signal-to-noise ratio and by the spherical and chromatic aberration of the finel probe-forming lens. The image is displayed on a cathode-ray tube (CRT) scanned in synchrony. The CRT beam intensity can be modulated by any of the different signals that result from the electron-specimen interactions.

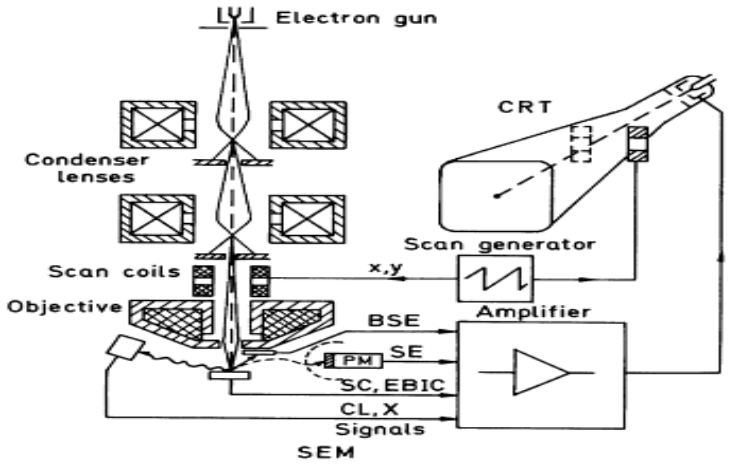


**Figure 1.18** Schematic Ray Path for a Scanning Electron Microscope (SEM)

Secondary electrons (SE) are emitted from very near the surface of the sample, with energies of a few electron volts. The SE yield increases with decreasing angle between beam and specimen surface. Backscattered electrons (BSEs) have very high energies and low yields compared to secondary electrons. The ET detector may be used to collect only BSEs by making the grid bias slightly negative so as to exclude secondary electrons. However, only those electrons travelling in line-of-sight towards the detector will contribute to the

relatively low signal and therefore images will show very strong shadowing contrast and a low signal-to-noise ratio (Kelsall, 2005).

### 1.10.2 X-Ray Photoelectron Spectroscoy (XPS)

X-Ray photoelectron spectroscopy (XPS) is well known surface analysis technique for solid materials. It gives informations about the percentage of atomic composition, empirical formula, the thickness of coated surface. XPS spectra is obtained the surface which is exposed to beam of X-ray at the same time, while measuring the kinetic energy and electrons that are emitted from the top 1-10 nm of materials.

The kinetic energy of these emitted electrons is characteristic for each element hence the position and intensity of the peaks in an energy spectrum provide chemical state and quantitative information.

**Figure 1.19** X-Ray Photoelectron Spectrometer.

When X-ray hits the sample surface, it excites the sample electrons. Normally the binding energy of sample electrons is lower than X-ray and they jump out of the sample atom. Besides, most of them are reabsorbed by the sample.

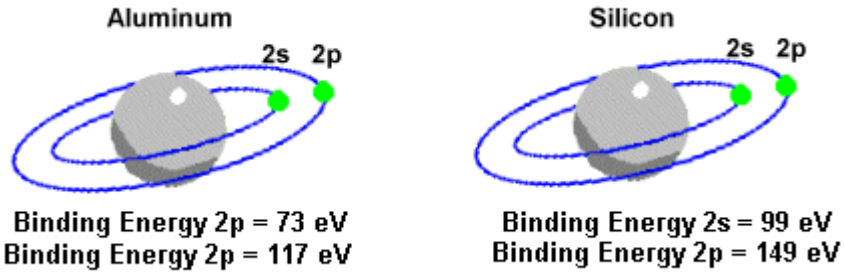


**Figure 1.20** Binding energies of different orbitals for aluminum and silicon .

As it shown in Figure 1.20, every element and their every orbital have orbitals have different binding energies. For an unknown sample, XPS spectra help recognize the element or composition.

# 2. EXPERIMENTAL

## 2. 1 Instrumentation

Electrochemical experiments were conducted with Autolab PGSTAT101 electrochemical Workstation and a conventional three-electrode system which is consist of a working electrode (GCE, Au/PPAP/GO/GCE, Au/PCR/GCE), a KCl-saturated Ag/AgCI electrode used as reference electrode and a platinium wire as the counter electrode. Cyclic and differential pulse techniques were used for the electroanalytical studies. The pH measurements were made with WTW handled 330i ion analyzer meter pH. Philips XL30SFEG, Micro Tech Polar 10 spatter Coater Scanning Electron Microscopy and Q-Scope Atomic Force Microscopy were used for the characterization of bare and modified electrode surfaces. As well as, Bandelin Sonorex model ultrasonic bath was used for preparing of solutions and cleaning the electrodes.

## 2. 2 Reagents and Solutions

Graphene oxide (GO) was synthesed in the laboratory conditions. p-Aminophenol (Fluka), acetic acid ($CH_3COOH$) (Merck), o-phosporic acid (Merck), chloroauric acid ($H_2AuCI_6$), sodium hydroxide (NaOH) (Riedel de

Haen), alimuna ( $Al_2O_3$) (Baikowski), sodium dodecil sulphate ($C_{12}H_{25}NaOsO_4S$) (SDS), cresol red, hyrochloric acid (HCI) (Merck), sodium arsenit ($NaAsO_2$) (Merck), nickel sulphate ($NiSO_4$) (Merck), copper sulphate ($Cu(SO_4)_2.3H_2O$) (Merck), chloroplatinic acid ($H_2PtCI_6$), N,N-dimethyl formamide (DMF) (Merck) (Sigma-Aldrich), graphite (Sigma Aldrich) were used in experimental studies.

As(III) stock solutions were prepared by making appropriate dilutions of the As(III) stock solution (0.1 M) with 0.1 M HCl. Standard solutions were also prepared freshly before use and they were dissolved by ultrapure water Millipore Milli Q system (18.2 M Ω).

Buffer solutions were prepared from acetic acid/sodium acetate, sodium dihydrogen phosphate/disodium monohydrogen phosphate (PBS). Supporting electrolyte was purged with a $N_2$ stream prior to each measurement.

## 2. 3 Methods

### 2. 3. 1 Pre-conditioning of GCE

Prior to experiments, the GCE was polished with different grade of alumina powders (0.05-3 micron) on a synthetic cloth and then sequentially sonicated in ultrapure water and anhydrous ethanol for 3 minutes. Then, the GCE was electrochemically cleaned by keeping 10 minutes at constant potential at 1.0V.

### 2. 3. 2 Preparation of graphene oxide

2 gram graphite powder and 17 gram $NaClO_3$ were taken into a glass beaker which was kept in an ice bath then 50 mL concentrated $HNO_3$ was added. This mixture was stirred for 24 hour in the room temperature with magnetic stirrer. The mixture was decanted with 1 L pure water to increase the pH value. To make it easier, ultra pure water's pH was adjusted 8 with 0.1 M NaOH. The mixture was separated falcon tubes, alkaline water was added and santifigurated until neutralize. Finally, mixture was evaporized at $110^0$ C in oven. Dried powder was

called graphene oxide. 50 mg graphene oxide powder and 5 mL DMF was mixed and stored room temperature to use it next experiments.

### 2. 3. 3 Preparation of graphene oxide modified GCE

A 15 µL graphene oxide suspension was injected on the pre-conditioned bare GCE surface. The solvent (DMF) of the suspension on the GCE surface was evaporated at $60^{o}$ C for more than one hour.

### 2. 3. 4 Preparation of Poly(p-aminophenol) film modified GCE

Electrochemical polymerization of p-aminophenol was carried out in 0.5 M $HClO_4$ solution containing 5 mM SDS and 5 mM p-aminophenol by cyclic voltammetry. The polymerization voltammograms were obtained by repetitive seven number of potential cycles from -0.5 to 2.0 V vs. Ag/AgCI (sat. KCI) at a scan rate of 100 mV/s.

### 2. 3. 5 Preparation of poycresol red film modified GCE

Electrochemical polymerization of polycresol red was performed in 0.1 M HCI by cyclic voltammetry. The polymerization voltammograms were obtained by repetitive 20 potential cycles from -1.0 to 2.0 V using Ag/AgCI (sat.KCI) and platinium wire at a scan rate of 100 mV/s.

### 2. 3. 6 Preparation of Au, Pt, Cu, Ni metal nanoparticles modified GO/GCE, GO/PPAP/GCE, PPAP/GO/GCE and PCR/GCE

The metal nanoparticles were electrochemically deposited on the GO/GCE, PPAP/GO/GCE, GO/PPAP/GCE and PCR/GCE by cyclic voltammetry (CV). For GO/PPAP/GCE and PPAP/GO/GCE modification, Au nanoparticles deposited by CV scanning between -1.2 and 0.2 V in $HAuCl_4$ with a scan rate of 50 mV/s for 20 cycles respectively. Also, for PCR/GCE modification, Au nanoparticles deposited by CV scanning between -1,2 and 0,2 V in $HAuCl_4$ with a scan rate of

50 mV/s for 15 cycles. For Au/PPAP/GO/GCE; Ni, Cu, and Pt nanoparticles were deposited onto the PPAP/GO/GCE before the deposition of Au nanoparticles. Cu nanoparticles deposited between -1,2 and 0.00 V and Ni nanoparticles deposited between 0.00 and 0.80 V by cyclic voltammetry. The bimetallic particles effect was also examined with Au-Ni, Au-Cu and Au-Pt. The obtained metal nanoparticles modified electrodes were ready for use after the final wash with ultra pure water.

### 2. 3. 7 Preparation of arsenic samples

Mineral water sample was purchased at local stores. First of all, pH was checked. It was 7,4. Because of optimum pH is 1.0 for As determination, it was adjusted 1.0 with concentrated HCl.

## 3. RESULTS AND DISCUSSION

This thesis was composed of two different studies. The first is synthesis of graphene oxide and used for preparation of working electrode material, its modification by using polymer (p-Aminophenol) and differet kind of metal nanoparticles for arsenic detection.

Second chapter was developed an metal nanoparticles modified polycresol red film electrodes for arsenic detection.

### 3. 1 Preparation of Poly(p-aminophenol) Film Modified GCE

Figure 3.1 shows the consecutive cyclic voltammograms of p-aminophenol (PPAP) for electropolimerization on GO modified GCE surface in 0.5 M $HClO_4$ solution containing 5mM SDS and 5mM p-aminophenol by cycling the potential from -0.5 to 2 V vs. Ag/AgCl (sat.KCl) at a scan rate of 100 mV/s for 7 cycles . An irreversible oxidation peak was appeared at 1.60 V for p-AP without the

corresponding cathodic processes in the reverse scan. On the other hand, an oxidation and a reduction peaks were observed at around +0.65 and +0.30 V respectively. The generation of the peaks might be attributed to the intermediate species during the oxidation process of the AP (Ojani, 2009) .The peak current increasing with cycles of CV indicates that, an electropolymerization takes place and increase the content of polymer on the GO/GCE surface. Increasing of the irreversible oxidation peak current showed the increasing of polymer omount on the surface of the electrode by consecutive potential cycles showing electropolymerization takes place on the GO/GCE surface. The oxidation of p-amino phenol can be easily occured on the electrode surface in the presence of SDS which was leading more monocation radical's formation on the electrode surface.

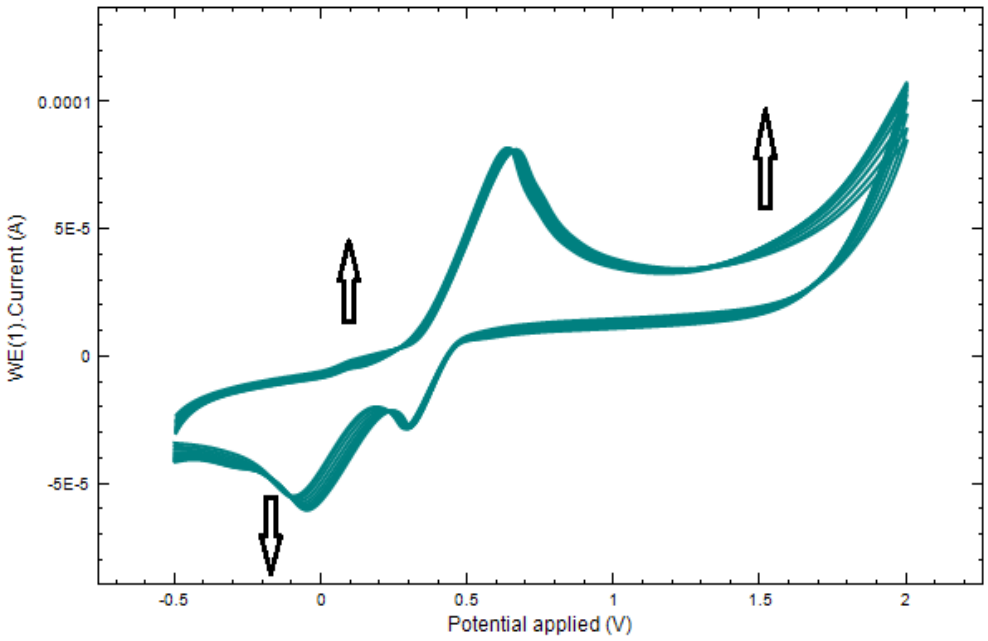


**Figure 3.1** Cyclic voltammogram of p-Aminophenol electropolymerization in a 5.0 mM p-Aminophenol monomer/ 0.5 M $HClO_4$ solution on GCE in the presence of 5.0 mM SDS at a scan rate of 100 $mVs^{-1}$. The arrows indicate the trends of current during CVs.

### 3. 2 Deposition of Au Nanoparticles on PPAP/GO/GC Electrode From Chloroauric Acid Solution

Electrochemically deposition of Au nanoparticles on the PPAP/GO/GCE surface was carried out from 3 mM chloroauric acid  0.1 M HCl solution mixture by concecutive potential scans from -1.10 to 0.40 V (Figure 3.2). Two reduction

peaks were appeared at 0.04V and -0.25 V for concecutive reduction of Au species on the electrode surface during the cathodic current- potential scan while observing of an oxidation peak at -0.10 V on anodic current-potential scan.

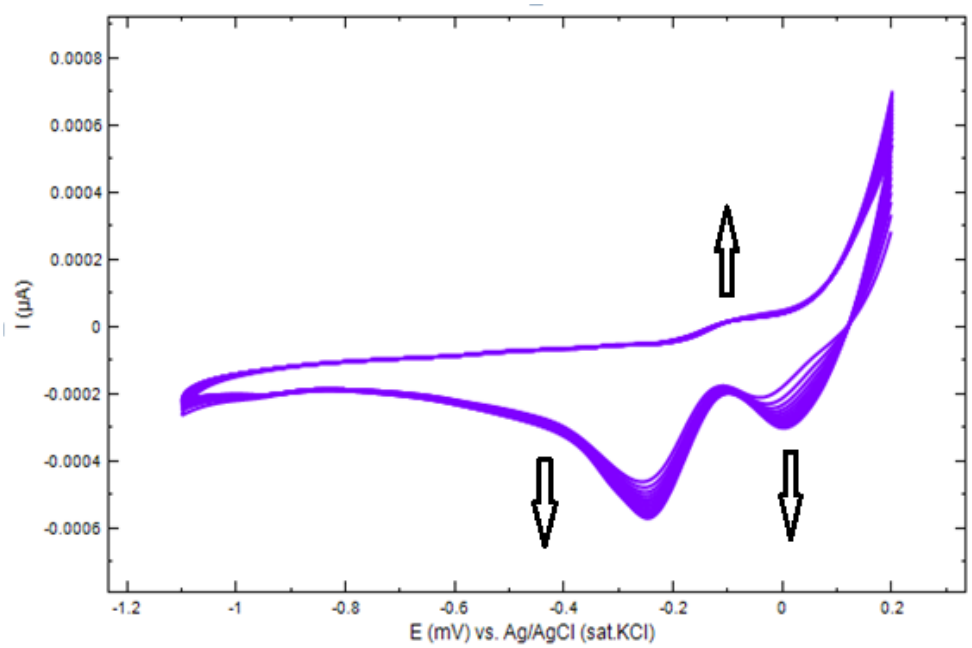


**Figure 3.2** Au deposition on PPAP/GO/GCE, at 50 mV/s for 15 cycles in 3 mM $HAuCl_4$.

It is easily seen from the CV results that, Au nano particles formed with Au (III) ions reductions at -0.25 V and oxidation at -0.1 V. Increasing of both reduction and oxidation peaks by increasing the cycle numbers of current potential showed that nano Au particles were formed on the electrode surface.

### 3. 3 Voltammetric Behaviour of Cu/PPAP/GO/GCE, FPt/PPAP/GO/GCE and Ni/PPAP/GO/GCE.

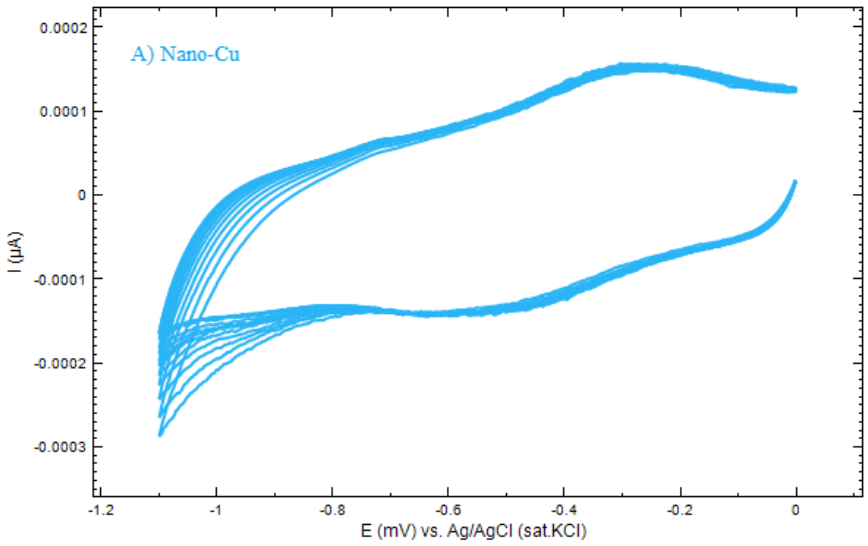


**Figure 3.3** Cu deposition on PPAP/GO/GCE, between -1,5 and 0.0 V at a scan rate 50 mV/s.

CV results showed that, Cu nanoparticles gives reduction peak at - 0,5 V and oxidation peak at + 0.5 V. Increasing the cycle numbers increased the current of reduction and oxidation peak.

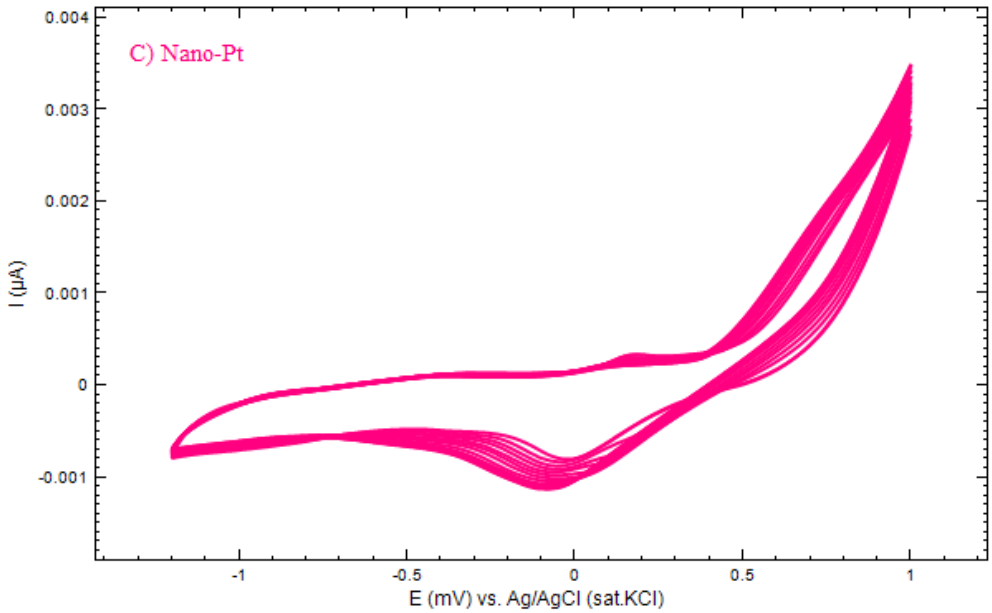


**Figure 3.4** Pt deposition on PPAP/GO/GCE, between -1.2 and 1.0 V at a scan rate 50 mV/s.

CV results of Pt nanoparticles showed that reduction peaks of Pt were at –1.0 V and two oxidation peaks of Pt nanoparticles were at 1.2 V and 0.8 V. As increasing the cycle numbers of Pt, reduction and oxidation peak current increased.

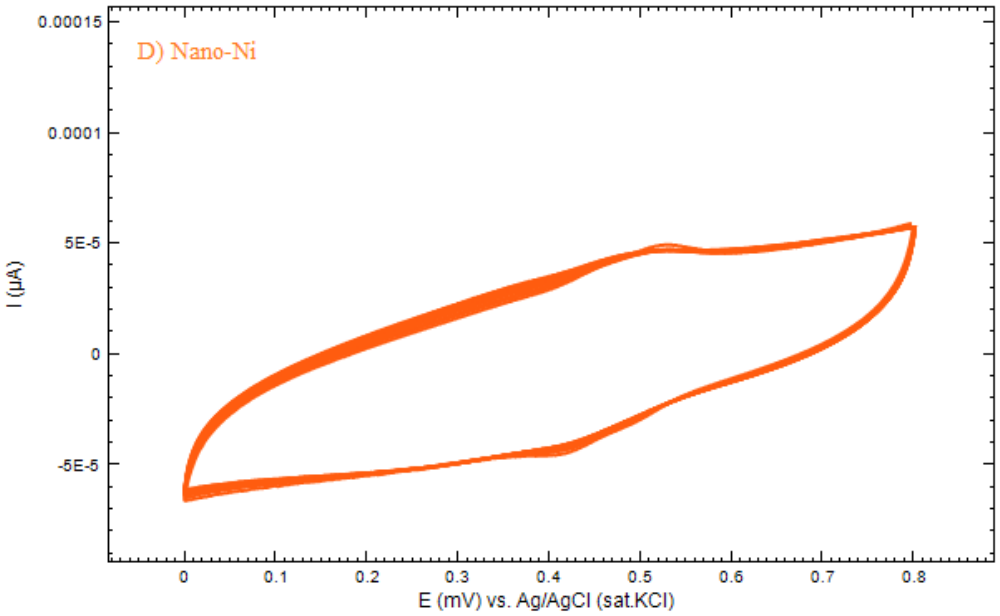


**Figure 3.5** Ni deposition on PPAP/GO/GCE, between 0.0 and 0.8 V at a scan rate 50 mV/s.

As it seen in the figure that, reduction peaks of Ni nanoparticles were at 0.42 V and oxidation peaks of Ni nanoparticles were at 0.5 V.

### 3.4. The Behaviour of Arsnic Oxidation on Au/PPAP/GO/GCE, Au/Pt/PPAP/GO/GCE, Au/Cu/PPAP/GO/GCE, Au/Fe/PPAP/GO/GCE and Au/Ni/PPAP/GO/GCE

To see the effect of different metal nanoparticles for electrochemical oxidation of arsenic; Pt, Cu, Fe and Ni nanoparticles (10 cyc) were deposited at the top of PPAP/GO/GCE electrode and then 15 cyc Au nanoparticles were deposited. $8.10^{-6}$ M As(III) response were calculated and compared with only Au/PPAP/GO/GCE electrode. As it seen in the Figure 3.6, the best response was taken from Au/PPAP/GO/GCE electrode and this electrode was chosen for working electrode.

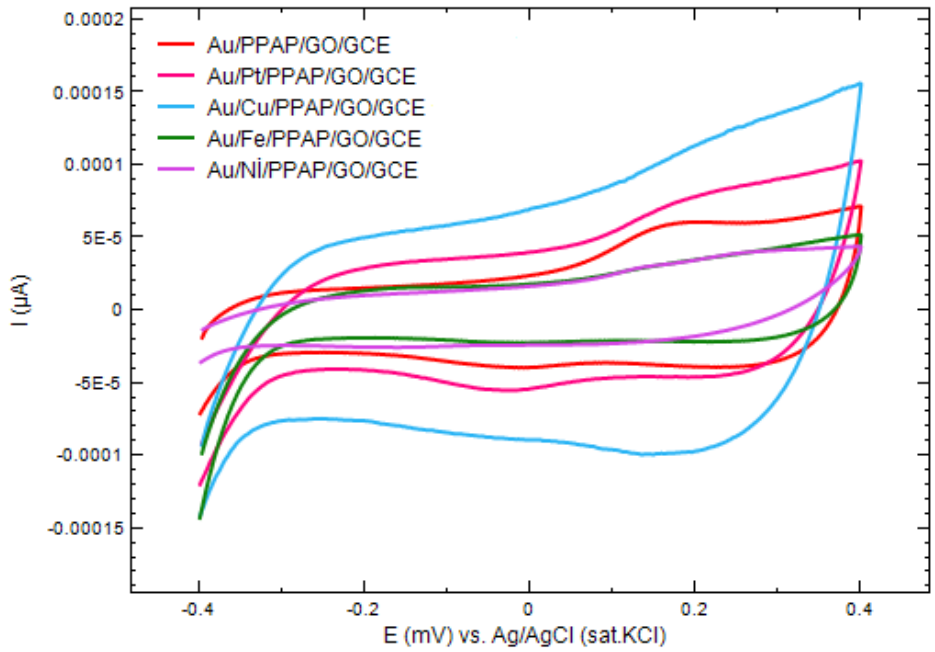


**Figure 3.6** The cyclic voltammetric behaviour of As(III) on Au/PPAP/GO/GCE, Au/Pt/PPAP/GO/GCE, Au/Cu/PPAP/GO/GCE, Au/Fe/PPAP/GO/GCE and Au/Ni/PPAP/GO/GCE.

## 3. 5 Surface Characterization of GO/GCE, PPAP/GO/GCE and Au/PPAP/GO/GCE

The surface morfology of GO/GCE, PPAP/GCE, PPAP/GO/GCE and Au/PPAP/GO/GCE were characterized by SEM. Figure 3.7 shows the image of graphene oxide modified GCE surface. As it seen in the Figure, the surface is not smooth. This rough area increases the conductivity of GCE because of increasing the active surface area.

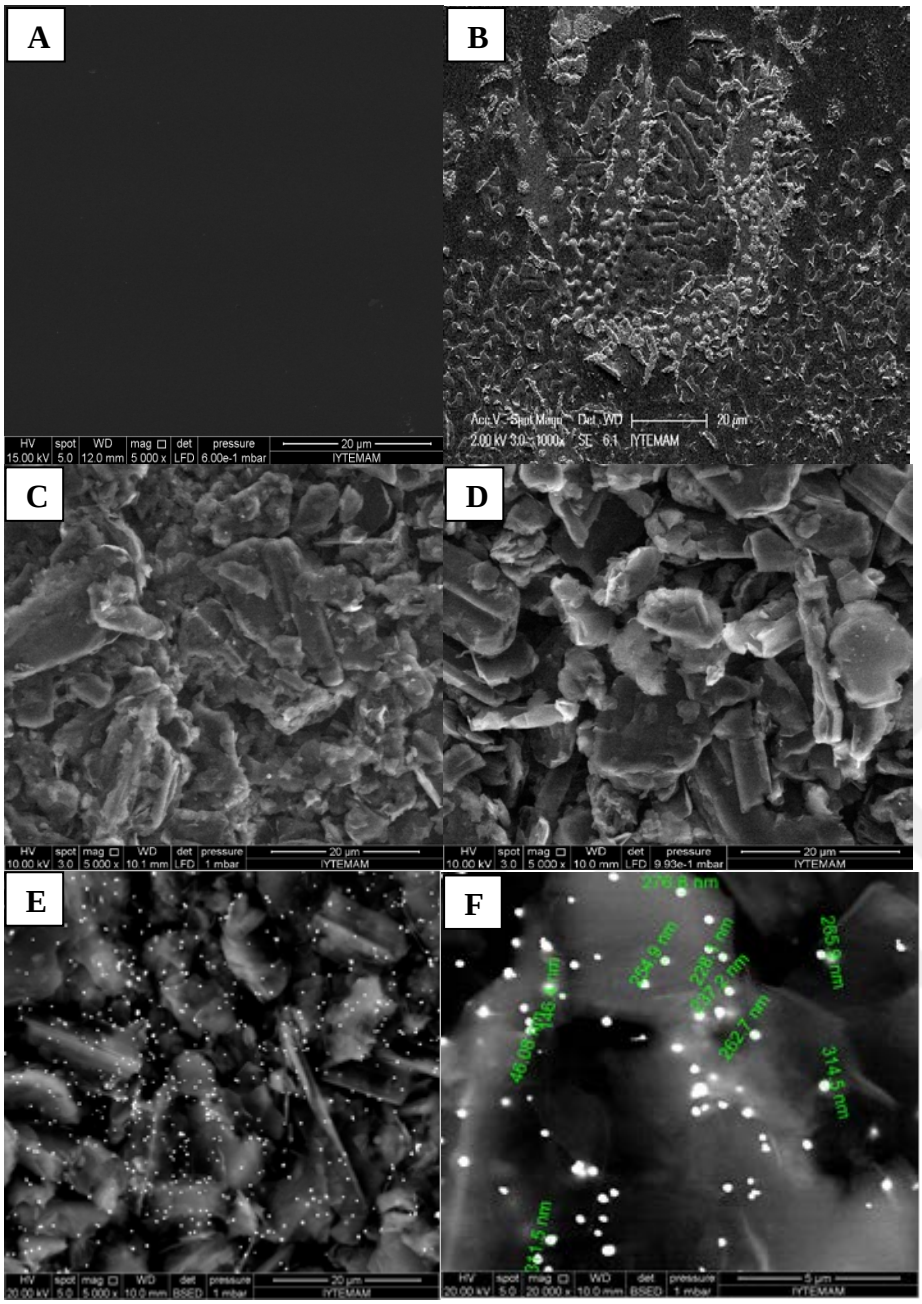


**Figure 3.7** SEM images of A) Bare GCE, B) PPAP/GCE, C) GO/GCE, D) PPAP/GO/GCE, E) and F) Au/PPAP/GO/GCE.

In Figure 3.7-A, as it is expected, the SEM image of smooth and homogeneous surface refers to the bare glassy carbon electrode. Compared with bare glassy carbon electrode surface, the morphology of the PPAP on GC electrode showed in Figure 3.7-B almost homogeneously distributed porous polymer surface. This porous polymer allow easily electrodeposited of metal nanoparticles on electrode surface. Figure 3.7-C shows the SEM images of graphene oxide modified GCE, as it seen in figure the surface is porous. In Figure

3.7-D, polymer film (PPAP) is modified GO/GCE electrode. Comparing to the Figure 3.7-C, it can be easily understand that the surface is more bright because of polymer film an homogenously spreaded to the graphene oxide surface. Figure 3.7-E and 3.7-F, show the SEM images of Au nanoparticles modified PPAP/GO/GCE surface. As it can be seen in the figure, shining small dots show the Au nanoparticles on the modified electrode surface. The surface structure was extremely different with the height of 311.5 nm suggested that Au nano particules deposited top of the polymer and graphene oxide GCE surface.

### 3. 6 Voltammetric Behaviour of As(III) at Bare and Modified Electrodes

Voltammetric behaviour of As(III) was investigated at different electrodes in 0.1 M HCl solution in Figure 3.8.

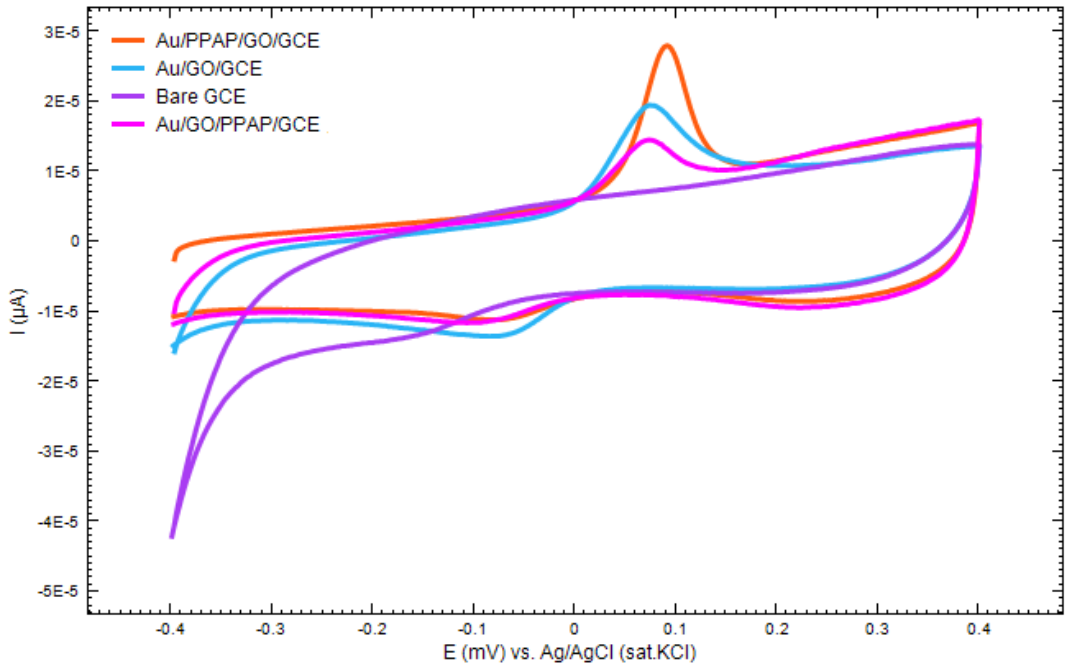


**Figure 3.8.** Cyclic voltammetric behaviors of $5.10^{-5}$ M As(III) in 0.1 M HCl on bare GCE, Au/GO/GCE, Au/GO/PPAP/GCE and Au/PPAP/GO/GC electrodes.

Figure 3.8 shows the cyclic voltammetric behaviors of $5.10^{-5}$ M As(III) in 0.1 M HCl on bare GCE, Au/GO/GCE, Au/GO/PPAP/GCE and Au/PPAP/GO/GC electrodes in the potential scaning range of – 0.4 V – (+ 0.4 V). There was no any electrochemical signal on bare GCE but a well defined irreversible oxidation peaak was apperaed at 0.05 V on Au/GO/GCE, at 0.06 V on

Au/GO/PPAP/GCE and at 0.09 V on Au/PAP/GO/ GCE. The highest peak current and small peak width was obtained on Au/PPAP/GO/GCE for As oxidation.

On the other hand, substantial increases in the peak current was also observed at Au nanorticles modified PPAP/GO/GCE. Using PPAP after GO/GCE increased the peak current more than using GO after PPAP/GCE.

### 3. 7 Optimization Studies of Arsenic

### 3. 7. 1 Effect of supporting electrolyte pH on cyclic voltammetric behaviour of As at Au/PPAP/GO/GCE.

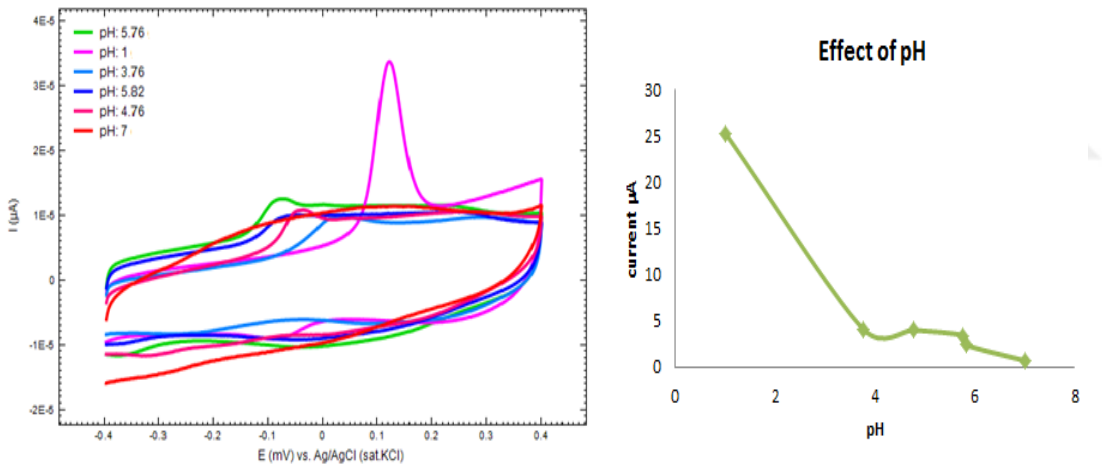


**Figure 3.9** Cyclic voltammograms for $5.10^{-5}$ M As(III) at Au/PPAP/GO/GCE in various pH (1.0 to 7.0) at a scan rate of 100 mV/s.

The effect of pH on the peak currents of electrochemical oxidation of As were investigated for $5.10^{-5}$ M As (III) at Au/PPAP/GO/GCE (Figure 3.10) by CV techniques in the pH range of 1.0-7.0. These results indicated that electrochemical investigation and determination of As(III) should be study in acidic solutions.

**Table 3.1.** The effect of pH on cyclic voltammetric behaviour of As(III) at Au/PPAP/GO/GCE.

| pH | E (mV) | İ (µA) |
|---|---|---|
| **1** | **120 mV** | **25.27** |
| 3.76 | 17 mV | 4.12 |
| 4.76 | -43 mV | 4.0 |
| 5.76 | -82 mV | 3.43 |
| 5.82 | -82 mV | 2.4 |
| 7 | -102 mV | 0.7 |

While pH is increasing, peak potential shifted negative values and peak current decreased respectively. Therefore HCl was chosen for supporting electrolyte.

### 3. 7. 2 Optimization of HCl concentration

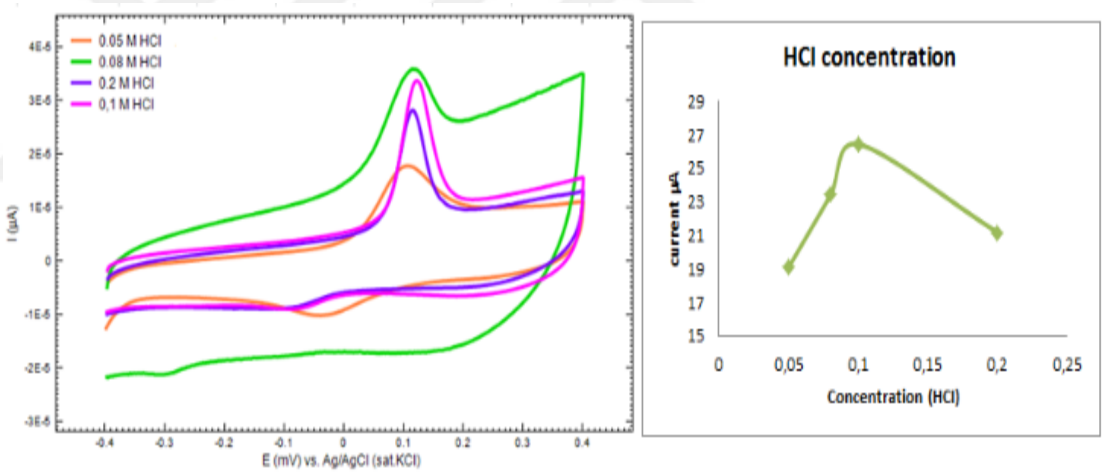


**Figure 3.10** Cyclic voltammograms of As(III) in different HCI concentration at Au/PPAP/GO/GCE.

To obtain optimum HCl concentration for As(III) voltammetric determination, the concentration was changed in the range between 0.05 -0.2 M. CV results shows that, the highest arsenic oxidation peak current obtained in 0.1 M HCl supporting electrolyte in the presence of $5.10^{-5}$ M As (III) at Au/PPAP/GO/GCE electrode. Table 3.2 indicates that arsenic oxidation peak current and potential in different HCI concentrations.

**Table 3.2** The effect of HCI concentration on As(III) cyclc voltammetric behaviour.

| $C_{HCI}$ | E (mV) | İ (µA) |
|---|---|---|
| 0.05 M | 85 | 19.11 |
| 0.08 M | 100 | 23.40 |
| **0.10 M** | **112** | **26.43** |
| 0.20 M | 115 | 21.17 |

### 3. 7. 3 Optimization of p-aminophenol concentration

Figure 3.11 demostrated the effect of aminophenol concentration on the voltammetric behaviour of $5.10^{-5}$ M As(III) solution in 0.1 M HCI. Variation of aminophenol concentration caused desirable change on peak current of arsenic and the optimum peak characteristics (24.15 µA and 127 mV) were obtained for $1.10^{-3}$ M of aminophenol monomer. Consequently, it was chosen optimum monomer concentration $1.10^{-3}$ M for preparation Au/PPAP/GO/GCE for further studies.

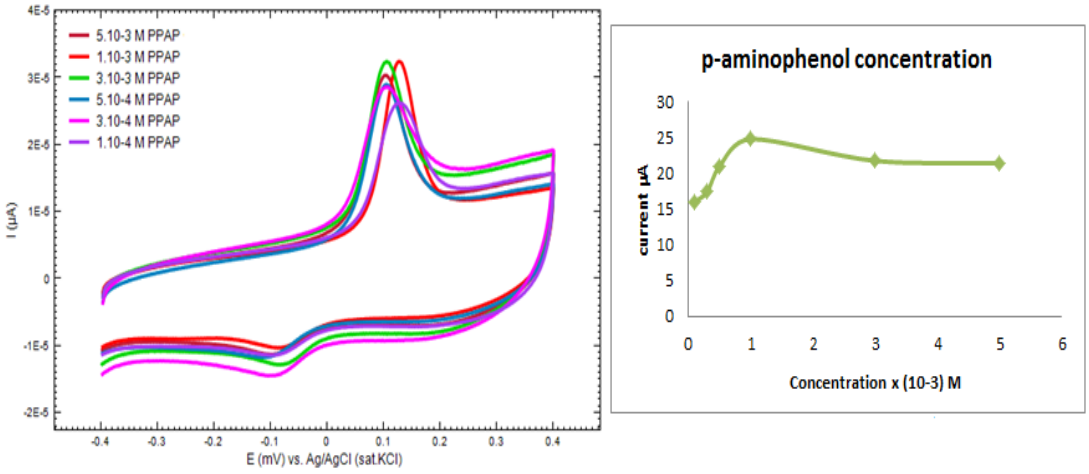


**Figure 3.11** Effect of p-aminophenol concentration on arsenic

**Table 3.3** The effect of p-aminophenol concentration on As(III) cyclic voltammetric behaviour.

| $C_{p\text{-aminophenol}}$ | E (mV) | İ (µA) |
|---|---|---|
| $5.10^{-3}$ M | 103 | 21.40 |
| $3.10^{-3}$ M | 103 | 21.73 |
| **$1.10^{-3}$ M** | **127** | **24.15** |
| $5.10^{-4}$ M | 103 | 21.00 |
| $3.10^{-4}$ M | 103 | 17.45 |
| $1.10^{-4}$ M | 127 | 16.00 |

As can be followed from Table 3.3., the best results were obtained by using $1.10^{-3}$ M aminophenol by means of oxidation peak potential and current of arsenic.

### 3. 7. 4 Optimization of Poly(p-aminophenol) cycle number

Figure 3.13 demonstrated the effect of potential scan cycle number on the electropolimerizatation of p-aminophenol on GO modified GCE for $5.10^{-5}$ M As(III) in 0.1 M HCI solution. Figure 3.12 inset shows the oxidation peak currents for arsenic increased from 3 to 7 cycles of aminophenol and then decreased for higher cycle numbers. This decrease can be explained to increase the electrode resistance and capaticance by increasing the polymer content on the GO/GCE surface. For future studies, seven cyclic numbers was choosen as optimum value.

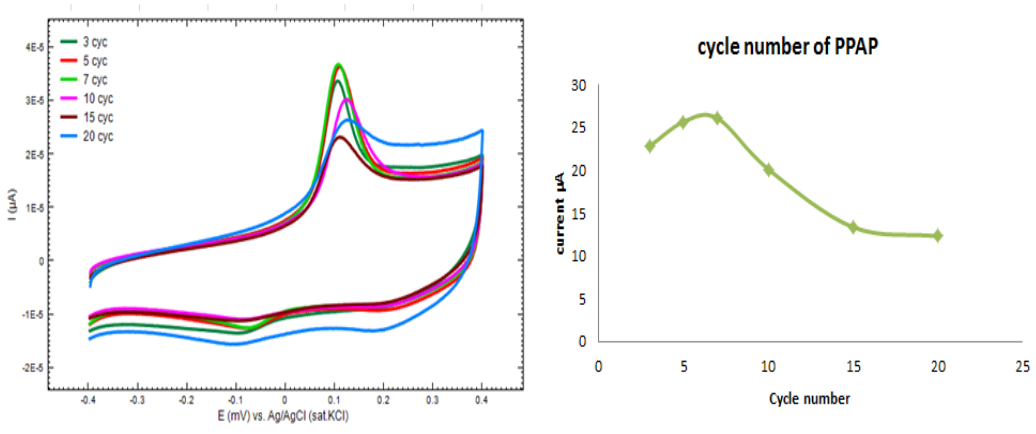


**Figure 3.12** The effect of poly(p-aminophenol) cycle number of arsenic

**Table 3.4** The effect of poly(p-aminophenol) cycle number of arsenic

| Cycle number of p-AP | E (mV) | İ (µA) |
|---|---|---|
| 3 | 105 | 22.84 |
| 5 | 107 | 25.67 |
| **7** | **107** | **26.07** |
| 10 | 125 | 20.13 |
| 15 | 124 | 13.37 |
| 20 | 125 | 12.31 |

Table 3.4 shows that peak potential shifted positive values by increasing cycle number of p-AP.

### 3. 7. 5 The Influence of chloroauric acid concentration for Au Nanoparticles formation and their effect on voltammetric behaviour of arsenic

The effect of chloroauric acid concentration during the Au nanoparticles formation on the PPAP/GO/GCE and their effect on arsenic oxidation reaction was investigated in the concentration range of $3.10^{-3}$–$10^{-4}$ M for 10 cycles of current potentials scan. Table 3.5 shows the values of current and potential by increasing the $AuCI_4^-$ concentrations for arsenic oxidation.

The voltammetric behaviour of $10^{-5}$ M As(III) in 0.1 M HCI was studied on Au/PPAP/GO/GCE by varying chloroauric acid concentration in figure 3.13. The maximum peak current was obatined at Au/PPAP/GO/GCE which prepared with $3.10^{-3}$ M chloroauric acid concentration, therefore, it was chosen for further studies.

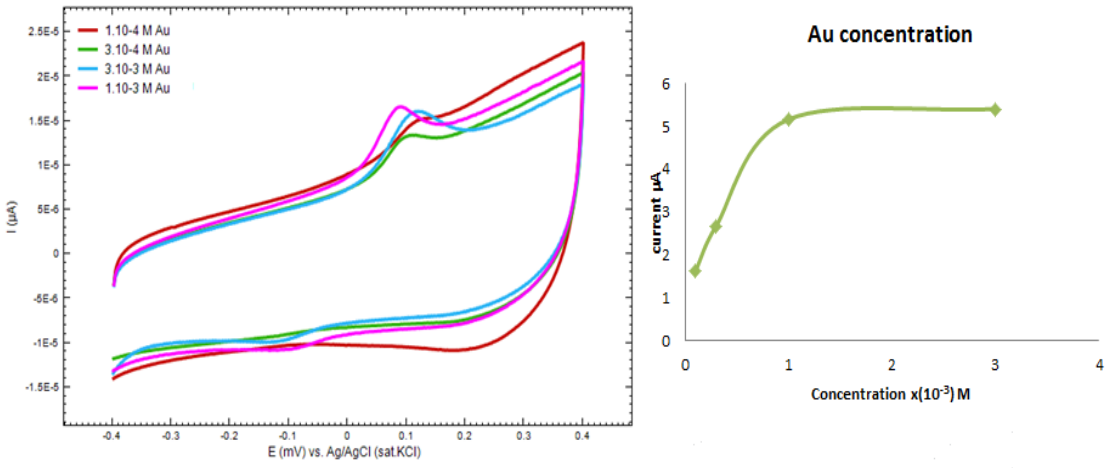


**Figure 3.13** The effect of $AuCI_4^-$ concentrations on As(III) cyclic voltammetric behaviour.

**Table 3.5** The effect of $AuCI_4^-$ concentrations of the electrooxidation of arsenic

| C $_{AuCI_4^-}$ (M) | E (mV) | İ (µA) |
|---|---|---|
| **$3.10^{-3}$** | **110** | **5.40** |
| $1.10^{-3}$ | 83 | 5.16 |
| $3.10^{-4}$ | 98 | 2.68 |
| $1.10^{-4}$ | 117 | 1.62 |

### 3. 7. 6 The influence of Au nanoparticles cycle number on arsenic oxidation

Au nanoparticles ($3.10^{-3}$ M) modified PPAP/GO/GC electrodes prepared with different coverage depending on the cycle number of CV that was examined by changing the cycle numbers Au deposition to obtain most appropriate surface toward arsenic oxidation. When the CV of $10^{-5}$ M As (III) voltammetric in 0.1 M HCl was compared for modified electrodes, which obtained under the same experimental conditions, 20 cycles gold deposition on PPAP/GO/GCE surface obviously provide the desirable change in peak current (Fig. 3.14).

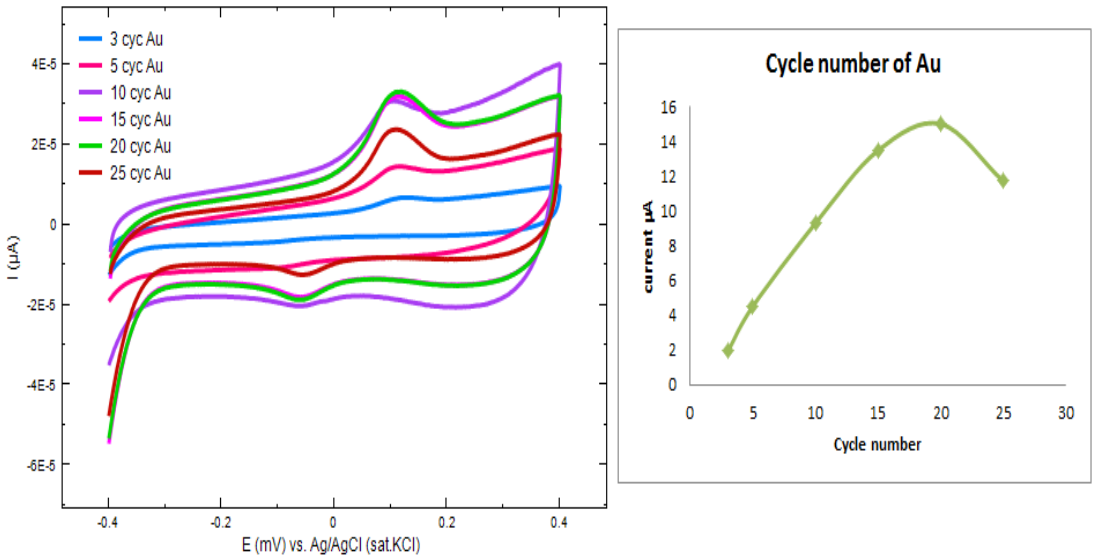


**Figure 3.14** Cyclic voltammograms for As(III) at different cycle number of Au ($3.10^{-3}$ M) particle deposition.

**Table 3.6** The effect of cycle number of Au the for electrooxidation of arsenic.

| Cycle number of Au | E (mV) | İ (µA) |
|---|---|---|
| 3 | 117 | 1.94 |
| 5 | 105 | 4.53 |
| 10 | 98 | 9.30 |
| 15 | 120 | 13.48 |
| **20** | **107** | **15.01** |
| 25 | 107 | 11.71 |

As it seen on Table 3.6 above, peak current and peak potential values are given.

### 3. 7. 7 Scan rate study at $Au_{(20cyc)}$ -PPAP/GO/GCE

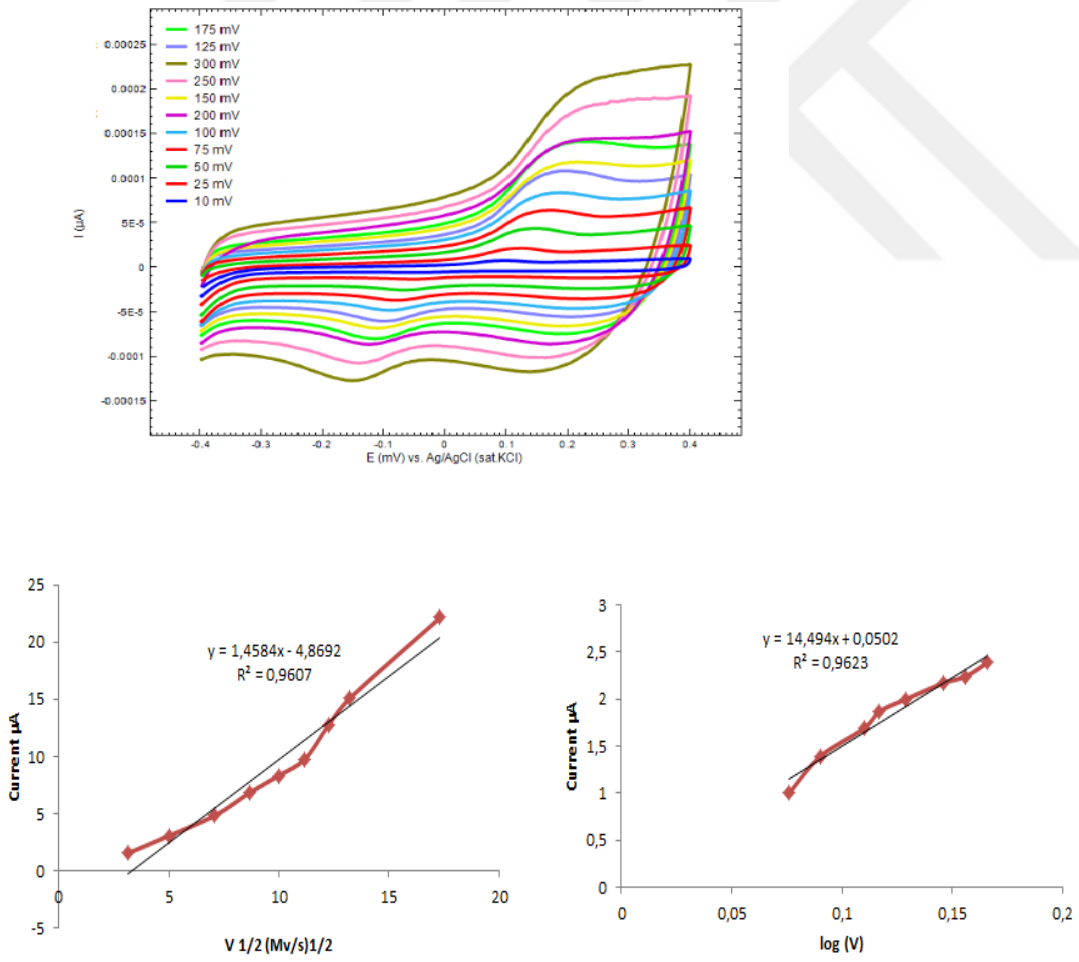


**Figure 3.15** Cyclic voltammogram behaviour of As(III) on $Au_{(20cyc)}$ -PPAP/GO/GC electrode at different scan rates. ( 10, 25, 50, 75, 100, 125, 150, 175, 200, 250, 300 mV/s ).

In order to confirm the electrode behaviour on the oxidation of arsenic, a series of cyclic volatmmograms were recorded at $Au_{(20cyc)}$-PPAP/GO/GC electrode by varying potential scan rate. The oxidation peak current increased linearly with the square root of the scan rate (Figure 3.15), suggesting that arsenic oxidation reaction at this modified electrode was controlled by diffusion. The oxidation peak potential of arsenic shifted positive values with increasing the scan rate, indicating that the electrode reaction was irreversible.

### 3. 7. 8 Differential pulse voltammetric determination of arsenic

Determination of arsenic is critical importance in human health especially in tap water. Since differential pulse voltammetry has a much current sensitivity and better separation the analyte peaks than CV, the electroanalytical technique was used for determination of arsenic.

Limit of detection values were calculated from (S/N:3) and calibration curves. The average value of backgroud current estimated from 7 different voltammograms.

Initial studies with DPV was focused on the electrochemical respons of increasing As(III) concentration on Au/PPAP/GO/GCE in 0.1 M HCI. Electrode response was given in Figure 3.16. The arsenic oxidation was observed between 0,07 and 0.12 V on Au/PPAP/GCE. The electrochemical respons of arsenic was increased linearly with the increasing of arsenic concentration in the range of $10^{-6}$ M – $2.10^{-5}$ M at Au/PPAP/GCE. LOD was calculated as $4.0x10^{-7}$ M (S/N =3). The linear regression equations of Au/PPAP/GCE could be expressed as $R^2$= 0.9964.

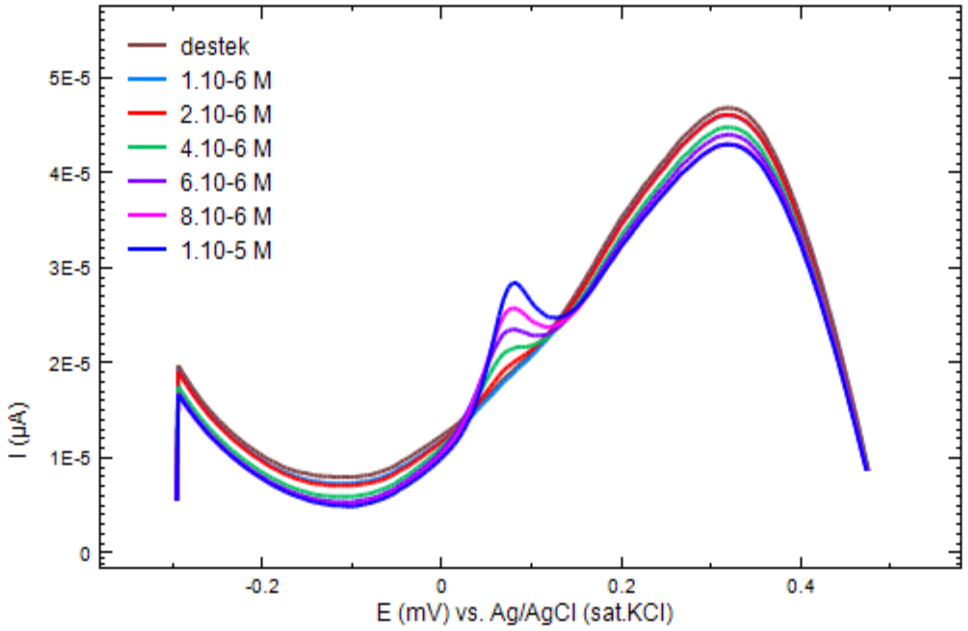


**Figure 3.16** Differential pulse voltammograms at Au/PPAP/GO/GCE for increasing concanterations of arsenic in 0.1 M HCI, with scan rate 20 mV/s and pulse amplitude 50 mV.

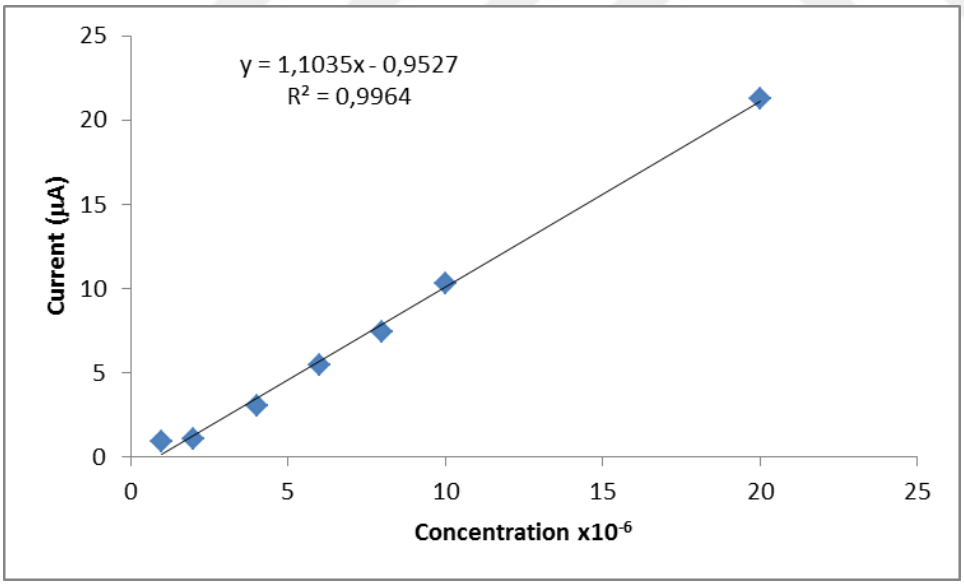


**Figure 3.17** Corresponding calibration curve of increasing arsenic concentrations in 0.1 M HCI. Arsenic concentrations: $10^{-6}$, $2.10^{-6}$, $4.10^{-6}$, $6.10^{-6}$, $8.10^{-6}$, $10^{-5}$, $2.10^{-5}$ M

**Table 3.7** As concentration range, potential and current.

| C (M) As | E (mV) | İ (µA) |
|---|---|---|
| $1.10^{-6}$ | 67 | 0.93 |
| $2.10^{-6}$ | 67 | 1.09 |
| $4.10^{-6}$ | 67 | 3.06 |
| $6.10^{-6}$ | 67 | 5.49 |
| $8.10^{-6}$ | 72 | 7.45 |
| $1.10^{-5}$ | 77 | 10.30 |
| $2.10^{-5}$ | 92 | 21.29 |

### 3. 7. 9 Sample analysis

The method was applied to the mineral water samples which could be contain arsenic. Because of mineral water's neutral media, pH was adjusted to 1 with 5 M HCI aqueus solution. Figure 3.18 shows the standart addition DP voltammograms obtained from mineral water sample. As it can be seen from the figure, standart addition graph was constructed.

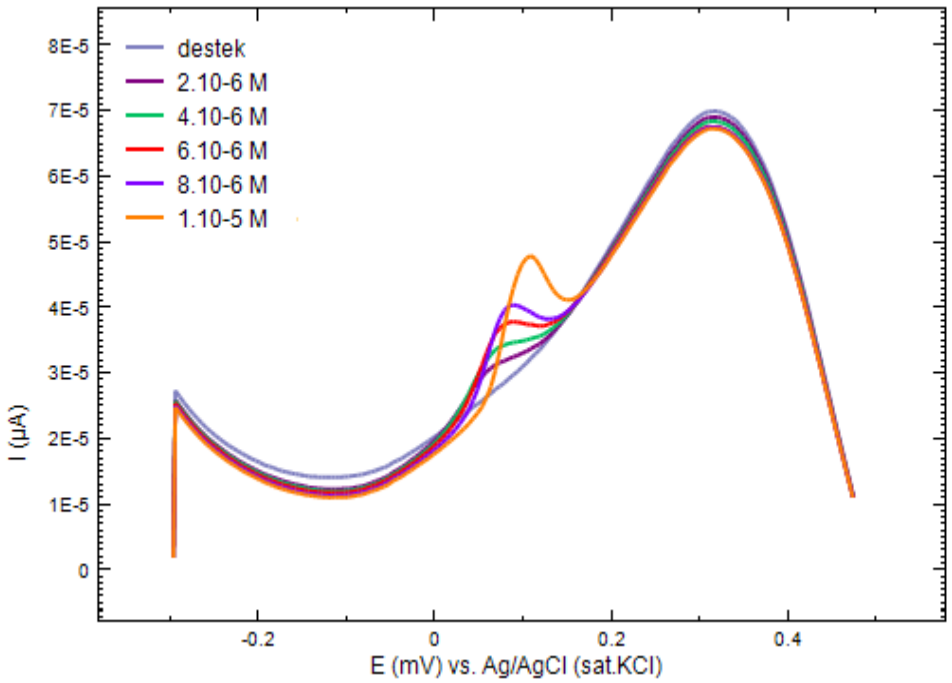


**Figure 3.18** Differential pulse voltammograms at Au/PPAP/GO/GCE for increasing concanterations of arsenic in mineral water, with scan rate 20 mV/s and pulse amplitude 50 mV.

Figure 3.19 shows the the standard addicion as Au/PPAP/GO/GCE obtained for arsenic sample. The linear regression equations of Au/PPAP/GCE could be expressed as $R^2$=0.9906 and y = 1.5452x- 0,7518. Recovery was calculated % 78.

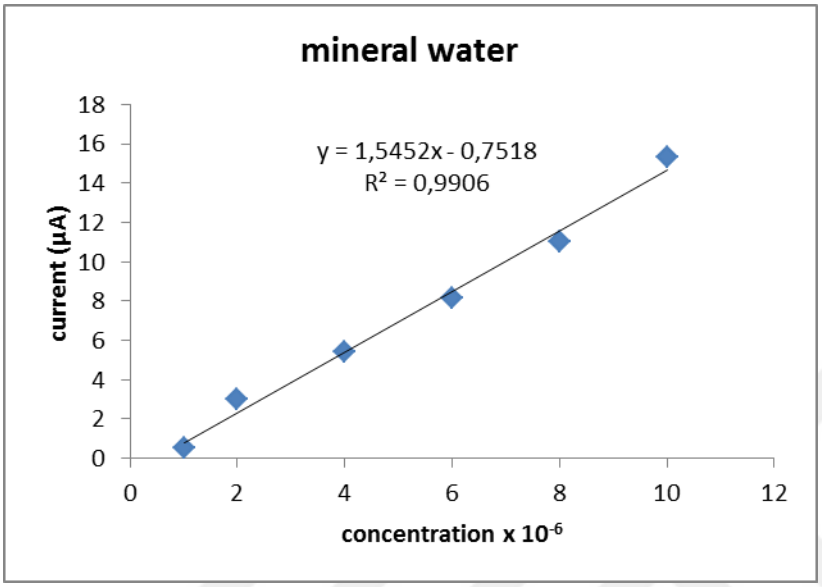


**Figure 3.19** Standard addition curve of increasing arsenic concentrations. Arsenic concentrations: $10^{-6}$, $2.10^{-6}$, $4.10^{-6}$, $6.10^{-6}$, $8.10^{-6}$, $10^{-5}$.

## 3. 8 Preparation of Polycresol Red (PCR) Film Modified GCE

Cresol red was dissolved in ultra pure water. $10^{-2}$ M stock solution was prepared and it was diluted everyday freshly. The electrochemical polymerization of CR was carried out in the presence of 0.1 M HCI. As following in Figure 3.20 an irreversible reduction peak was observed at – 0.75 V during the first cathodic potential-current scan. In the second current potential scan two reversible oxidation and reduction peak was observed at 0.1 V and 0.75 V and 0.8 V. The increasing of peak current depending on cycles number shows that the increasing the content of polymer on the electrode surface.

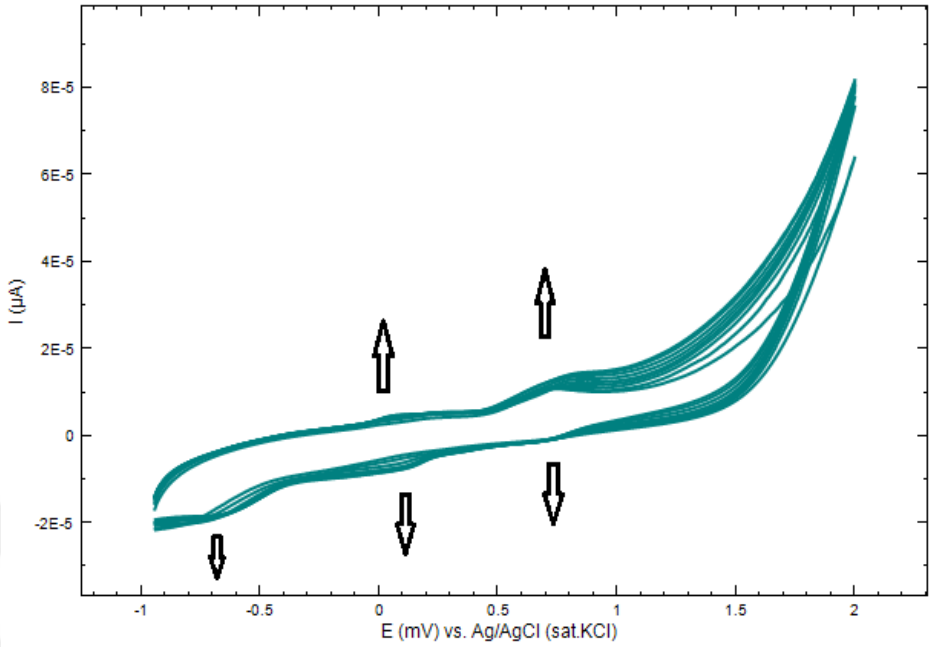


**Figure 3.20** Cyclic voltammograms of polycresol red electropolymerization on GCE surface in 0.1 M HCI, $10^{-3}$ cresol red by cycling the potential from -0.9 to +2.0 V vs. Ag / AgCl (sat. KCl) at a scan rate of 100 mV /s for 10 cycles.

## 3. 9 Deposition of Au Nanoparticles on Polycresol Red Covered GCE From Chloroauric Acid Solution

Electrochemically deposition of Au nanoparticles on the PCR/GCE surface was carried out from 1mM chloroauric acid + 0.1 M HCl solution mixture by concecutive potential scans from -1.10 to 0.40 V (Figure 3.21). Two reduction peaks were appeared at -0.05V and -0.32 V for concecutive reduction of Au species on the electrode surface during the cathodic current- potential scan while observing of an oxidation peak at -0.10 V and -0.5 V.

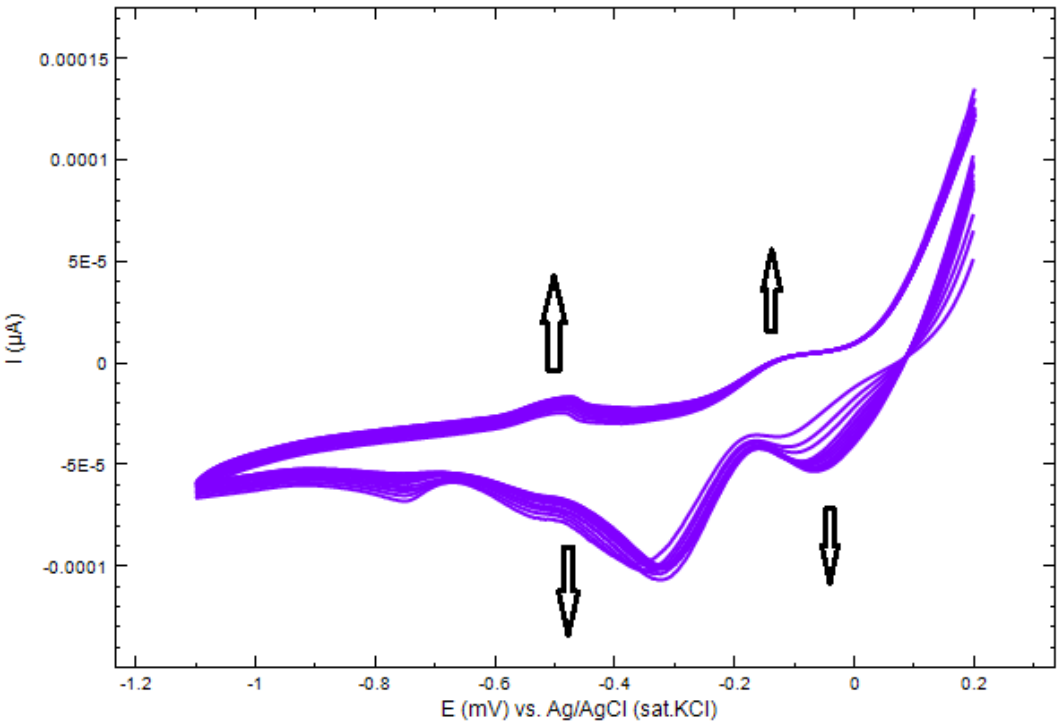


**Figure 3.21** Electrodeposition of Au nanoparticles on PCR/GCE surface by cyclic voltammetry at a 50 mV/s scan rate, between – 1.1 V and 0.2 V.

### 3. 10 Voltammetric Behaviour of Arsenic(III) at Bare and Modified Electrodes

Voltammetric behaviour of As(III) was also examined in 0.10 M HCl solution (Fig.3.22). in the presence of $5.10^{-5}$ M As(III) in the potential scaning range between the range of – 0.4 V – (+ 0.4 V) at bare GCE, PCR/GCE and Au/PCR/ GCE. There was no any electrochemical signal for bare GCE and PCR/GCE. A well defined irreversible oxidation peaak was apperaed at 0.15 V on Au/PCR/GCE. A reduction peak was occured at -0.06 V due to the Au species formed during the anodic current potential scan.

Figure 3.22 shows the cyclic voltammograms of bare GCE, PCR/GCE and Au/PCR/GCE in 0.1 M HCI supporting solution for $5.10^{-5}$ M As. Bare GCE and PCR/GCE didn't give any response towards to arsenic, but Au nanoparticles modified PCR/GCE electrode give oxidation peak of arsenic at 0.18 V and reduction peak at – 0.16 V.

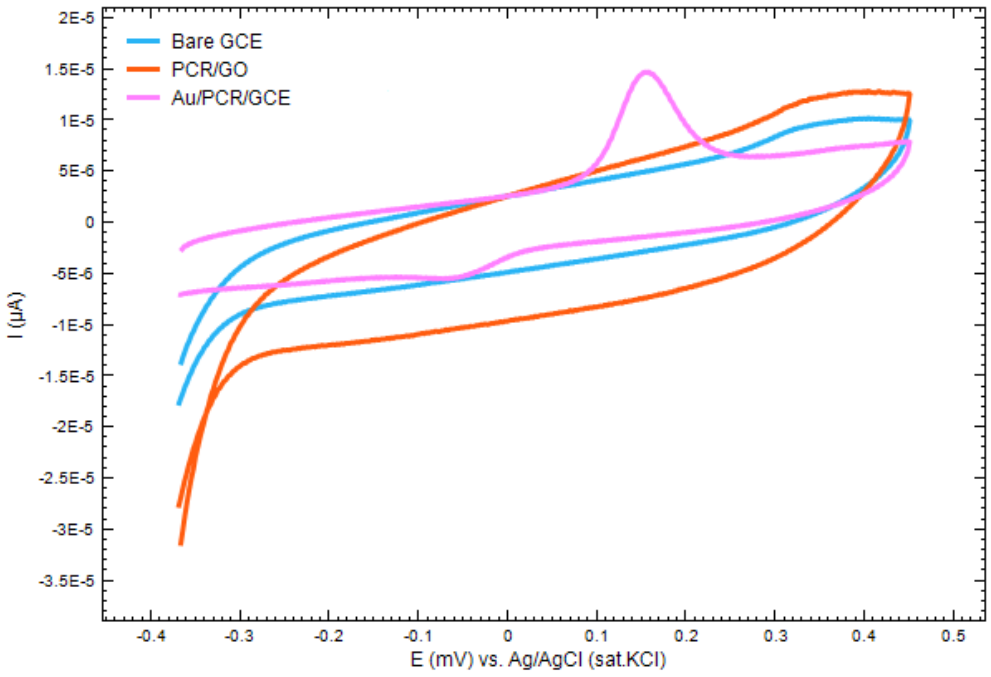


**Figure 3.22** Cyclic voltammetric behavior of GCE, PCR/GCE and Au/PCR/GCE for $5.10^{-5}$ M As(III) in 0.1 M HCI supporting solution at a 100mV/s scan rate.

### 3. 11 Surface Characterization of PCR/GCE and Au/PCR/GCE

The surface morphology of PCR/GCE and Au/PCR/GCE were characterized by SEM. To get a good surface image, addition to the using conventional secondary electron dedector, an in-lens dedector was used. The in-lens detector is located inside the electron column of the microscope and is arranged rotationally symmetric around the optical axis. Due to a complicated magnetic field at the pole piece, the secondary electrons are collected with high efficiency. Especially, at low voltages and small working distances, images with high contrast can be obtained. Besides information about morphology and surface topography, the in-lens detector images have high resolution. On the other hand, in the images recorded by the conventional secondary electron detector, the topographic information is dominant. In Figure 3.23, and 3.24 the differences can be seen easily.

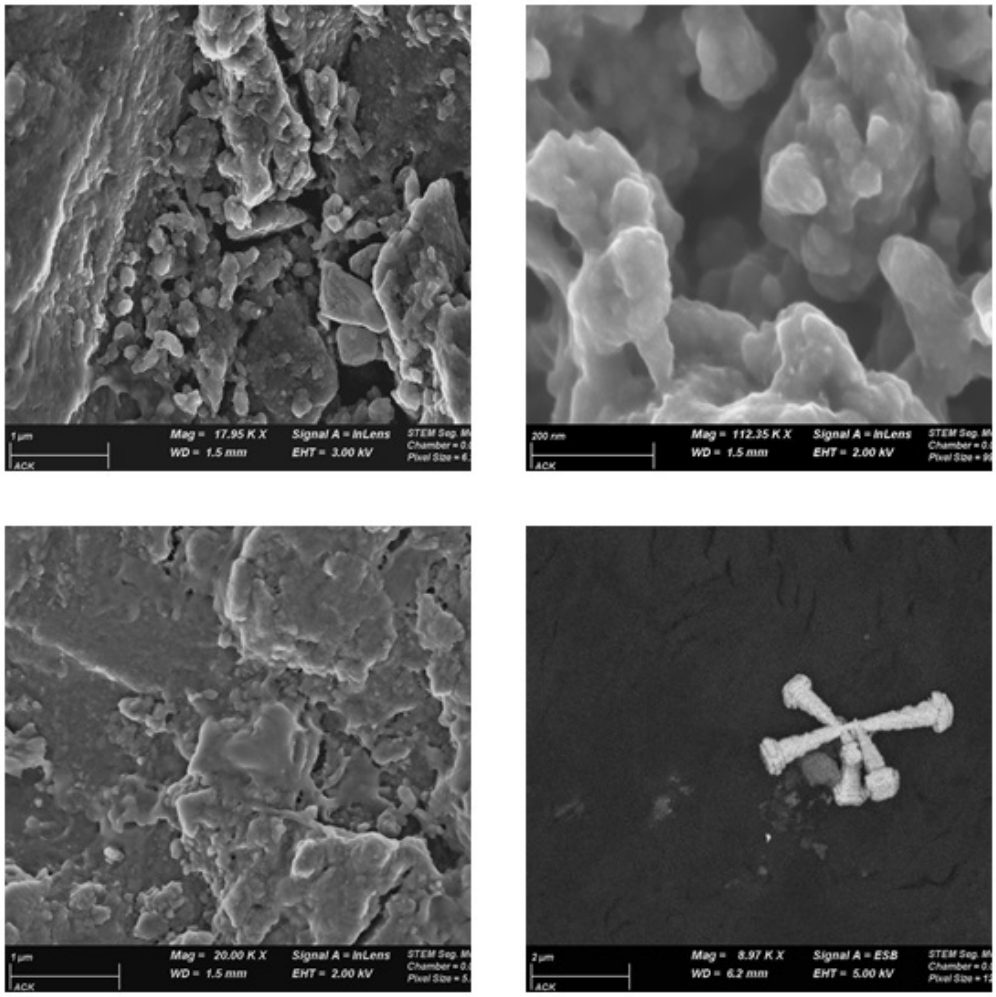


**Figure 3.23** SEM images of PCR modified GCE surface with using in-lens.

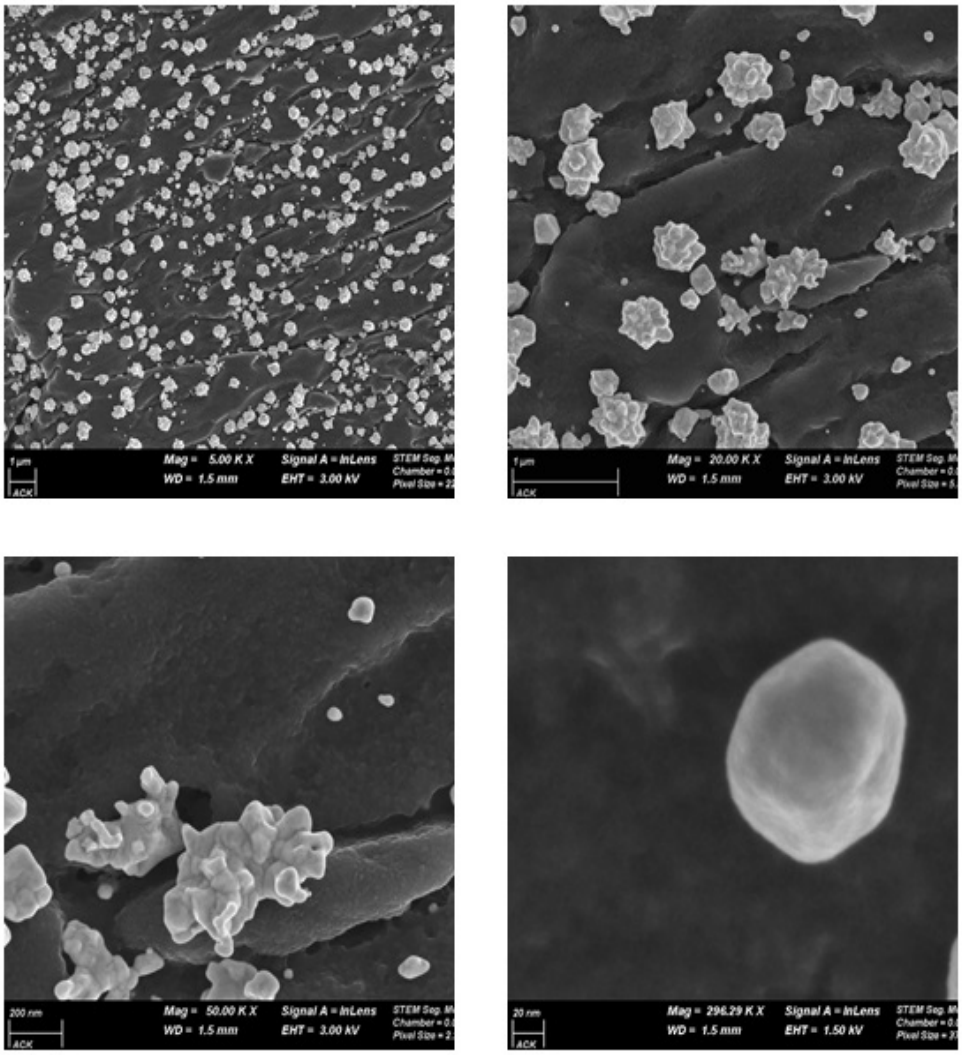


**Figure 3.24** SEM images of Au/PCR modified GCE surface with using in-lens.

In Figure 3.24, according to the top two pictures, nanoparticles were calcultaed 430 nm, 468 nm, 660 nm and 466 nm.

### 3. 12 Chemical Characterization of Modified Electrodes by XPS

To identify the electrodes surface chemical composition in PCR/GCE and Au/PCR/GCEs, XPS measurements were carried out on polymer films. Figure 3.25 shows detailed spectra of C1s, O1s and Au4$f_{7/2}$ and 4$f_{5/2.}$

The curve fitting of the C1s peaks for PCR and $PCR_{ox}$ had been done assuming three components at 284.7, 286.2, 289.9 eV respectively (Figure 3.25-

a). These value could be correspond to $sp^2$ carbon in the polymer chain, C=O bond on PCR/GCE surface. The fitted O1s spectra of the PCR modified GC electrodes were indicated in Figure 3.25-c. Only an oxygen structure was observed with the PCR/GCE (Figure 3.25-c) at BE 532.44. The BE signal could be assigned to -C=O bond on the electrode surface of PCR/GCE. Figure 3.25-d shows the Au4f spectrum resolved into two spin–orbit components. The $Au4f_{7/2}$ and $4f_{5/2}$ peaks were appeared at a binding energy (BE) of 84.08 and 87.78 eV, respectively, and were assigned to metallic Au (Bakır et al., 2011; Zheng et al., 2010) on PCR/GCE surface.

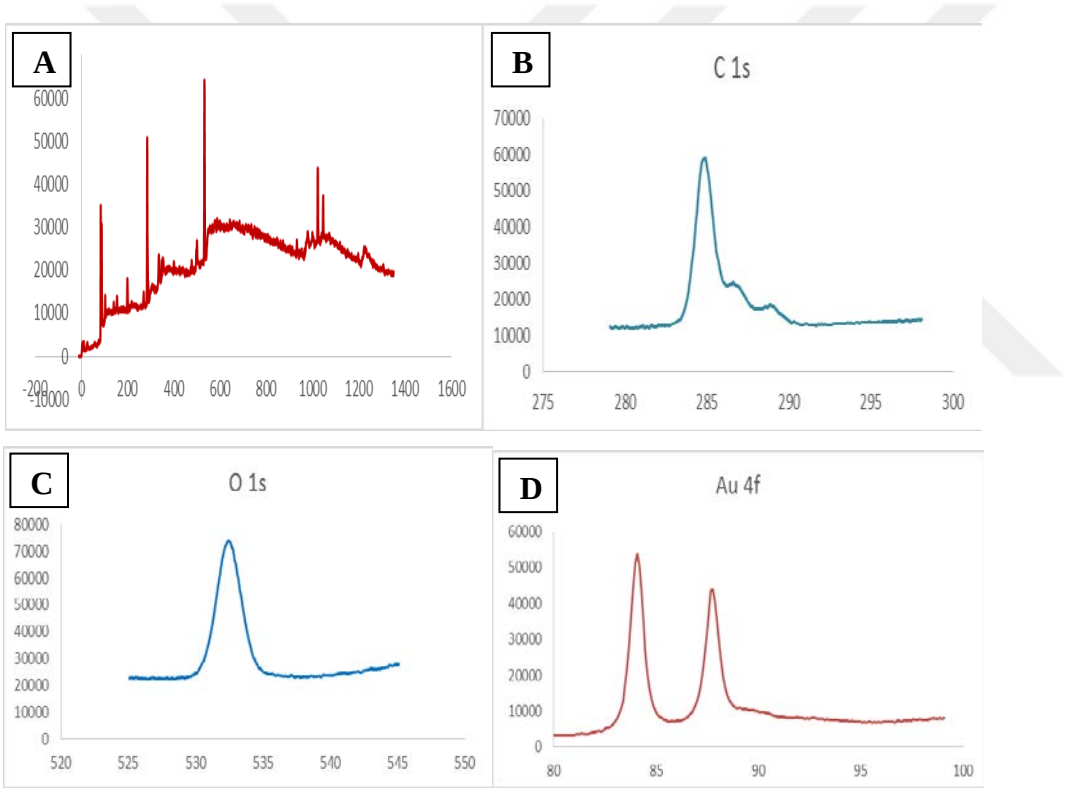


**Figure 3.25** XPS spectra of PCR/GCE and Au/PCR/GCE.

**Table 3.8** % Atomic percentage of some elements on nanocomposite surface

| Name | Start BE | Peak BE | End BE | Height CPS | FWHM eV | Area (P) CPS.eV | Area (N) KE^0.6 | Atomic % |
|---|---|---|---|---|---|---|---|---|
| Au 4f7 | 99 | 84,14 | 79 | 29322,56 | 1,26 | 45844,25 | 61,91 | **1,39** |
| Si 2s | 163,42 | 154,14 | 145,02 | 2931,01 | 2,15 | 6700,54 | 93,61 | **2,11** |
| Cl 2p | 204,75 | 199,33 | 193,95 | 6688,23 | 2,79 | 19112,4 | 113,92 | **2,56** |
| C 1s | 298 | 285,23 | 279,96 | 28580,37 | 2,28 | 90885,74 | 1290,24 | **29,02** |
| N 1s | 410 | 400,42 | 395,24 | 2136,37 | 1,24 | 8205,15 | 68,75 | **1,55** |
| O 1s | 538,9 | 532,39 | 527,3 | 37141,06 | 1,64 | 111875,94 | 622,39 | **14** |
| Zn2p | 1052 | 1022,34 | 1015 | 15531,4 | 1,51 | 81202,94 | 71 | **1,6** |
| Au4f Scan A | 89,68 | 87,78 | 79,58 | 35091,76 | 0,76 | 31133,57 | 23,56 | **0,53** |
| Au4f Scan B | 89,68 | 84,08 | 79,58 | 48340,88 | 0,74 | 41926,22 | 31,68 | **0,71** |
| C1s Scan A | 292,98 | 289,08 | 282,28 | 5102,67 | 1,18 | 7049,45 | 100,27 | **2,26** |
| C1s Scan B | 292,98 | 287,08 | 282,28 | 9872,39 | 1,53 | 17670,43 | 251,09 | **5,65** |
| C1s Scan C | 292,98 | 284,78 | 282,28 | 45800,6 | 1,33 | 71256,45 | 1011,35 | **22,75** |
| O1s Scan A | 540,48 | 532,44 | 527,58 | 50897 | 2,13 | 126990,61 | 706,5 | **15,89** |

It is easily seen on the table 3.8, the surface material mostly consist of C which exist in polycresol red. The molecular formula of cresolred is $C_{21}H_{17}NaO_5S$ so oxygen's percentage is high. Au 4f scannings also indicates that the electrode composite surface material have Au nanoparticles.

### 3.13 Electrochemical characterization of modified electrodes by EIS

Electrochemical impedance spectroscopy is pratical tool for the characterization of modified surfaces. The surface resistance is measured by changing frequencies of applied alternative current. Surface resistance changed by changing surface modification. Figure 3.26 shows the Nyquist curves of bare GCE, PCR/GCE and Au/PCR/GCE. The radius of the semi circles are the sign of the conductivity of the surfaces. For comprasion the smallest semicircle was observed for Au/PCR/GCE probably due to high conductivity of gold nanoparticles.

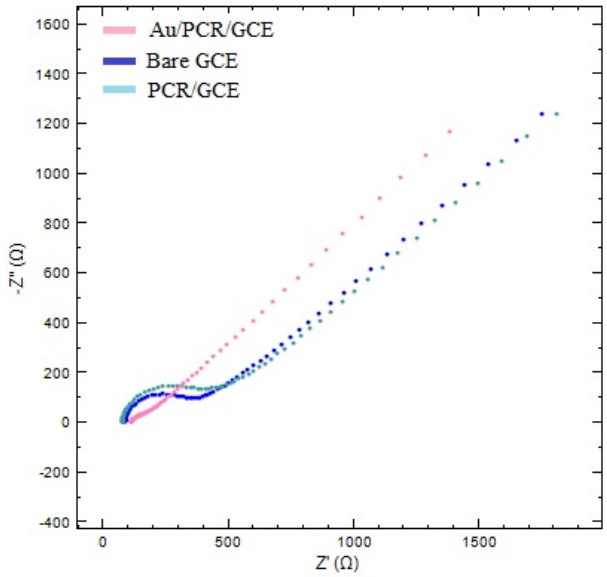


**Figure 3.26** The Nyquist curves of bare GCE, PCR/GCE and Au/PCR/GCE obtained in the frequency range of 0.1 to 30000 Hz.

## 3. 14 Optimization Studies of Arsenic at Au/PCR/GCE

### 3. 14. 1 Opti/mization of HCI Concentration

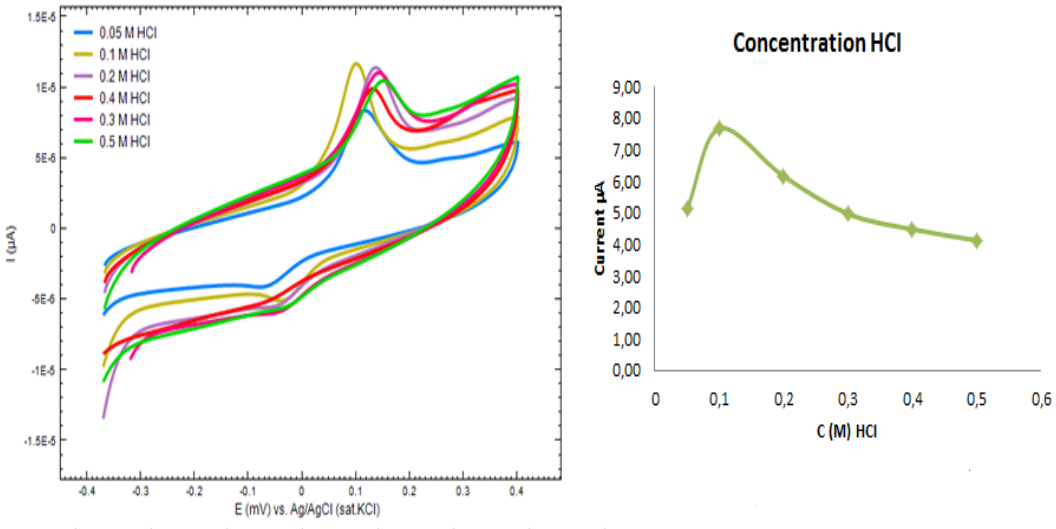


**Figure 3.27** Cyclic voltammograms for $10^{-5}$ M As(III) on Au/PCR/GCE at different HCI concentrations at 100 mV/s scan rate.

The effect of HCl concentrations on the voltammetric behaviour of arsenic(III) was investigated in the concentration range of 0.05 - 0.50 M at Au/PCR/GCE. Figure 3.27 shows that the highest peak current was observed in 0.1 M HCI solution. Potential and current values are given in Table 3.8 above.

**Table 3.9** The effect of HCI concentration for arsenic oxidation.

| $C_{(HCl)}$ M | E (mV) | i (µA) |
|---|---|---|
| 0.05 | 113 | 5.11 |
| **0.1** | **98** | **7.67** |
| 0.2 | 132 | 6.16 |
| 0.3 | 141 | 4.97 |
| 0.4 | 130 | 4.48 |
| 0.5 | 147 | 4.13 |

### 3. 14. 2 The effect of cresol red concentration on voltammetric behaviour of As(III)

Figure 3.28 shows that the effect of CR concentration on the voltammetric behaviour of $5.10^{-5}$ M As(III) in the presence of 0.1 M HCI supporting electrolyte solution. All polymer film surface were prepared by 10 cycles of current potential curve as mentioned in Experimental section of 2.3.5. Optimum Cresol Red concentration was obtained as $10^{-3}$ M by monitoring of As signal. Therefore the $10^{-3}$ M CR concentration will be used for further studies.

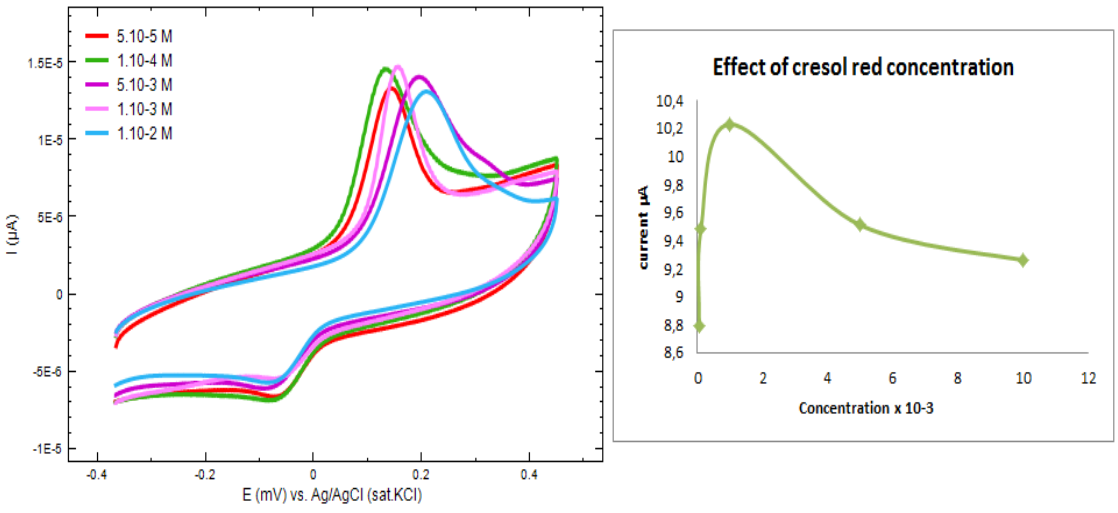


**Figure 3.28** Effect of cresol red concentration for Arsenic(III)

**Table 3.10** The effect of cresol red concentration for electrooxidation of As(III).

| $C_{PCR}$ (M) | E (mV) | İ (µA) |
|---|---|---|
| $10^{-2}$ | 206 | 9.26 |
| $5.10^{-3}$ | 189 | 9.51 |
| **$10^{-3}$** | **152** | **10.23** |
| $10^{-4}$ | 130 | 9.87 |
| $5.10^{-5}$ | 142 | 8.79 |

## 3. 14. 3 The Effect of Cycle Number of Cresol Red for Arsenic

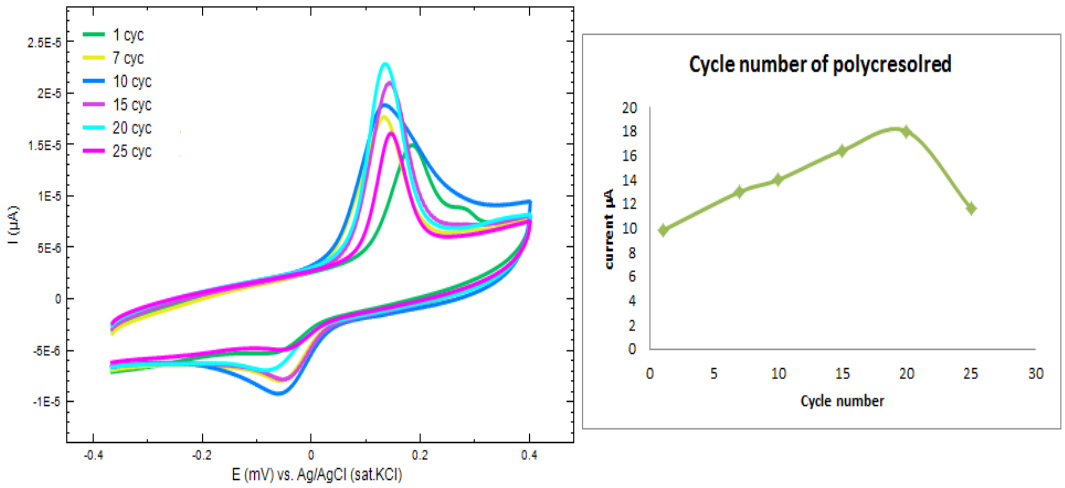


**Figure 3.29** Cycle effect of PCR on arsenic(III) voltammetric behaviour .

The effect of cycle number for the response in the presence of $5.10^{-5}$ M As in 0.1 M HCI supporting solution is shown in Figure 3.29 The peak current for arsenic oxidation increased from 1 cycle to 20 cycles of PCR then decreased at 25 cycle in the presence of Au particles. The decreasing peak current can be explained to increase the electrode resistance and capaticance by increasing the polymer content on the GCE surface. Table 3.10 shows the changes of current and potential values by changing cycle number of PCR.

**Table 3.11** The effect of PCR cycle number for electrooxidation of As(III).

| Cycle number of PCR | E (mV) | İ (µA) |
|---|---|---|
| 1 | 181 | 9.82 |
| 7 | 130 | 13.00 |
| 10 | 154 | 14.00 |
| 15 | 142 | 16.43 |
| **20** | **132** | **18.00** |
| 25 | 145 | 11.63 |

### 3. 14. 4 The Effect of Cycle Number for Au Nanoparticles

For the optimization of Au deposition on the PCR/GCE surface, the cycle number effect between 3 to 20 prepared from $3x10^{-3}$ M $AuCl_4^-$ solution on the electrochemical oxidation of arsenic was also investigated (Figure 3.30). The amount, the size even the shape of the deposited Au nano particles were controlled by changing the cyclic number (n) in electrodeposition process. The maximum peak current was obtained for arsenic electrooxidation on Au/PCR/GCE which was prepared after 15 cycling Au deposition. Table 3.11 shows the changes of current and potential values by changing cycle number of Au.

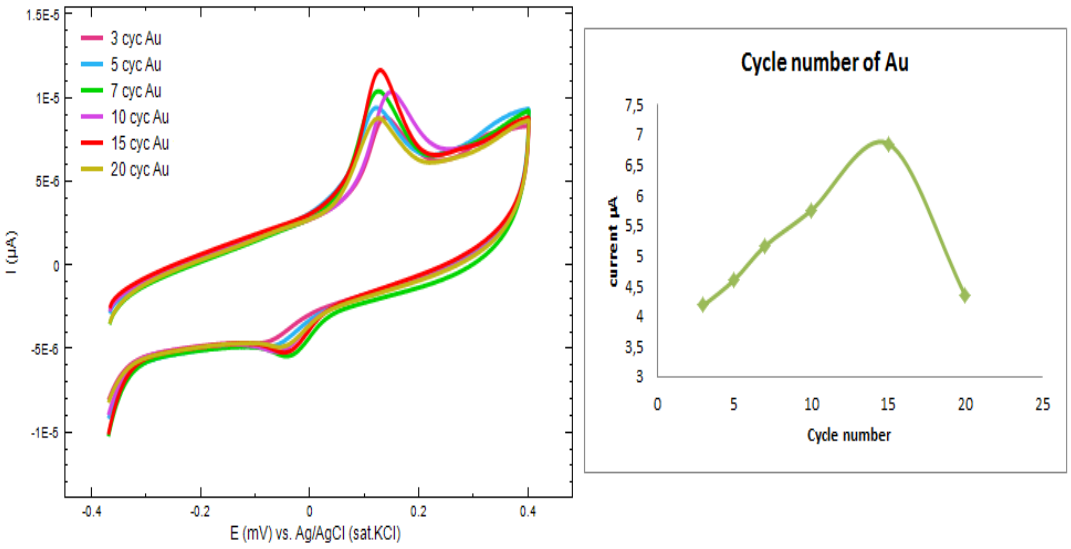


**Figure 3.30** Effect of different cycle numbers of Au ( from $3.10^{-3}$ M $AuCl_4^-$) for voltammetric behaviour of $10^{-5}$ M As (III).

**Table 3.12** The effect of Au cycle number of arsenic.

| Cycle number of Au | E (mV) | İ (µA) |
|---|---|---|
| 3 | 135 | 4.18 |
| 5 | 118 | 4.60 |
| 7 | 145 | 5.16 |
| 10 | 120 | 5.75 |
| **15** | **128** | **6.85** |
| 20 | 123 | 4.34 |

## 3. 14. 5 Scan Rate Study at $Au_{(15\ cyc)}$-PCR/GCE

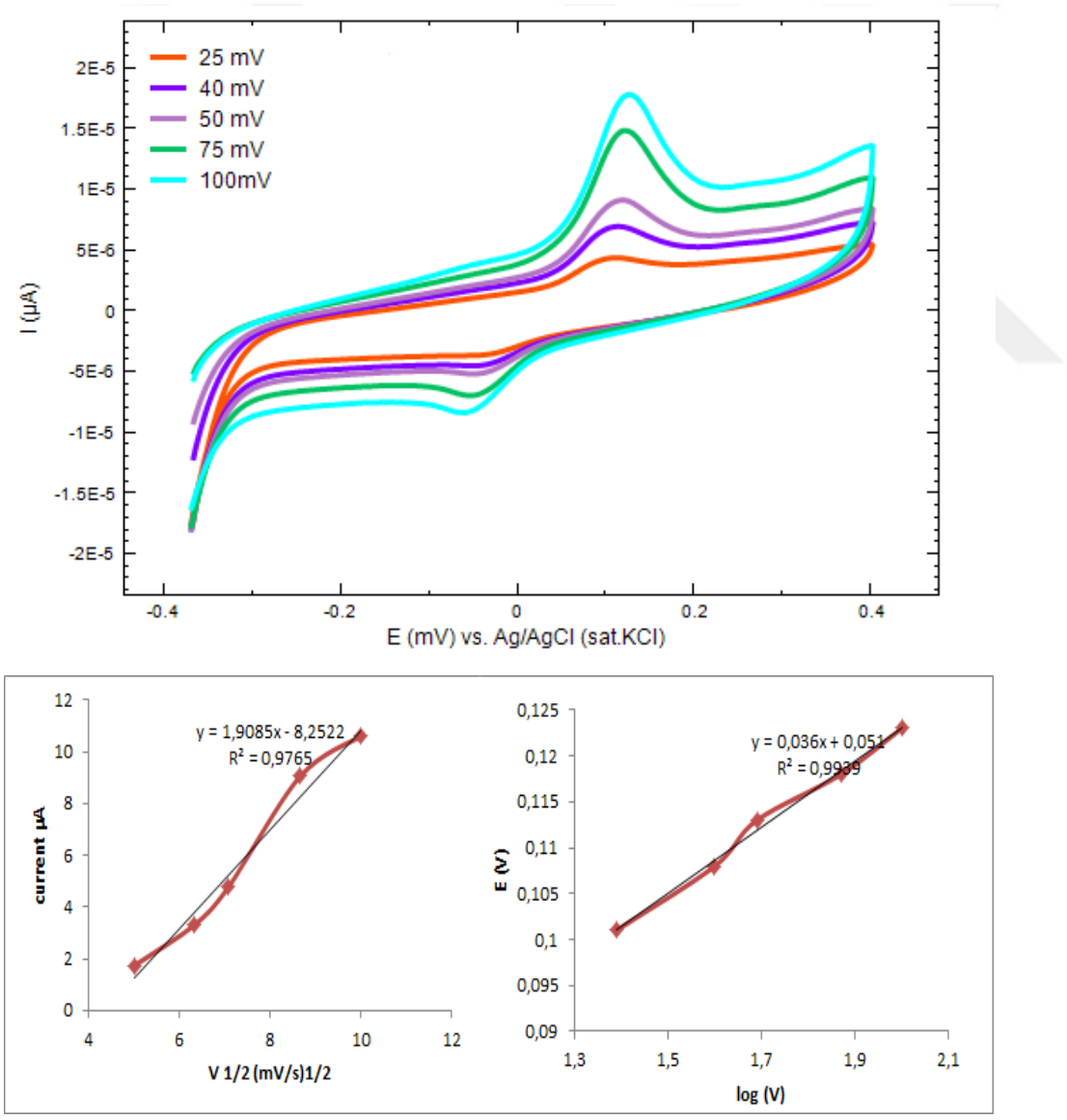


**Figure 3.31** Cyclic voltammograms of different scan rates for $10^{-5}$ M As (III) on Au/PCR/GCE surface ( 25, 50, 75, 100, 150 mV/s ).

In order to confirm the electrode behaviour on the oxidation of arsenic, a series of cyclic volatmmograms were recorded at Au nanoparticles modified PCR/GCE by varying potential scan rate. The oxidation peak current increased linearly with the square root of the scan rate (Figure 3.31), suggesting that arsenic oxidation reaction at this modified electrode was controlled by diffusion. The reduction peak potential of arsenic shifted negative values with increasing the scan rate, indicating that the electron transfer was irreversible. As well as, the oxidation peak potential was shifted positive values. For $10^{-5}$ M As(III), the highest peak current was at 100 mV/s scan rate.

### 3. 14. 6 Differential Pulse Voltammetric Determination of Arsenic

The differential pulse voltammetric results were obtained under following conditions; step potential: 5 mV, amplitude: 50 mV, modulation time: 0.05 s, interval time: 4 s and scan rate 20 $mV.s^{-1}$. Limit of detection values were calculated from (S/N:3) and calibration curves. The average value of background current estimated from 5 different measurements. LOQ values were calculated for estimation of linear ranges. The oxidation peak current of arsenic was increased linearly with the increase of As(III) concentration in the range $1.0x10^{-7}$ -7.0. $10^{-7}$ M (Figure 3.32 and 3.33) at Au/PCR/GCE. LOD was calculated $5.7x10^{-8}$ M (S/N =3). The linear regression equations of this modified electrode could be expressed at $R^2$ = 0,9921.

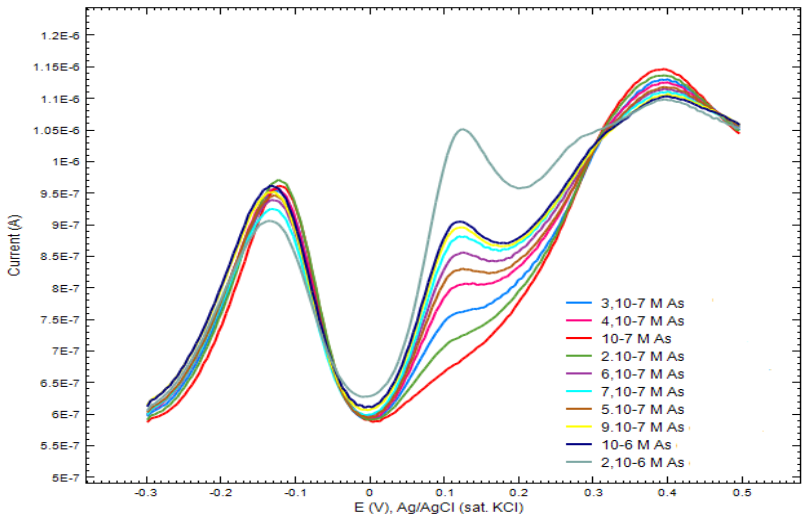


**Figure 3.32** Differential pulse voltammograms at Au/PCR/GCE for increasing concentrations of arsenic in 0.1 M HCI supporting solution with scan rate 20 mV/s and pulse amplitude 50 mV/s.

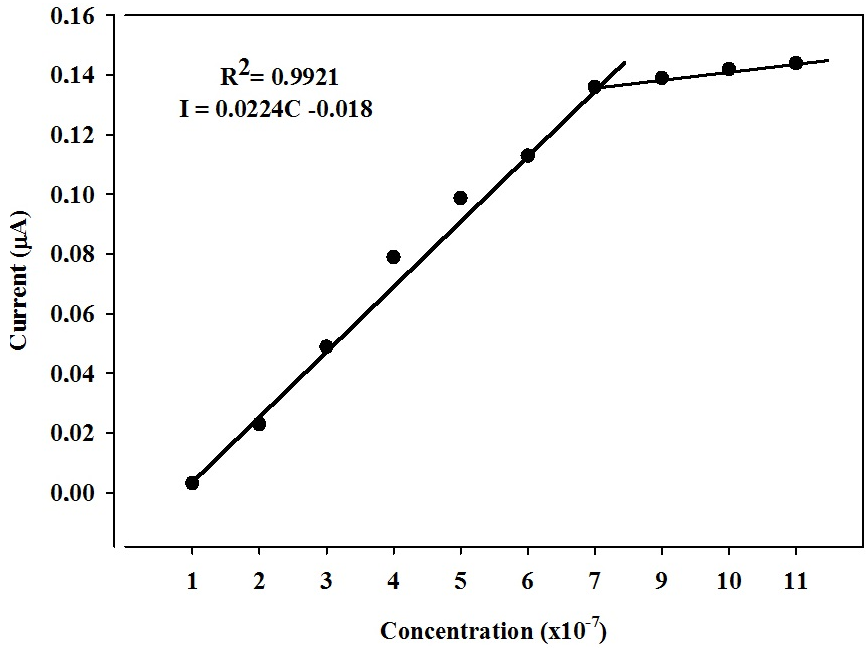


**Figure 3.33** Corresponding calibration curve of increasing arsenic concentrations in 0.1 M HCI for increasing As (III) concentrations $1.10^{-7}$ to $1.10^{-6}$ M.

**Table 3.13** As concentration range, potential and current for Au/PCR/GCE.

| C (M) As | E (mV) | İ (µA) |
|---|---|---|
| $1.10^{-7}$ | 0.102 | 0.0033 |
| $2.10^{-7}$ | 0.102 | 0.023 |
| $3.10^{-7}$ | 0.103 | 0.049 |
| $4.10^{-7}$ | 0.107 | 0.079 |
| $5.10^{-7}$ | 0.102 | 0.098 |
| $6.10^{-7}$ | 0.107 | 0.113 |
| $7.10^{-7}$ | 0.107 | 0.136 |
| ***$8.10^{-7}$*** | ***0.107*** | ***0.139*** |
| ***$9.10^{-7}$*** | ***0.107*** | ***0.142*** |
| ***$1.10^{-6}$*** | ***0.107*** | ***0.144*** |
| ***$2.10^{-6}$*** | ***0.113*** | ***0.244*** |

### 3. 14.7 Sample analysis

Mineral water sample was degazed in ultrasonic bath approximately one hour to remove gases and carbonates. According to the optimization studies, arsenic gives good response in acidic media so the pH of mineral water was adjusted to 1.0 with concentrated HCI. After that, 15 mL sample was put into a cell and measured by DPV. Arsenic was not detected in mineral water, afterthen measurements were carried out by conducting spike-recovery studies. Five identical measurements were made and the percentage of recoveries with standard error of Arsenic (III) is presented in Table 3.14.

**Table 3.14.** Percentage recovery of Arsenic(III) from mineral water.

| Arsenic spiked (µM) | Arsenic found (µM) | Recovery (%) | RSD (n=3) |
|---|---|---|---|
| 0,6 | 0,45 | 75 | 6,0 |
| 1 | 0,94 | 94 | 4,3 |
| 2 | 1,88 | 94 | 4,5 |

For ground water and tap water, another Au/PCR/GCE electrode was prepared. Firstly, calibration curve was prepared and then it was used for detection of arsenic in ground water and tap water. To get an acidic media, their pH were adjusted to 1.0 value with concentrated HCl. According to the measurements, arsenic was not detected and then recovery studies were performed by spike the standart solution of As(III).

**Table 3.15.** Percentage recovery of Arsenic(III) from ground water.

| Arsenic spiked (µM) | Arsenic found (µM) | Recovery (%) | RSD (n=3) |
|---|---|---|---|
| 0,5 | 0,45 | 90 | 3,8 |
| 0,6 | 0,55 | 91 | 3,2 |
| 1 | 1,12 | 112 | 2,7 |

**Table 3.16** Percentage recovery of Arsenic(III) from tap water.

| Arsenic spiked (μM) | Arsenic found (μM) | Recovery (%) | RSD (n=3) |
|---|---|---|---|
| 0,3 | 0,306 | 102 | 3,4 |
| 0,4 | 0,304 | 76 | 5,4 |
| 0,5 | 0,55 | 110 | 3,0 |

### 3.14.8 Repeatability and stability of Au/PCR/GCE

Repeatability and stability studies were avaluated using DPV technique. In order to study repeatability, the same electrode was used within a day and the relative standart deviation (RSD) of the peak currentswas 0.65 % for arsenic (n=3).

The stability of Au/PCR/GCE electrode was also examined. The modified electrode was stored in the supporting electrolyte during the stability experiments. As it shown in Figure 3.36, after 4 days, the current is % 92.

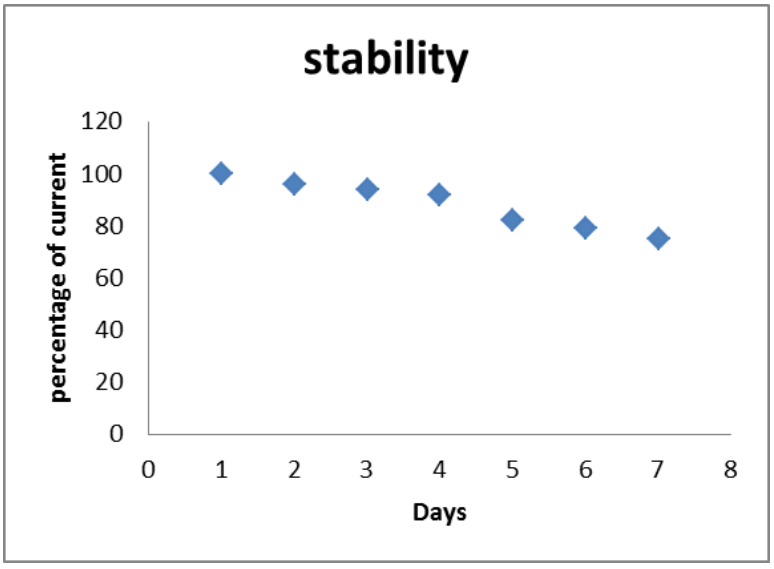


**Figure 3.34** Percentage of current for each day for $10^{-6}$ M concentration of As (III).

# 4. GENERAL DISCUSSION AND CONCLUSION

Analytical chemistry and especially electrochemistry need new type of electrode materials for catalytic and selective electrode materials catalytic, oxidative and all kind of selective electrode reactions. For this target, nano materials and different composite materials have been used recently. The properties of nanoparticles are different from bulk materials and isolated molecules by virtue of their unique optical, electronic, magnetic, chemical properties and high effective surface area. For these reason, nano structured materials have been used in various applications such as catalysis, fuel cells, nanodevices, biosensors and optoeletronics.

Extraordinary role of nanomaterials in modern electroanaltyical chemistry is supported by the electrocatalytic ability of carbon based modified electrodes such as carbon nanotubes, graphene oxide, graphene. The modification is enhanced analytical properties as active surface area, high electronic conductivity of the surface. Furthermore, to improve unique properties of grephene, the modification could be combined with metal nanoparticles which they can be synthesized and modified chemically or electrochemically. As well as, to make more effective surface area, graphene oxide can be modified with not only metal nanoparticles but also conductive polymers such as PPAP. To prepare an effective metal nanoparticles which is attached on the polymer and graphene oxide modified electrodes, an electrochemically deposition procedure is rapid, simple and reproducible.

Arsenic pollution in the environment is the most important problem in all over the world recently. Arsenic is exist in earth’s crust and it is transmitted to ground water. The problem which we concern is arsenic pollution in tap water, drinking water and mineral water. Because of inorganic forms of arsenic is more toxic than organic forms, different techniques have been developed to eliminate As(III) and As(V) forms from water. Arsenic oxidation reaction can be proceeded by three electron loosing on electrode surface. Preparation of higher catalytic electrode surface is a key factor for enhancing the performance of the electrodes.

For this aim, in this thesis, new electrode materials were prepared using graphene oxide, PPAP and different nano particles modified electrodes. Au/GO/GCE, Au/PPAP/GO/GCE and Au/GO/PPAP/GCE are prepared. The Au/PPAP/GO/GCE showed best results for arsenic. Without using PPAP, Au/GO/GCE is not effective as the others. Using PPAP directly to the GCE surface is not effective as using it after graphene oxide. It can be explained that graphene oxide increases the conductivity of GC electrode more than PPAP. After choosing the Au/PPAP/GO/GCE electrode, different nanoparticles such as Cu, Fe, Ni, Pt nanoparticles were deposited onto the PPAP/GO/GCE surface to increase before Au. Results showed that Au/Cu/PPAP/GO/GCE, Au/Ni/PPAP/GO/GCE and Au/Pt/PPAP/GO/GCE are not effective as Au/PPAP/GO/GCE. It can be say that these nanoparticles (Cu, Ni, Pt) decreased the synergic effect of Au-PPAP. GO/GCE, PPAP/GO/GCE and Au/PPAP/GO/GCE were characterized by SEM and Au nanoparticle size was also revealed.

In another study, cresol red was used as a conductive polymer. Cresol red was polymerized by electrochemical method directly onto the GCE surface. Au nanoparticles were deposited on the PCR/GCE surface. Results showed that PCR increased the peak current of As (III). It was observed that conductivity of Au/PCR was more than Au/PPAP/GCE.

The main goal of the thesis is that preparation and characterization of new electrode material for detection of arsenic. For this aim, graphene oxide was synthized an used as a composite electrode material and then modified. For modification, conductive polymer and nanoparticles were used. It was seen that electrocatalytic activitiy was increased in the presence of metal nano particles and conductive polymers onto the composite electrode surface. Using different nanoparticles and polymer materials, the best response was taken from Au/PPAP/GO/GCE and Au/PCR/GCE. The presence of Au as nanoparticles size was revealed by SEM.

**REFERENCES**

**Abid, A. D., Anderson, D. S., Das, G. K., Kennedy, M., 2013,** Novel lanthanide-labeled metal oxide nanoparticles improve the measurement of in vivo clearance and translocation. Particle and Fibre Toxicology, 1-10.

**Antollini. E. and Gonzales, E.R., 2009,** Polymer support for low-temparature fuel cell catalysts, applied Catalysis A: General, 365:1-19 pp.

**Bakır Ç. C., 2011, Doğan, N., Polat, R., Dursun, Z.,** Electrocatalytic reduction of oxygen on bimetallic copper–gold nanoparticles–multiwalled carbon nanotube modified glassy carbon electrode in alkaline solution, Journal of Electroanalytical Chemistry, 275-280.

**Bard, A. and Faulkner, L. R., 2001,** Electrochemical methods, John Wiley&Sons, New York.

**Beng Khoo, S., Zhu, J., 1998,** Poly(pyrogallol) film on glassy carbon electrode for selective preconcentration and stripping voltammetric determination of Sb(III), Analytica Chimica Acta, 15-27.

**Biallozor, S., Kupniewska, A., 2005,** Conducting polymers electrodeposited on active metals - review article, Synthetic metals, 443-449.

**Brodie, B. C., 1859,** "On the Atomic Weight of Graphite". Philosophical Transactions of the Royal Society of London 149: 249**.**

**Bobacka, J., Mousavi, Z., Lewenstam, A., Ivaska, A., 2009,** Poly(3,4-ethylenedioxythiophene) (PEDOT) doped with carbon nanotubes as ion-to-electron transducer in polymer membrane-based potassium ion-selective electrodes, Journal of Electroanalytical chemistry, 246-252.

**REFERENCES (Contiuned)**

**Camacho, L. M., Parra, R. R., & Deng, Sh. 2011,** Arsenic removal from groundwater by MnO2-modified natural clinoptilolite zeolite: Effects of pH and initial feed concentration. Journal of Hazardous Materials, 189, 286-293.

**Cao, G., 2004,** Nanostructures and Nanomaterials, Synthesis, Properties and Applications, Imperial College Pages.

**Cheetham, A.K., Rao, C.N.R. and Mülker, A.,** 2004, The Chemistry of nanomaterials, Wiley, VCH.

**Chen, W., Lin, X., Huang, L., Luo, H., 2005,** Electrochemical characterization of polymerized cresol red film modified glassy carbon electrode and seperation of electrocatalytic responses for ascorbic acid and dopamine oxidation. Microchimica Acta, 101-107.

**Cui, H., Yang, W., Li, X., Zhao, H., Yuan, Z., 2012,** An electrochemical sensor based on a magnetic $Fe_3O_4$ nano particles and gold nanoparticles modified electrode for sensitive determination of trace amounts of arsenic(III), Analytical Methods, 4176-4183.

**Doria G., Conde J., Veigas B., Giestas L., Almeida C., Assuncao M., et al. 2012.** Noble metal nanoparticles for biosensing applications. Sensors (Basel) 12, 1657–1687.

**Dresselhaus, M.S., Linb., Y.M., Rabine, O., Jorioa, A., Filho, A.G.S., Pimentad, M. A., Saitof, R., Samsonidzeb, Ge.G. and Dresselhaus G.,** 2003, Nanowires and nanotubes material science and engineering C 23:129-140pp.

**Giacomino, A., Abollino, O., Lazzara, M., Melandrino, M., Mentasti, E., 2011,** Determination of As(III) by anodic stripping voltammetry using a lateral gold electrode: Experimental conditions, electron transfer and monitoring of electrode surface,Talanta, 1428-1435.

**REFERENCES (Contiuned)**

**Gibbon, V. K., Salaün, P., Kalle Uroic, M., Feldmann, J., McArthur, J. M., Berg, C. M. G., 2011,** Voltammetric determination of As in high Fe and Mn groundwaters. Talanta, 85, 1404–1411.

**Hathoot, A.A., Yousef, U.S, Shatla A.S. and Abdel-Azzem, M.,** 2012, Voltammetric simultaneous determination of glucose, ascorbic acid and dopamine on glassy carbon electrode modified by NİNPS@poly1,5-diaminophthalene, Electrochimica Acta 85:531-537 pp.

**Haudy, J.R., Ventra, M. and Lahmani, M.,** 2006, Nanomaterials and Nanochemistry, European Materials Research Society, Berlin, France.

**Heflin, J. R., Vente, M., Evoy, S., 2004,** Introduction to nanoscale science and technology, Kluwer Academic Publisher, Boston.

**Hummers, W. S., Offeman, R. E., 1958,** "Preparation of Graphitic Oxide". Journal of the American Chemical Society 80 (6): 1339.

**Jain, C.K., Ali, I., 2000**, Arsenic: occurrence, toxicity and speciation techniques, Water Research, 4304-4312.

**Kelsall, R., 2005,** Nanoscale Science and Technology, Wiley, 472 pages.

**Khan, M., Haque, A., Kim, K., 2013**. Electrochemical determination of uric acid in the presence of ascorbic acid on electrochemically reduced graphene oxide modified electrode, Journal of Electroanalytical Chemistry. Volume 700, 1 July 2013, Pages 54–59.

**Kosynkin, D. V., Higginbotham, A. L., Sinitskii, A., Lomeda, J. R., Dimiev, A., Price, B. K., Tour, J. M., 2009.** "Longitudinal unzipping of carbon nanotubes to form graphene nanoribbons". Nature 458 (7240): 872–876.

**Krause, R. V., Arotiba, O. A., Sampath, S., Mamba, B. B., Ndlovu, T., 2014,** Voltammetric detection of arsenic on a bismuth modified exfoliated graphite electrode, Electrochimica Acta, 48-53.

**REFERENCES (Contiuned)**

**Kumaravel, A., Chandrasekaran, M., 2010,** A novel nanosilver/nafion composite electrode for electrochemical sensing of methyl parathion and parathion, Journal of Electroanalytical Chemistry, 231-235.

**Lan, Y., Luo, H., Ren, X., Wang, Y., Liu, Y., 2012,** Anodic stripping voltammetric determination of arsenic(III) using a glassy carbon electrode modified with gold-palladium bimetallic nanoparticles, Microchimica Acta,153-161.

**Li, Z., Chen, L., Meng, S., Guo, L., Huang, J., Liu, Y., Wang, W., Chen, X., 2015,** Field and temperature dependence of intrinsic diamagnetism in graphene: Theory and experiment, American Physical Society Phys. Rev. B **91**, 094429.

**Li, D., Li, J., Jia, X., Han, Y., Wang, E., 2012**, Electrochemical determination of arsenic (III) on mercaptoethylamine modified Au electrode in neutral media, Analytica Chimica Acta, 23-27.

**Liu, Y., Huang, Z., Xie, Q., Sun, L., Gu, T., Li, Z., Bu, L., Yao, S., Tu, X., Luo, X., Luo, S., 2013,** Electrodeposition of electroreduced graphene oxide-Au nanoparticles composite film at glassy carbon electrode for anodic stripping voltammetric analysis of trace arsenic(III), Sensors and Actuators B: Chemical, 894-901.

**Lu, X., Zhang, W., Wang, C., Wen, T., Wei, Y., 2011** One-dimensional conducting polymer nanocomposites: Synthesis, properties and applications, 627-712.

**Luzan, S.M., You, S., Szabo, T., Talyzin, A.V., 2013,** Effect of synthesis method on solvation and exfloliation of graphite oxide, Carbon, 171-180.

**MacDiarmid, A.G., Huang, Z., Wang, P-C., Feng, J., Xia, Y., Whitesides, G.M., 1997,** Selective deposition of films of polypyrrole, polyaniline and nicke on hydrophobic/hydrophilic patterned surfaces and applications, Synthetic Metals, 1375-1376.

**REFERENCES (Contiuned)**

**Mu, S., 2009,** Direct determination of arsenate based on its electrocatalytic reduction at the poly(aniline-co-o-aminophenol) electrode, Electrochemistry Communications, 1519-1522.

**Muraviev, D. N., 2005,** Inter-matrix synthesis of polymer stabilised metal nanoparticles for sensor applications, Contributions to Science, 19-32.

**Ojani, R., Raoof, J. B., and Fathi, S.,** Poly(o-aminophenol) film prepared in the presence of sodium dodecyl sulphate: aplication for nickel-ion dispersion and the elecctrocatalytic oxidation of methanol and ethylene glycol, Electrochimica Acta, vol. 54, pp. 2190–2196, 2009.

**Osteryoung, J. G., Osteryoung, R. A., 1985,** Square wave voltammetry, American Chemical Society, pp 101A-110A.

**Prakash, S., Chakrabarty, T., Singh, A. K., Shahi, V. K., 2012,** Silver nanoparticles built-in chitosan modified glassy carbon electrode for anodic stripping analysis of As(III) and its removal from water, Electrochimica Acta, 157-164.

**Rahman, M.A; Won, M-S; Shim, Y-B., 2003,** Characterization of an EDTA bonded conducting polymer modified electrode: Its application for the simultaneous determination of heavy metal ions, Analytical Chemistry, 1123-1129.

**Rajakovic, L. V., Markovic, D. D., Lekic, B. M., Dukic, A. R., Rajakovic-Ognjanovic, V. N., 2013,** Arsenic Removal from Water Using Industrial By-Products, Journal of Chemistry, 1-9.

**Rajkumar, M., Chiou, S-C., Chen, S-M., Thiagarajan, S., 2011,** A novel poly (Taurine)/nano gold modified electrode fort he determination of arsenic in various water samples, International Journal of Electrochemical Science, 3789-3800.

**REFERENCES (Contiuned)**

**Ramesha, G. K., Sampath, S., 2011,** In-situ formation of graphene–lead oxide composite and its use in trace arsenic detection, Sensors and Actuators B, Chemical, 306-311.

**Rawal, R., Chawla, S., Pundir, C.S., 2011,** Polyphenol biosensor based on laccase immobilized onto silver nanoparticles/multiwalled carbon nanotube/polyaniline gold electrode, Analytical Biochemisrty,196-204.

**Ren, X., Meng, X., Tang, F., 2005,** Preparation of Ag–Au nanoparticle and its application to glucose biosensor, Sensors and Actuators B: Chemical, 358-363.

**Renedo, O.D., Martinez, M.J.A., 2007,** A novel method for the anodic stripping voltammetry determination of Sb(III) using silver nanoparticle-modified screen-printed electrodes, Electrochemistry Communications, 820-826.

**Rivas, G. A. and Rubianes, M.D.,** 2007, Dispersion of multi-wall carbon nanotubes in polyethilenamine: A new alternative for preparing electrochemical sensors, Electrochemistry Communications, 9:480-484 pp.

**Rosenauer, A., 2003,** Transmission electron microscopy of semiconductor nanostructures. An Analysis of Composition and Strain State, 238 pages.

**Sahoo, P.K., Panigrahy B., Sahoo, S., Li, D., Bahadur, D., 2013** In situ synthesis and properties of reduced graphene oxide/Bi nanocomposites: As an electroactive material for analysis of heavy metals, Biosensors and Bioelectronics, 293-296.

**Sayyah, S. M., Mohamed, F., Shaban, F., 2014,** Adsorption of Pb (II) ions from aqueous solutions using polycresol film fabricated by cyclic voltammetry, IOSR Journal of Applied Chemistry, 56-64.

**REFERENCES (Contiuned)**

**Sun, V., Wang, X., Wang, Y., Ju, X., Xu, L., Li, G., Sun. Z.,** 2013, Application of graphene–SnO2 nanocomposite modified electrode for the sensitive electrochemical detection of dopamine, Electrochimica Acta, 317-322.

**Tang, L., Li, X., Ji, R., Teng, K. S., Tai, G., Ye, J., Wei, C., Lau, S. P. 2012** "Bottom-up synthesis of large-scale graphene oxide nanosheets". Journal of Materials Chemistry 22 (12): 5676.

**Taniguchi, T., Aoun, S. B., Dursun , Z., Koga, T., Bang, G. S. and Sotomura, I.,** 2004, Effect of metal ad-layers on Au(111) electrodes on electrocatalytic oxidation of glucose in an alkaline solution, J. Electroanal. Chem. 467:175-183 pp.

**Toor, S. K., Devi, P., Bansod, B. K. S., 2015,** Electrochemical Detection of Trace Amount of Arsenic (III) at Glassy Carbon Electrode Modified with Au/Fe3O4 Nanocomposites, 1107-1113.

**Torres, A. C., Barsan. M., Brett, C. M. A., 2014,** Simple electrochemical sensor for caffeine based on carbon and Nafion-modified carbon electrodes, Food Chemistry, 215-220.

**Vasantha, V. S., Chen, Shen-Ming., 2009**, Synergistic effect of a catechin-immobilized poly(3,4-ethylenedioxythiophene)-modified electrode on electrocatalysis of NADH in the presence of ascorbic acid and uric acid, Electrochimica Acta, 665-674.

**Wallace, G. G., Spinks, G. M., Kane-Magnuire, L. P. and Teasdale, P. R.,** 2009, Conductive Electroactive Polymers, CRC pres, Taylor & Francis Group, New York, 263p.

**Wang, J., 2000,** Analytical electrochemistry, Chapter 2, John Wiley and Sons, NY.

**Wang, J., 2001,** Analytical Electrochemistry, WILEY-VCH.FF**.**

**Wang, J., 2006,** Analytical electrochemistry, 3 rd ed., Wiley, VCH.

**REFERENCES (Contiuned)**

**Xiao, L., Wildgoose, G. G., Compton, R. G., 2008,** Sensitive electrochemical detection of arsenic (III) using gold nanoparticle modified carbon nanotubes via anodic stripping voltammetry, Analytica Chimica Acta, 44-49.

**Yuan, B., Xu, C., Deng, D., Xing, Y., Liu, L., Pang, H., Zhang, D., 2013,** Graphene oxide/nickel oxide modified glassy carbon electrode for supercapacitor and nonenzymatic glucose sensor, electrochimica Acta, 708-712.

**Zhang, Y., Li, Q, Sun, L., Zhai, J., 2009,** The electrocatalytic reduction and removal of arsenate by poly(aniline-co-o-aminophenol), Journal of Electroanalytical Chemistry, 47-52.

**Zhang, Z., Yin, J., 2014**, Sensitive detection of uric acid on partially electro-reduced graphene oxide modified electrodes, Electrochimica Acta, 32-37.

## CURRICULUM VITAE


**Name** : Meryem Gökduman

**Date of Birth** : March, 22, 1988

**Place of Birth** : İzmir, Turkey

**Nationality** : Republic of Turkish

**Marital Status** : Single

**Adress** : 58 Sokak Özyağan Apt No:23 D:3 Bornova-İZMİR

**Phone Number** : +90 5548041369

**E-mail** : meryemgokduman@hotmail.com.tr


**Education** : 2007-2012, BSc Degree in Chemisty Department of Ege University, İzmir, Turkey

: 2012-2015 MSc Degree in Chemistry Department of Ege University, İzmir, Turkey.